



## 47 **Introduction**

48

49 Climate change and eutrophication can alter aquatic environments in many ways, including  
50 increasing water temperatures and reducing water oxygen levels. These changes can pose  
51 strong physiological challenges for aquatic ectotherms, such as fish, whose thermal tolerance  
52 windows and geographic distribution are strongly influenced by water temperature and  
53 oxygen availability (Sunday et al., 2012; Comte and Olden, 2017). Ectothermic organisms  
54 experience temperature-dependent increases in metabolic rate during warming, which elevate  
55 their oxygen demand (Fry and Hart, 1948). The oxygen- and capacity-limited thermal  
56 tolerance (OCLTT) hypothesis proposes that aerobic performance is constrained at high  
57 temperatures when oxygen transport can no longer meet the rising metabolic demand for  
58 standard metabolism (Pörtner, 2010; Pörtner et al., 2017). Evidence for a link between  
59 thermal performance and oxygen limitation, however, varies among species and life stages  
60 (Ern et al., 2016, 2017; Silva-Garay et al., 2025; Andreassen et al., 2022; McArley et al.,  
61 2022; Raby et al., 2025), with most research focusing on juvenile and adult stages. A recent  
62 meta-analysis suggested that due to oxygen limitation, fish embryos have narrower thermal  
63 windows than larvae and adults (Dahlke et al., 2020), creating a developmental bottleneck  
64 under climate change. However, this analysis relies partly on imputed thermal tolerance data  
65 due to gaps in the available literature and is influenced by methodological differences among  
66 studies (Pottier et al., 2022; Cowan et al., 2023). As a result, further research is needed to  
67 clarify the role of oxygen availability during warming in early life stages (Du and Shine ,  
68 2022; Pottier et al., 2022; Cowan et al., 2024).

69

70 Fish embryos face respiratory constraints distinct from those of juveniles and adults. Elevated  
71 temperatures accelerate metabolism, increasing oxygen demand and developmental rates,  
72 which can compromise the completion of essential developmental milestones (Kamler, 1994;  
73 Barrionuevo and Burggren, 1999). These vulnerabilities may be amplified by underdeveloped  
74 respiratory and circulatory systems, and by limited or absent behavioral capacity to escape  
75 environmental extremes (Warkentin, 2007). Unlike later life stages that rely on active  
76 ventilation, embryos obtain oxygen primarily through passive diffusion across the chorion,  
77 perivitelline fluid, and embryonic tissues including the yolk sac membrane, which can act as  
78 additional diffusion barriers (Hayes et al., 1951; Rombough, 1989; Warkentin, 2007). After  
79 hatching, larvae still rely largely on cutaneous diffusion, as their gills and circulatory systems  
80 develop (De Silva, 1974; Wells and Pinder, 1996; Rombough, 1999). Although embryos can  
81 initially tolerate low water oxygen levels well, their oxygen requirements generally increase  
82 throughout development. It has been suggested that oxygen requirements peak close to  
83 hatching when the surrounding egg envelope may become a critical barrier to oxygen  
84 diffusion (Rombough, 1989; Czerkies et al., 2001). This diffusion-dependent oxygen uptake  
85 could thus create a physiological bottleneck that limits the embryos' ability to meet rising  
86 metabolic demands under warming or hypoxic conditions (Hassell et al., 2008). As a result,  
87 embryonic development may become oxygen-limited, with severity and duration varying  
88 among species and environmental conditions.

89

90 Embryos can hatch prematurely in response to external stressors, such as warming and  
91 hypoxia, a strategy that can come at the cost of underdeveloped physiological and behavioral  
92 functions (Alderdice et al., 1958; Keckeis et al., 1996; Wood et al., 2019). Premature  
93 hatching may optimize fitness by balancing the trade-offs of remaining within the protective  
94 chorion and emerging as a free-swimming larva, but can also be a maladaptive consequence  
95 of a stressor (Cowan et al., 2024; Warkentin, 2011). Despite this flexibility, environmental  
96 stressors can still impose substantial developmental constraints (Cowan et al., 2024). Both

97 elevated temperatures and low water oxygen levels impair yolk conversion efficiency,  
98 reducing the energy available for growth and organogenesis (Kamler, 1994; Kamiński et al.,  
99 2006). Prolonged or severe hypoxia during embryogenesis can lower metabolic rates, delay  
100 organ development, and reduce growth, often resulting in reduced hatching success and the  
101 emergence of smaller or malformed larvae (Miller et al., 2008; Garside, 1966, Czerkies et al.,  
102 2001). While high temperatures and aquatic hypoxia can restrict development by reducing  
103 oxygen supply relative to demand, the effects of hyperoxia are still poorly understood.  
104 Because hyperoxia can increase tissue oxygen supply capacity in fish (Skeeles et al., 2022)  
105 and may enhance oxygen diffusion across the embryonic and larval respiratory surfaces, it  
106 has the potential to alleviate oxygen-limitation at high temperatures, when metabolic demand  
107 is greatest.

108 Many studies have explored the effects of water temperature or oxygen on fish early  
109 development in isolation (Kamiński et al., 2006; Hassell et al., 2008; Schnur et al., 2014;  
110 Negrete et al., 2024), yet few have examined their interactive impacts, despite the fact that  
111 these environmental stressors often co-occur in nature. This study investigates whether and  
112 how combinations of temperature and oxygen availability during embryogenic development  
113 influence developmental performance in wild-caught zebrafish (*Danio rerio*). Zebrafish  
114 inhabit subtropical freshwater habitats in South Asia, where diel oxygen fluctuations and  
115 episodic heatwaves are common. Although their embryonic development under normoxic,  
116 optimal conditions (~28.5 °C) is well characterized (Kimmel et al., 1995), environmental  
117 stressors can have major physiological impacts. Previous work has shown that adult zebrafish  
118 upper thermal tolerance limits are unaffected by water oxygen across moderate hypoxia to  
119 hyperoxia, regardless of acclimation history (Silva-Garay et al., 2025). However, zebrafish  
120 larvae thermal tolerance can be constrained by oxygen availability, due to oxygen-limited  
121 brain function (Andreassen et al., 2022), suggesting heightened oxygen sensitivity early in  
122 development.

123 To test whether early fish development is constrained by oxygen availability under warming,  
124 we exposed zebrafish embryos to a matrix of 50 temperature-oxygen combinations and  
125 quantified developmental rate, heart rate, yolk sac depletion, hatching success, larval growth,  
126 and survival to first feeding. We also measured juvenile critical thermal maximum (CT<sub>max</sub>) in  
127 fish reared from these embryos to assess developmental carryover effects. Under an oxygen-  
128 limitation framework, hypoxia was expected to exacerbate and hyperoxia to alleviate  
129 temperature effects if development is oxygen limited. Understanding how oxygen availability  
130 constrains early development under warming is essential for improving predictions of fish  
131 vulnerability to climate change.

132  
133  
134  
135

## 134 **Materials and methods**

### 136 **Study Species and Embryo Collection**

137 Zebrafish (*Danio rerio*) originated from a wild population collected in West Bengal, India  
138 (2016; Morgan et al., 2019; Sundin et al., 2019) and were maintained in freshwater aquaria at  
139 the NTNU Animal Facility (Trondheim, Norway). Two independent breeding groups  
140 produced embryos for experiments conducted in April (*Experiment 1*) and September  
141 (*Experiment 2*) 2024. Parental fish were kept in well-aerated freshwater at 28 °C under a

142 14:10 h light:dark cycle and fed dry flakes (TetraPro, Tetra Sales, USA) three times daily. A  
143 total of 42 adults were used for breeding in *Experiment 1* and 110 in *Experiment 2*.

144 Embryos were collected soon after fertilization, photographed, and staged between the one-  
145 cell (0 hours post-fertilization, hpf) and cleavage stages ( $\sim 3/4$  to  $2 1/4$  hpf) following Kimmel et  
146 al. (1995). From each breeding group, randomly mixed subsets of embryos were distributed  
147 among 50 glass beakers (800 mL): 750 embryos (15 per beaker) in *Experiment 1* and 1250  
148 (25 per beaker) in *Experiment 2*. Beakers contained 300 mL water and were sealed with  
149 plastic lids fitted with an aeration tube (PE200; 1.4 mm ID) to provide continuous mixing.  
150 Embryos were maintained under the same photoperiod and were not fed during embryonic  
151 development or early hatching. All procedures were approved by the Norwegian Food Safety  
152 Authority (permit 8578).

153

## 154 **Experimental Setup**

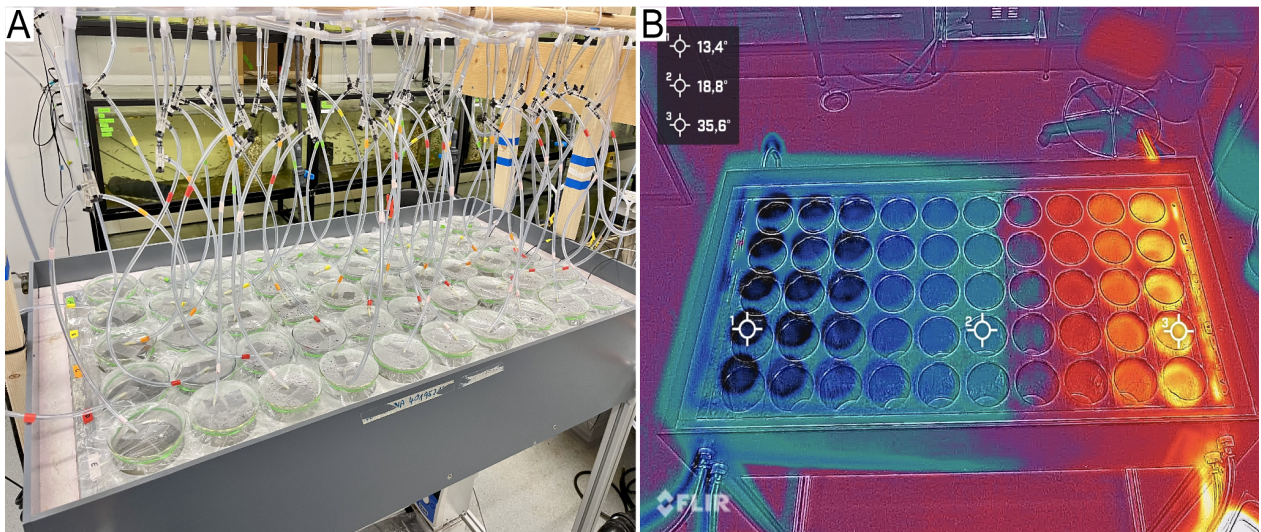
155

### 156 *Thermal Gradient Table*

157

158 An aluminum thermal gradient table was used to expose embryos to 50 simultaneous  
159 temperature-oxygen combinations during development and early larval stages. The system,  
160 adapted from Thomas et al. (1963), consisted of a thick aluminium slab (122.2 x 53.8 x 17  
161 cm) with 50 wells (Thomas et al., 1963; Myrvold, 2020; Haugen, 2022) arranged in a 10 x 5  
162 grid, accommodating 800 mL glass beakers. Each row corresponded to a distinct temperature  
163 treatment (Fig. 1A; Fig. S15–S18). A stable linear thermal gradient was generated by  
164 circulating cooled and heated water at opposite ends using a cooler (Titan 200, Aqua Medic,  
165 Germany) and heater circulator (Grant Instruments, GD100), each regulated by built-in  
166 thermostats. Water from each bath was pumped to the respective edges of the table with an  
167 Eheim Universal 1000 pump (Germany), producing a consistent cold-to-warm gradient  
168 across the aluminium slab (Fig. 1B).<sup>3</sup>

169



170

171 **Fig. 1: Aluminum thermal gradient table used to generate 50 temperature-oxygen**  
172 **combinations. (A)** Ten temperature treatments combined with five oxygen levels (12.5, 25,  
173 50, 100, and 200% air saturation) supplied through gas mixing lines. **(B)** Thermal image of  
174 the gradient surface (FLIR One Pro, Teledyne FLIR LLC).

175

## 176 *Oxygen Treatments*

177

178 Five water oxygen levels (12.5, 25, 50, 100, and 200% air saturation) were supplied to  
179 columns of the thermal gradient table via five independent air lines. Oxygen concentration  
180 were regulated using manual gas flow controllers (RS Pro, 500 ml/min) that mixed air with  
181 nitrogen (50 L, 99.6% N<sub>2</sub>; hypoxia) or oxygen (50 L, 99.5% O<sub>2</sub>, Linde Co.; hyperoxia); while  
182 ambient air provided normoxia (Fig. S17). The mixed gas was delivered to each column via a  
183 10 mm diameter outflow tube. Each beaker was aerated through an individual air tube tightly  
184 inserted through the lid and fitted with an air valve, providing gentle bubbling. Treatment  
185 order was randomized across columns (i.e., *Experiment 1*: 100, 12.5, 25, 200, and 50 % air  
186 sat.; *Experiment 2*: 25, 200, 12.5, 50, and 100 % air sat.) Dissolved oxygen (DO<sub>2</sub>) was  
187 continuously monitored at the warmest position using fiber-optic probes (Fig. S2), and DO<sub>2</sub>  
188 and temperature were verified twice daily in all beakers (FireStingO<sub>2</sub>, PyroScience GmbH).

189

190

## 191 **Experimental Protocol**

192

### 193 *Experiment 1 - Wide thermal range*

194

195 *Experiment 1 (April 2024)* examined embryo development and hatching across a wide  
196 thermal gradient (15.7-39.3 °C: 15.7, 18.1, 20.3, 22.5, 25.2, 27.3, 29.4, 32.0, 35.6, and 39.3  
197 °C) at five oxygen levels (12.5, 25, 50, 100, and 200% air saturation). Embryos (15-16 per  
198 beaker) were transferred by pipette into sealed beakers containing 300 mL normoxic water at  
199 28 °C (control). High-resolution images were taken to document initial developmental stage  
200 before placement on the gradient table. DO<sub>2</sub> levels in the 300 mL water reached target values  
201 within ~20 minutes, while temperatures stabilized within 1-2 hours (with extreme ends of the  
202 gradient table requiring the longest to equilibrate). Embryos were photographed  
203 approximately every 8 hours (see imaging methods). Once hatching began, 30-second videos  
204 of larvae were recorded. During each sampling event (2-3 min per beaker), lids were removed  
205 only briefly (~30 seconds), minimizing disruption to environmental conditions. The  
206 experiment continued for 15 days, until all surviving embryos had hatched.

207

### 208 *Experiment 2 - Upper thermal range*

209

210 *Experiment 2 (September 2024)* examined embryo responses over a narrower, warmer  
211 thermal range (27.8-37.1 °C: 27.8, 28.4, 29.5, 30.4, 31.4, 32.4, 33.3, 34.5, 35.8, and 37.1 °C).  
212 Embryos (24-26 per beaker) were processed as in *Experiment 1*. Target temperatures were  
213 reached within ~1 hour (Fig. S1) and target DO<sub>2</sub> levels within 20 min after beakers were  
214 placed on the gradient table. Embryonic development was documented with video recordings  
215 every 12 hours, with additional photographs collected once hatching began. The experiment  
216 lasted seven days, concluding when all surviving embryos had hatched.

217

218 Dead embryos and larvae were identified by discoloration (e.g., white, cloudy, or opaque  
219 appearance) and lack of response to gentle water flow applied via pipette and were removed  
220 during sampling. After hatching, larvae remained in their original beakers until just before the  
221 onset of exogenous feeding (~2-3 days post-hatching, treatment depending). At that point, a  
222 subset of larvae from five temperature treatments across all oxygen levels were transferred to  
223 control tanks (28 °C, normoxia) for later assessment of critical thermal maximum (CT<sub>max</sub>)  
224 during the juvenile stage.

225

## 226 **Data Collection**

### 227 *Imaging Setup*

228 Two imaging stations were used to capture high-resolution images of embryos and larvae.

### 229 *Embryo Imaging*

230 Embryos were imaged using a custom-built glass platform using a camera (Sony Alpha 7C,  
231 Sony Corp.) fitted with a macro lens (Sony FE 2.8/50 Macro, Sony Corp.) mounted below the  
232 platform and oriented upward, allowing close-up imaging of embryos resting on the beaker  
233 bottom within a 40 mm field of view. Illumination was provided by a side-mounted LED  
234 flood light (133×173×59 mm, 30W, 2400 lumens) positioned 12-15 cm from the focal point  
235 to enhance image contrast. In *Experiment 1*, still images were collected (6000×4000 pixels;  
236 Fig. 2A). In *Experiment 2*, 30-second videos (3840×2160 pixels) were recorded using the  
237 same setup (Fig. 2B).

### 238 *Larval Imaging*

239 Larvae were imaged using a larger LED light platform (470×280×9 mm, Lightcraft Ultraslim  
240 A4 Lightbox) placed beneath the beaker for uniform illumination. A second camera (Sony  
241 Alpha 7C) equipped with a macro lens (Sony FE 2.8/90 Macro G OSS) was positioned above  
242 the platform pointing downward, capturing larvae swimming in the water column. Beaker  
243 lids were briefly removed (~0.5-1 min) during sampling. In *Experiment 1*, 30-second videos  
244 were collected (1280×720 pixels), while *Experiment 2* used still images (6000×4000 pixels).

## 245 **Data Analysis**

246

247 Embryo and larval performance were assessed using fitness-related traits including embryo  
248 survival, yolk sac area, and heart rate, hatching success, larval length at hatch, and survival to  
249 first feeding stage. Metrics were extracted from time-series images and videos.

250

### 251 *Yolk Sac Area*

252

253 Yolk sac surface area (YSA, mm<sup>2</sup>) was measured at three developmental time points starting  
254 at 24 hpf, using *ImageJ* (Abràmoff et al., 2004). For each treatment, five embryos were  
255 analyzed and two perpendicular yolk sac diameters (length (*l*) and height (*h*) in mm) were  
256 measured. YSA was calculated using the ellipse area formula:

257

258

$$YSA = \frac{\pi \cdot l \cdot h}{4}$$

259

260 Image calibration was 390 pixels mm<sup>-1</sup> (*Experiment 1*) and 325 pixels mm<sup>-1</sup> (*Experiment 2*).

261

262 Thermal performance curves were generated using embryonic yolk consumption, quantified  
263 as the percentage reduction in yolk area relative to the mean initial area (at 0 hpf). Yolk area  
264 was measured at 24, 48, and 72 hpf (*Experiment 1*), and at 24, 36, and 48 hpf (*Experiment 2*):

265

266

$$\% \text{ yolk consumed} = \frac{(\text{initial yolk area} - \text{yolk area at time } t)}{\text{initial yolk area}} \times 100$$

267  
268  
269  
270  
271  
272  
273  
274  
275  
276  
277  
278  
279  
280  
281  
282  
283  
284  
285  
286  
287  
288  
289  
290  
291  
292  
293  
294  
295  
296  
297  
298  
299  
300  
301  
302  
303  
304  
305  
306  
307  
308  
309  
310  
311  
312  
313  
314  
315

### *Embryo Heart Rate Measurement*

Embryo heart rate was quantified by amplifying subtle pixel-level motion associated with cardiac contractions using Eulerian video magnification (EVM; Lauridsen et al., 2019). This approach enhances small, periodic intensity changes in a video, such as those caused by heartbeats. Videos (1280x720 pixel) were first stabilized in *iMovie* to reduce camera shake by aligning successive frames. Stabilized videos were then processed in Python using the Laplacian pyramid-based motion magnification approach (Burt and Adelson, 1983). This approach enhances very small movements in the video by analyzing the image at multiple spatial scales and gently amplifying motion while reducing noise, making subtle body movements easier to detect. We used a configuration with eight pyramid levels, an amplification strength of 100. Motion signals with spatial wavelengths above 100 pixels were attenuated, and a mild post-filtering step (attenuation factor 0.4 applied to both the I and Q motion channels) was used to reduce noise while preserving biologically relevant movements. The temporary frequency band was restricted to 1.5-3.5 Hz.

To reduce background noise, videos were temporarily cropped around the embryo's heart, typically to a 10x10 pixel region (Fig. S3A). From this region, a vertical scan line (fixed x-coordinate) positioned over the clearest cardiac signal was used to extract a space-time image representing heartbeat dynamics (Fig. S3B). Heart rate was typically extracted from 5-30 s of recording, limited to periods of high image stability with minimal embryo movement. We then applied Fast Fourier Transform with SciPy 1.15.2 to this space-time image to obtain the frequency spectrum. The dominant peak frequency was taken as heart rate (Hz; Fig. S3C) and converted to beats per minute. Up to six embryos per treatment were analyzed across developmental time points (24-144 hpf) in *Experiment 2*. When background noise prevented reliable frequency detections for six embryos, we analyzed as many individuals as possible.

### *Survival and Hatching*

Embryo survival was assessed visually and confirmed using image recordings. Hatching success was calculated as the proportion of hatched embryos relative to the number of fertilized embryos per beaker. Fertilization was verified by observing early cleavage stages, such as blastula or blastocyst formation, which became visible at ~24 hours post-fertilization (hpf) in *Experiment 1* and ~12 hpf in *Experiment 2*, depending on temperature and oxygen conditions. In addition, survival to the first feeding stage was defined as the proportion of fertilized embryos surviving through hatching and yolk sac absorption, at which point larvae were removed and the treatment was terminated. Larvae showing severe pathological stress (e.g., spiral swimming, edema, spinal deformities) were excluded. Exclusions were not applied to larvae exhibiting delayed but otherwise viable development.

Cumulative hatching and survival to first feeding were visualized using 2D plots and 3D surface plots. For the latter, cumulative survival ratios were smoothed using a kernel-based normalization (*image.smooth*, *Fields* package, R Core Team, 2024). This method applies local averaging to the observed data to estimate a continuous surface.

### *Larval Length*

316 Larval total length (mm; head to caudal fin tip) was measured from all post-hatch images and  
317 videos using *ImageJ*. Image scale calibration was 7.4 pixels mm<sup>-1</sup> (*Experiment 1*) and 35.2  
318 pixels mm<sup>-1</sup> (*Experiment 2*).

319

### 320 *CT<sub>max</sub> Testing*

321

322 To assess developmental effects on upper thermal tolerance, larvae from five developmental  
323 temperatures across all oxygen levels were reacclimated to control conditions until reaching  
324 the juvenile stage (*Experiment 1*: 28.0 ± 0.5 °C; *Experiment 2*: 27.0 ± 0.5 °C). Surviving  
325 individuals were maintained under control conditions for four weeks in *Experiment 1* (20.3,  
326 25.2, 29.4, 32.0, 35.6 °C) and six weeks in *Experiment 2* (27.8, 29.5, 31.4, 33.3, 35.8 °C)  
327 prior to critical thermal maximum (CT<sub>max</sub>) testing. During reacclimation, larvae were fed live  
328 artemia and commercial larvae feed (Zebrafeed, Sparos I&D, <100 to 600 μm) three times  
329 daily and were transitioned to a dry flake diet (TetraPro, Tetra Sales, USA) upon reaching the  
330 juvenile stage (~2-3 weeks post-fertilization).

331

332 CT<sub>max</sub> was defined as the temperature (°C) at loss of equilibrium (LOE; inability to remain  
333 upright for 3 s; Morgan et al., 2018). Trials followed the protocol of Morgan et al. (2018) and  
334 were conducted under control conditions (28 °C, normoxia; 100% air saturation). Groups of  
335 7-9 fish from each rearing condition were transferred from holding tanks to a CT<sub>max</sub> arena (9  
336 L; 25 × 22 × 18 cm) and allowed to acclimate for 15 min before temperature ramping began.  
337 Starting at 28 °C, water temperature was increased at a rate of 0.34 ± 0.02 °C min<sup>-1</sup>. Fish  
338 were fasted for 16-20 h prior to testing, and water in the CT<sub>max</sub> arena was replaced between  
339 trials to maintain water quality. Treatment order was randomized to minimize time-of-day  
340 and order effects, and trials were completed within a three-day period for *Experiments 1* and  
341 *2*. At LOE, fish were immediately removed, and temperature and time were recorded.  
342 Individuals were transferred to recovery tanks maintained at 28 °C, where all recovered  
343 equilibrium within 2 min. After a 30 min recovery period, fish were euthanized by ice  
344 immersion, and body mass (± 0.01 g) and total length (± 0.1 mm) were measured.

345

346

### 347 *Fulton's Condition Factor*

348

349 Using body mass (*W*) and total length (*L*) of the fish tested for CT<sub>max</sub>, we quantified the  
350 Fulton Condition Factor (*K*) as follows:

351

352

$$K = \frac{W}{L^3}$$

353

354

### 355 **Statistical Analysis**

356

357

#### 358 *Physiological Parameters Analysis*

359

360 Yolk consumption, heart rate, larval length, CT<sub>max</sub> and Fulton's condition factor were  
361 analyzed using linear models in R (*car* package; v4.4.1; R Core Team, 2024). Fixed effects  
362 included oxygen, temperature, their interaction, and developmental time when applicable.  
363 Temperature was centered to the coldest treatment and included as linear (*Temp<sub>1</sub>*) and  
364 quadratic (*Temp<sub>2</sub> = Temp<sub>1</sub><sup>2</sup>*) within each experiment to facilitate interpretation of model

365 coefficients and interaction terms:  $Response\ variable \sim Oxygen + Temp_1 + Temp_2 +$   
366  $Oxygen*Temp_1 + Oxygen*Temp_2 + hpf$ . Type II ANOVA was used for balanced designs and  
367 Type III for unbalanced designs or models with interactions. Alternative models were built,  
368 removing the quadratic term of temperature, when oxygen or temperature had a linear  
369 relationship with the response variable. Models were contrasted using Akaike Information  
370 Criterion (AIC) to identify the most parsimonious model structure that best fit the data  
371 (*MuMIn* package). We considered a difference of  $\Delta AIC > 2$  as evidence of substantial  
372 improvement in model fit (Burnham and Anderson, 2004). Estimates, standard errors, and p-  
373 values (with significance  $p < 0.05$ ) are reported in the Results section. Model assumptions  
374 were evaluated via residual diagnostics and homoscedasticity.

375

### 376 *Hatching Success Analysis*

377

378 Hatching and larval survival probability were analyzed using binomial generalized linear  
379 models (GLMs, *glm* package; Brooks et al., 2017) with a logit link and bias-reducing  
380 estimation (*brglmFit*) to mitigate small-sample and separation issues. Models included  
381 oxygen, temperature, their interaction, and  $\log(hpf)$  as fixed effects, with fertilized embryos  
382 specified as the binomial denominator:  $(Larval\ hatched, Initial\ embryos - Larval\ hatched) \sim$   
383  $Oxygen * Temperature + \log(hpf)$ . From these models, we estimated the time to 50%  
384 hatching ( $ET_{50}$ ) for each temperature–oxygen combination in both experimental runs by  
385 interpolating predicted hatching probabilities from the fitted curves using the functions  
386 *predict* and *approx*. Treatment effects were assessed by contrasting model predictions against  
387 control conditions (normoxia at 27.3 °C in *Experiment 1* and 27.8 °C in *Experiment 2*).

388

389 Quadratic temperature models were also fitted to characterize nonlinear responses:  $(Larval$   
390  $hatched, Initial\ embryos - Larval\ hatched) \sim Oxygen + Temp_1 + Temp_2 + Oxygen*Temp_1 +$   
391  $Oxygen*Temp_2 + \log(hpf)$ ; where  $Temp_1$  and  $Temp_2$  represent linear and quadratic  
392 temperature terms, respectively. This model was used to assess the effect of oxygen on  
393 thermal performance of both hatching success and survival to first feeding across  
394 temperatures. Model goodness-of-fit was evaluated using residual deviance (residual  
395 deviance/degrees of freedom  $\approx 1$ ) and diagnostic plots. Statistical significance was set at  $\alpha =$   
396 0.05. Parameter estimates reported in the Supplementary Materials correspond to log-odds  
397 coefficients, along with their standard errors, z-values, and associated p-values derived from  
398 the fitted GLMs.

399

400

## 401 **Results**

402

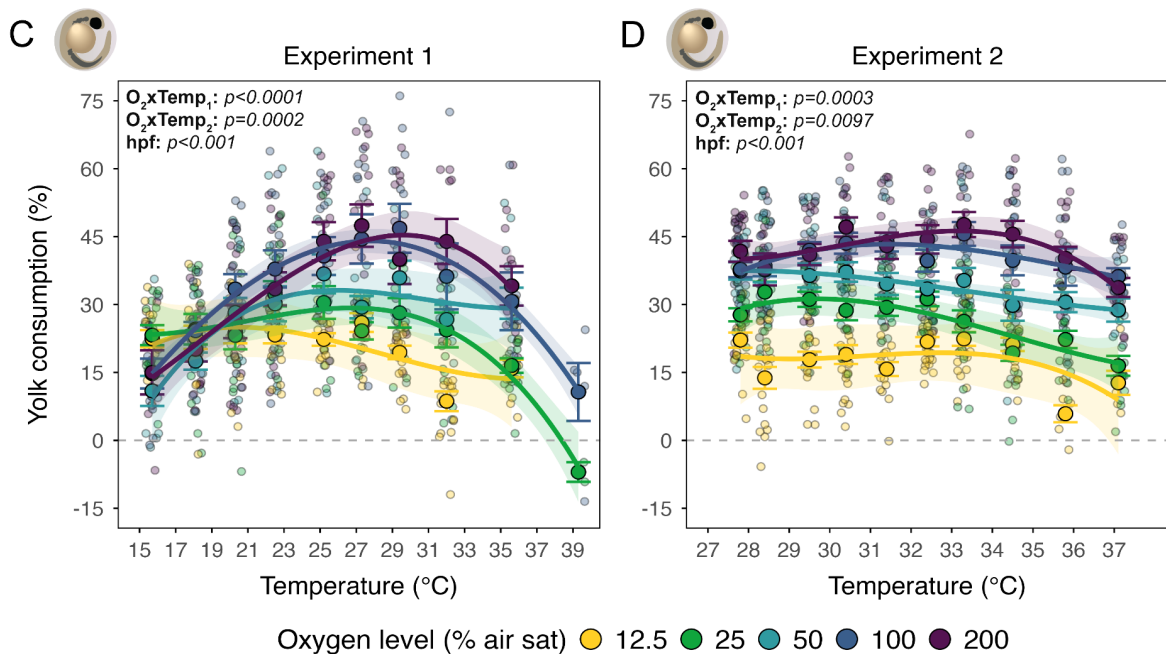
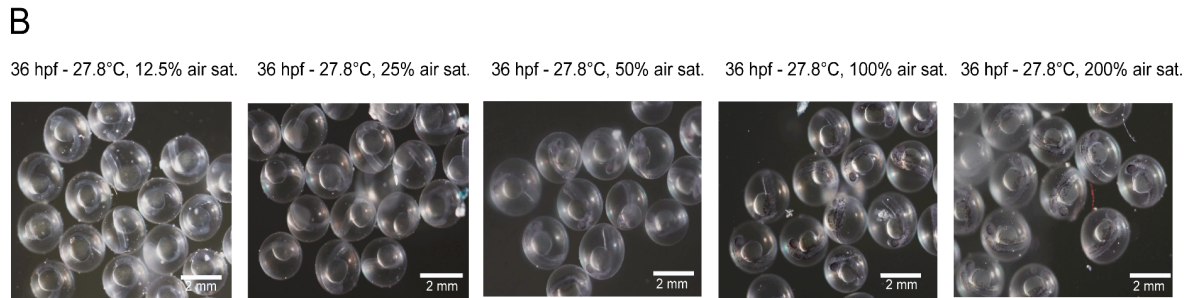
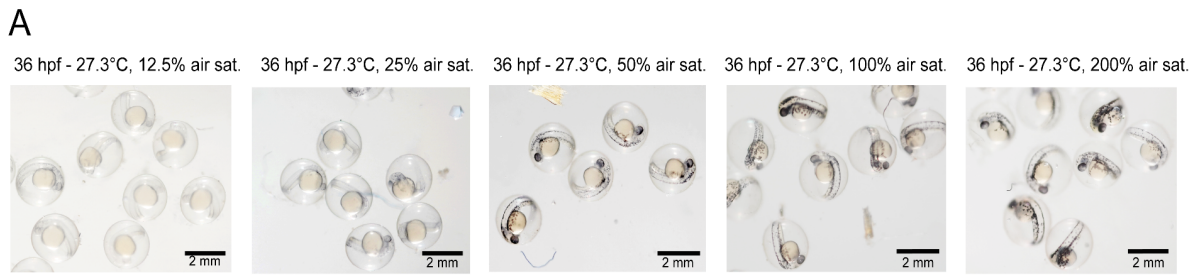
403

### 404 *Yolk Sac Area*

405 In *Experiment 1* (15.7 to 39.3 °C), yolk consumption was affected by temperature, oxygen  
406 availability, their interaction, and developmental time (all  $p < 0.001$ ; Fig. 2A-C; Fig. S4A-  
407 S5A; Table S1). Under normoxia, yolk utilization increased steeply with warming from the  
408 coldest treatment ( $Temp_1: \beta = 5.01 \pm 0.45, p < 0.001$ ) and declined above 32 °C ( $Temp_2: \beta =$   
409  $-0.195 \pm 0.020, p < 0.001$ ), forming a thermal performance curve with maximal yolk  
410 consumption between 22.5 - 32 °C. Oxygen level strongly altered this temperature  
411 dependence. At the lowest temperatures, severe hypoxia increased yolk consumption ( $\beta =$   
412  $7.66 \pm 2.88, p = 0.008$ ;  $\beta = 6.14 \pm 2.85, p = 0.032$ ), coinciding with delayed development and  
413 developmental arrest at 15.7 °C. Above 20.3 °C, however, hypoxia consistently reduced yolk

414 consumption ( $\beta = -10.19 \pm 1.52, p < 0.001$  at 12.5%;  $\beta = -5.03 \pm 1.51, p = 0.001$  at 25%;  $\beta = -$   
415  $7.15 \pm 1.54, p < 0.001$  at 50%). Severe hypoxia (12.5% and 25%) markedly flattened and  
416 narrowed the thermal performance curve by reducing the increase in yolk use with warming  
417 ( $O_2 \times Temp_1$ :  $\beta = -4.39 \pm 0.65, t = -6.78, p < 0.001$  for 12.5%;  $\beta = -2.68 \pm 0.63, p < 0.001$  for  
418 25%). Moderate hypoxia also reduced yolk use at warm temperatures ( $\beta = -1.34 \pm 0.67, p =$   
419  $0.048$ ), whereas hyperoxia did not differ from normoxia ( $\beta = -1.16 \pm 3.29, p = 0.47$ ).

420 In *Experiment 2* (27.8 - 37.1 °C), yolk sac dynamics mirrored those observed in *Experiment 1*  
421 ( $p < 0.001$  all; Fig. 2B-D; Fig. S4B-S5B; Table S2). Yolk consumption increased from 27.8  
422 °C ( $Temp_1$ :  $\beta = 2.74 \pm 0.74, p < 0.001$ ) and declined at the highest temperatures ( $Temp_2$ :  $\beta =$   
423  $-0.325 \pm 0.078, p < 0.001$ ). Severe hypoxia (12.5 and 25% air saturation) reduced yolk  
424 consumption across temperatures ( $\beta = -21.62 \pm 1.91, p < 0.001$  at 12.5%;  $\beta = -8.60 \pm 1.91, p$   
425  $< 0.001$  at 25%), whereas moderate hypoxia and hyperoxia did not differ from normoxia  
426 (Table S2, Fig. 3B). Unlike *Experiment 1*, oxygen-temperature interactions were weak in this  
427 warmer range, with only moderate hypoxia showing an interaction with temperature at high  
428 temperatures ( $O_2 \times Temp_2$ :  $\beta = 0.296 \pm 0.110, p = 0.007$ ).



429  
430  
431  
432  
433  
434  
435  
436  
437  
438  
439  
440  
441

**Fig. 2: Yolk consumption (%) of embryos across temperature and oxygen treatment.**

(A) Embryonic development progress at 36 hpf across oxygen levels at 27.3 °C in  
 Experiment 1. (B) Equivalent data at 27.8 °C in Experiment 2. (C-D) Yolk consumption (%  
 of initial area, mm<sup>2</sup>) across temperatures (x-axis) and oxygen levels (colors) in Experiment 1  
 (C; n = 2–9) and Experiment 2 (D; n = 2–11). Points show individual embryos; circles: means  
 ± s.e, lines: quadratic fits by oxygen level. Anova (type III) results in Table S1-S2.

### Heart Rate

#### Experiment 2

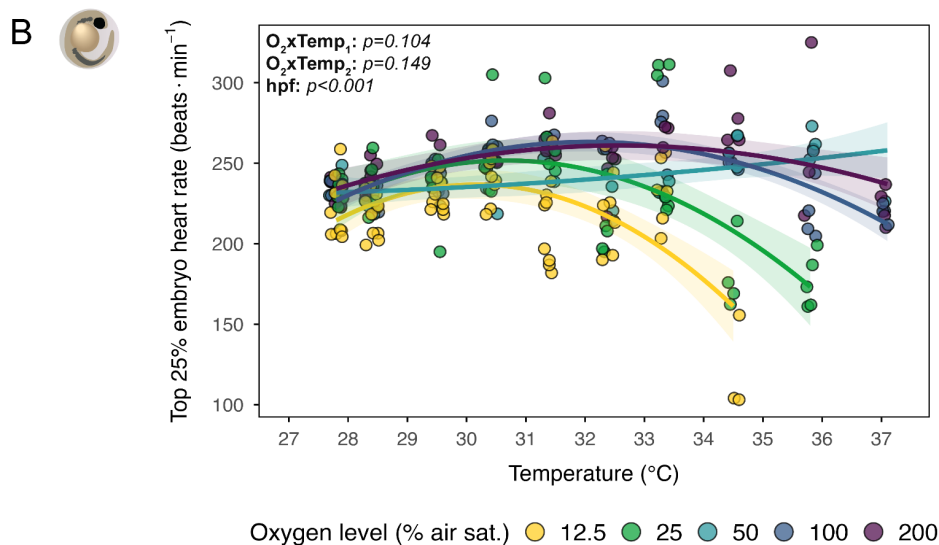
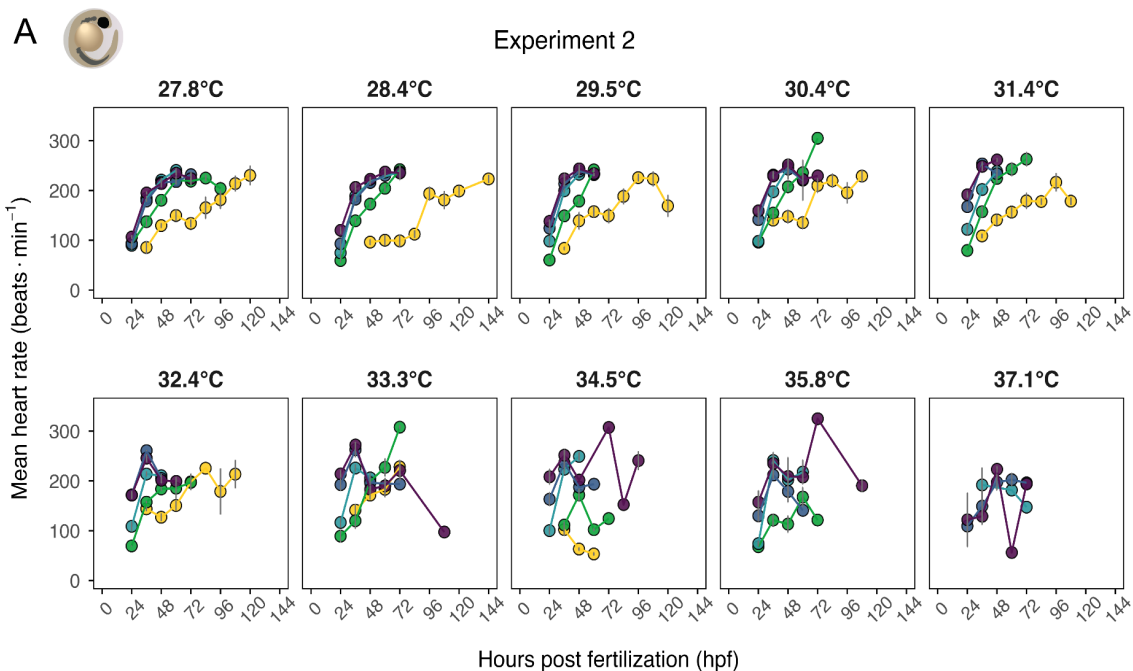
Embryonic heart rate exhibited nonlinear temporal dynamics and was strongly influenced by  
 oxygen level and temperature, but not by their interaction (Fig. 3A-B; Table S3). Centered at  
 27.8 °C under normoxia, heart rate increased with warming from the coldest treatment

444

445 (Temp<sub>1</sub>:  $\beta = 19.60 \pm 3.72$ ,  $p < 0.001$ ) and declined above  $\sim 33.3$  °C (Temp<sub>2</sub>:  $\beta = -2.19 \pm 0.41$ ,  
 446  $p < 0.001$ ), showing a unimodal thermal response. Heart rate increased with developmental  
 447 time ( $\beta = 1.63 \pm 0.08$ ,  $p < 0.001$ ) from its onset at  $\sim 24$  hpf and approaching a plateau prior to  
 448 hatching.

449  
 450 Severe hypoxia (12.5% air saturation) delayed the onset of heart activity and markedly  
 451 reduced heart rate across temperatures ( $\beta = -96.20 \pm 8.72$ ,  $p < 0.001$ ), while 25% air  
 452 saturation also reduced heart rates, with stronger effects at warmer temperatures ( $\beta = -19.15 \pm$   
 453  $8.91$ ,  $p = 0.032$ ). Heart rates under 50% and 200% air saturation did not differ from  
 454 normoxia. Oxygen-temperature interactions were generally weak, indicating that oxygen  
 455 mainly shifted overall heart rate rather than altering its temperature dependence; only 50% air  
 456 saturation showed detectable interaction effects (Temp<sub>1</sub>:  $\beta = -12.96 \pm 5.84$ ,  $p = 0.027$ ; Temp<sub>2</sub>:  
 457  $\beta = 1.44 \pm 0.67$ ,  $p = 0.032$ ). Increased variability in heart rate above 33.3 °C likely reflects  
 458 measurements from embryos that failed to hatch on time ( $\sim 48$  hpf) and exhibited delayed or  
 459 abnormal development.

460



461

462 **Fig. 3: Embryonic heart rate across temperature and oxygen treatments.**  
463 (A) Mean heart rate (beats min<sup>-1</sup>) of embryos in *Experiment 2* over developmental time,  
464 calculated as the average of individual embryo heart rates within each temperature-oxygen  
465 treatment (n = 1-8 embryos per time point). Colors indicate oxygen levels. Points show mean  
466 ± s.e. (B) Top 25<sup>th</sup> percentile of embryo heart rates (beats min<sup>-1</sup>) by temperature-oxygen  
467 treatment, calculated from measurements pooled across developmental time. Colored points  
468 representing individual measurements, lines show quadratic fits by oxygen level. P-values  
469 from type III Anova (Table S3).

470

471

## 472 ***Hatching Success***

473

474

### 475 *Experiment 1*

476

477 Across the wide thermal range (15.7-39.3 °C), hatching rate was influenced by temperature,  
478 oxygen level, their interaction, and developmental time (GLM, all  $p < 0.0001$ ; Fig. 4A; Table  
479 S4). Under normoxia, embryos showed a clear thermal window for successful development:  
480 hatching was delayed and reduced at 18.1 °C, increasing sharply from 20.3 to 35.6 °C (>75%  
481 hatching), and was fastest at 27.3-32 °C. No hatching occurred at the extreme temperatures  
482 (15.7 °C and 39.3 °C). Oxygen availability strongly modified this thermal response (Fig. 4C;  
483 see Fig. S6A-S7A-S8). At 18.1 °C, hatching was delayed and reduced across oxygen  
484 treatments, and especially under hypoxia ( $\leq 50\%$  air saturation;  $p < 0.001$ ) and hyperoxia  
485 (200% air saturation;  $p < 0.001$ ). Severe hypoxia (12.5% air saturation) showed hatching  
486 rates comparable to normoxia (~80-100%) between 20.3 and 27.3 °C but declined at 29.4 °C  
487 (~75%) and ceased at 32.0 °C. Hypoxia (25% air saturation) showed a similar pattern, with  
488 reduced hatching at 32.0 °C (~75% ;  $p = 0.001$ ) and complete suppression at higher  
489 temperatures. Both moderate hypoxia (50%) and hyperoxia (200%) reduced hatching at the  
490 warmest temperature (35.6 °C) only, where hatching declined to ~50% (both  $p < 0.001$ ;  
491 Table S5).

492 A GLM including the temperature-oxygen interaction provided the best fit for estimating  
493 time to 50% hatch (ET<sub>50</sub>; Table S5; Fig. S9A). Hatching time decreased steeply with  
494 warming, from: ~224-279 hpf at 18.1 °C and 126-200 hpf at 20.3 °C, to 51-79 hpf at 27.3 °C  
495 and 41-78 hpf at 32 °C (Table S6). Oxygen availability further modified this temperature  
496 dependence. At cooler temperatures ( $\leq 27.3$  °C), severe hypoxia (12.5-25%) accelerated  
497 hatching by ~20-70 h relative to normoxia, whereas at warmer temperatures hypoxia  
498 progressively delayed hatching by ~25-50 h. Hyperoxia delayed hatching only at the warmest  
499 temperature (35.6 °C).

500

501

### 502 *Experiment 2*

503

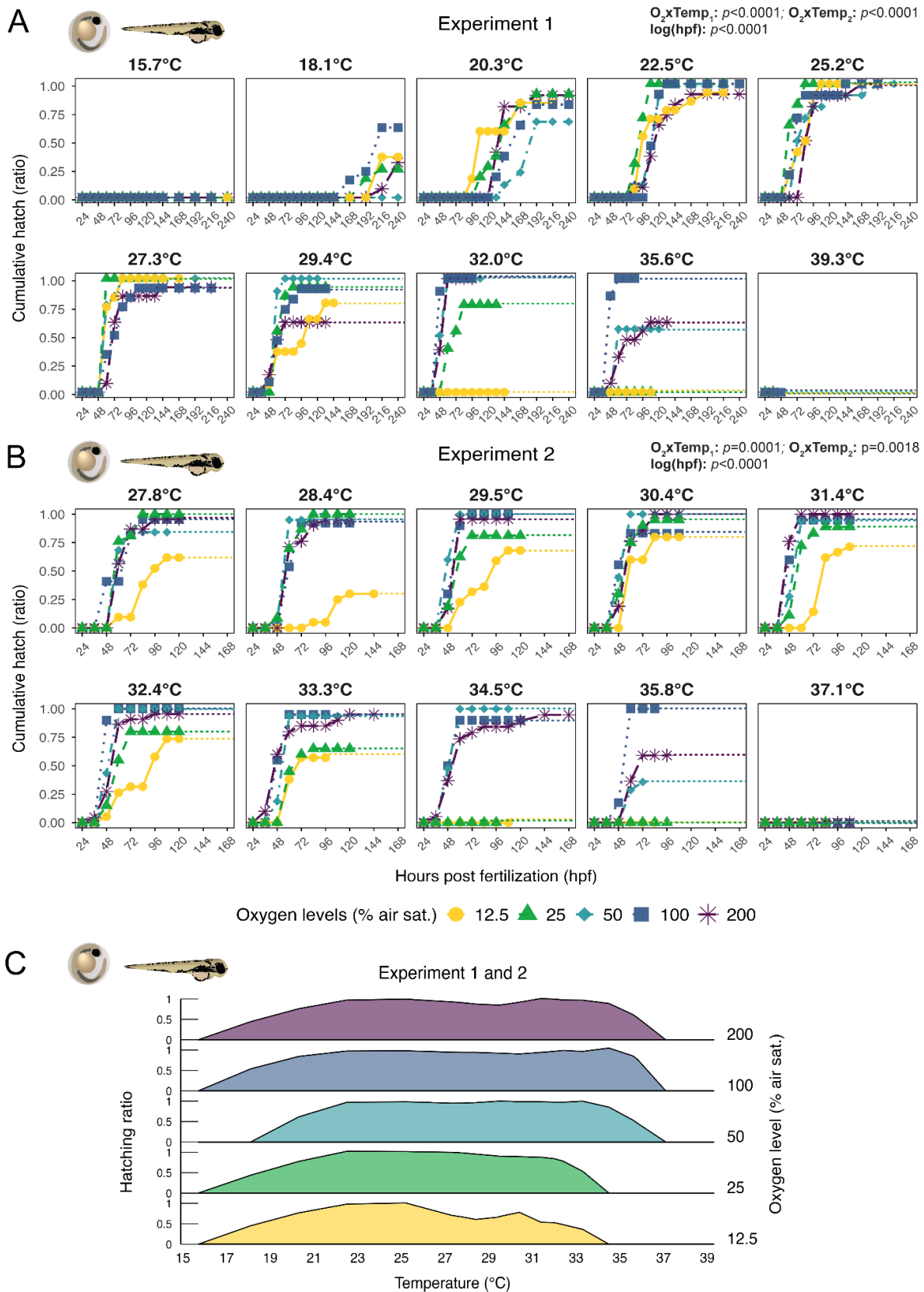
504 Within the warmer developmental range (27.8-37.1 °C), hatching success was again  
505 influenced by temperature, oxygen level, their interaction, and developmental time (GLM, all  
506  $p < 0.001$ ; Fig. 4B; Table S6). Under normoxia, hatching remained high (90-100%) from 27.8  
507 to 35.8 °C and failed entirely at 37.1 °C. Oxygen strongly modified this thermal window (Fig.  
508 4C; see Fig. S6B-S7B-S8). Severe hypoxia (12.5%) consistently reduced and delayed

509 hatching across most temperatures ( $p < 0.001$ ), with complete failure at 34.5 °C ( $p = 0.0002$ ;  
510 Table S7). Hypoxia (25%) produced hatching rates comparable to normoxia at 27.8-28.4 °C,  
511 but reduced hatching at 32.4 and 33.3 °C (both  $p < 0.001$ ) and suppressed hatching at 34.5  
512 °C, consistent with *Experiment 1*. Moderate hypoxia (50%) had little effect except at 35.8 °C,  
513 where hatching was strongly reduced and delayed ( $p = 0.001$ ). Hyperoxia (200%) did not  
514 improve hatching success relative to normoxia across this temperature range (27.8-35.8 °C);  
515 but reduced hatching to a ~50% at 35.8 °C ( $p < 0.001$ ), again mirroring *Experiment 1*.

516

517 Consistent with these patterns,  $ET_{50}$  estimates (GLM; Table S7; Fig. S9B) revealed strong  
518 oxygen effects across 27.8-37.1 °C. Severe hypoxia (12.5%) markedly delayed hatching  
519 throughout this thermal range, with  $ET_{50}$  occurring ~68-136 hpf later than under normoxia  
520 (41-62 hpf; Table S6). Hypoxia (25%) produced  $ET_{50}$  values comparable to normoxia at  
521 cooler temperatures (~56 hpf at 27.8-28.4 °C), but increasingly delayed hatching at warmer  
522 temperatures ( $ET_{50} \approx 59-80$  hpf), consistent with the temperature-dependent shift observed in  
523 *Experiment 1*. Hyperoxia delayed the hatching only at the warmest temperature (35.8 °C).

524



525  
 526  
 527  
 528  
 529

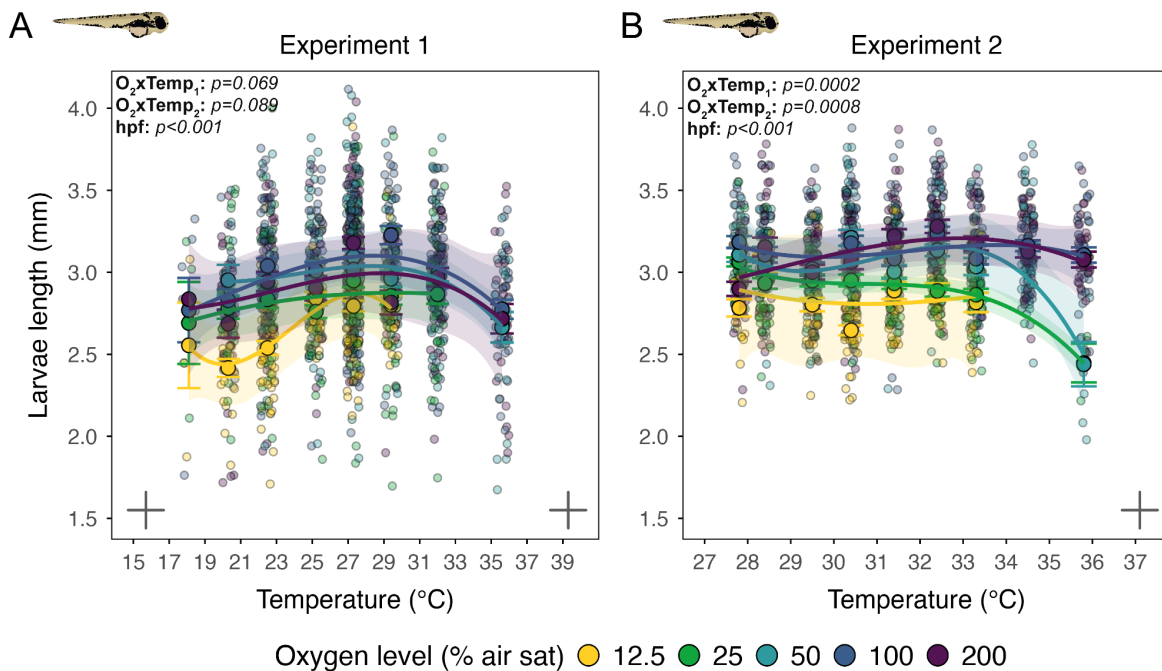
**Fig. 4: Hatching dynamics across temperature and oxygen treatments. (A)** Cumulative hatching ratio over time (hpf) across temperatures (panels) and oxygen levels (colors) in *Experiment 1* (n = 8-15). **(B)** Equivalent data for *Experiment 2* (n = 13-23). Symbols denote observed hatching ratios; dotted lines indicate periods when larvae were removed following

530 mortality or completion of hatching. P-values from binomial GLM (Table S4-S6). (C)  
 531 Maximum hatching ratio across temperatures combining *Experiment 1* and 2. The ridgeline  
 532 shows *LOESS*-smoothed maxima (span = 0.45).  
 533  
 534

### 535 *Larvae Length*

536  
 537 In *Experiment 1*, larval length varied with temperature, oxygen level, and developmental  
 538 time, but not with the interaction temperature-oxygen ( $p < 0.001$ ; Fig. 5A; Table S9; Fig.  
 539 S10A-S11). Under normoxia and centered at 18.1 °C, length increased with warming from  
 540 the coldest treatment (Temp<sub>1</sub>:  $\beta = 0.085 \pm 0.017$ ,  $p < 0.001$ ) and declined slightly at higher  
 541 temperatures (Temp<sub>2</sub>:  $\beta = -0.0042 \pm 0.0009$ ,  $p < 0.001$ ). Severe hypoxia (12.5% air  
 542 saturation) produced the largest reduction in length across temperatures ( $\beta = -0.423 \pm 0.139$ ,  
 543  $p = 0.002$ ), while hyperoxia caused a moderate decrease ( $\beta = -0.250 \pm 0.117$ ,  $p = 0.033$ ).  
 544 Hypoxia (25% air saturation) reduced length only above 22.5 °C ( $\beta = -0.145 \pm 0.042$ ,  $p =$   
 545  $0.001$ ), whereas 50% air saturation did not differ from normoxia. Oxygen-temperature  
 546 interactions were weak, suggesting that oxygen primarily shifted mean larval length without  
 547 substantially altering its temperature response. Larval length increased modestly with  
 548 developmental time ( $\beta = 0.00094 \pm 0.00025$ ,  $p < 0.001$ ).  
 549

550 In *Experiment 2*, larval length again varied with oxygen level and developmental time but  
 551 showed no temperature effects ( $p < 0.001$ ; Fig. 5B; Table S10; Fig. S10B-S12). Length was  
 552 no different across temperatures (Temp<sub>1</sub>:  $p = 0.44$ ; Temp<sub>2</sub>:  $p = 0.46$ ). Oxygen effects were  
 553 more pronounced: larvae reared in hypoxia were consistently smaller across temperatures,  
 554 with the strongest reduction at 12.5% ( $\beta = -0.410 \pm 0.062$ ,  $p < 0.001$ ), followed by moderate  
 555 reduction at 25%, 50%, and 200% air saturation (all  $p \leq 0.02$ ). As in *Experiment 1*, oxygen-  
 556 temperature interactions were weak, and mostly driven by responses under hyperoxia at 27.8  
 557 °C. Larval length also increased with developmental time ( $\beta = 0.00445 \pm 0.00042$ ,  $p < 0.001$ ).



558  
 559 **Fig. 5: Larval length across temperature and oxygen treatments.** (A) Larval length (mm)  
 560 in *Experiment 1* (n = 2-15). (B) Equivalent data for *Experiment 2* (n = 2-24). Points represent

561 individual larvae; colored circles indicate means  $\pm$  s.e., lines show third-degree polynomial  
562 fits. P-values from type III Anova (Table S9-S10).

563

564

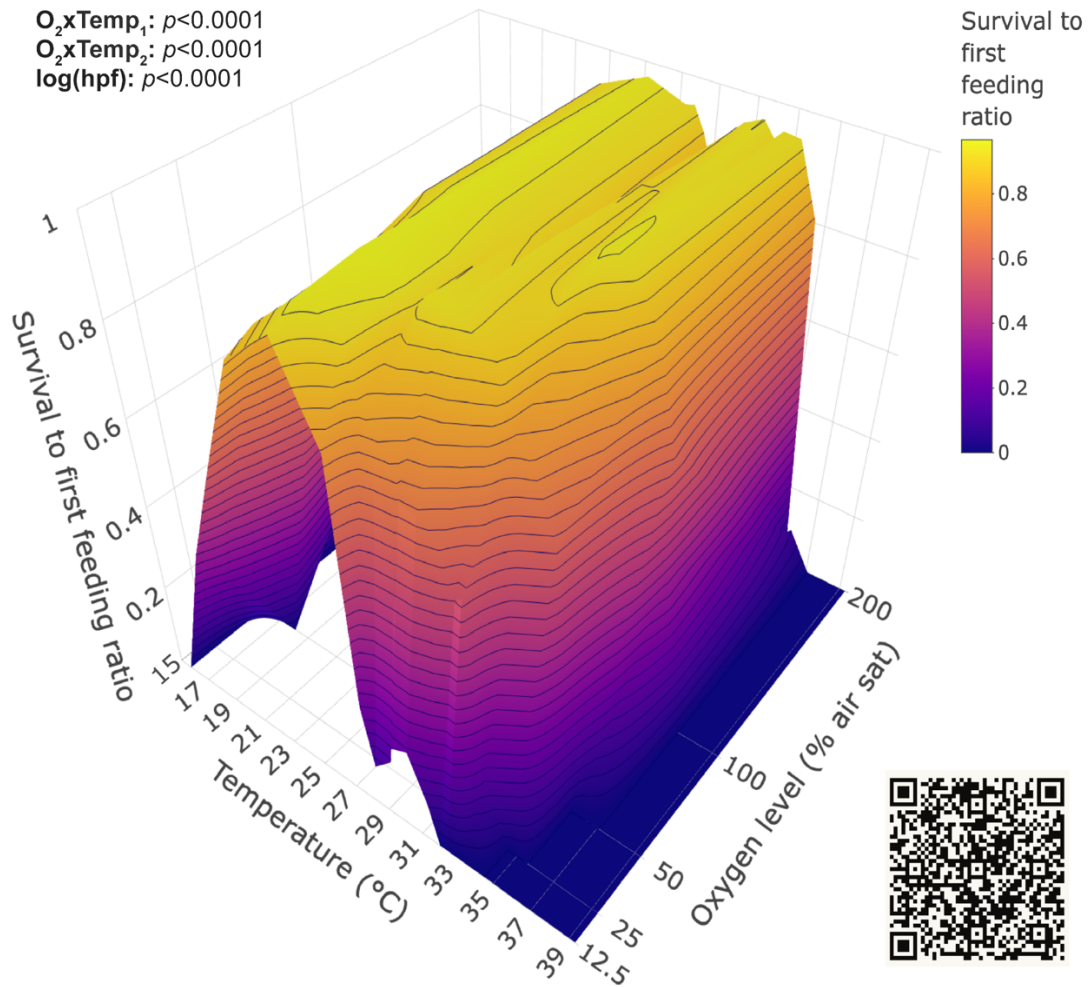
### 565 ***Survival To First Feeding Stage***

566

567 Survival to the first feeding stage showed significant main and interactive effects of  
568 temperature and oxygen level when results from *Experiments 1* and *2* were combined (Fig. 6;  
569 Table S11). At 18.1 °C, hatching was substantially delayed (~225-275 hpf), and surviving  
570 larvae exhibited retarded development, retaining large yolk sacs for an additional 48-72 h  
571 after hatching. Because the experiment was terminated at this point, these individuals were  
572 included in survival-to-first-feeding estimates, as they reflected delayed development rather  
573 than mortality. In contrast, under extreme warming (~35.6-35.8 °C) and hyperoxia, larvae  
574 that had consumed the yolk sac but exhibited severe deformities (e.g., spinal malformations  
575 or tissue swelling) were excluded from survival estimates.

576

577 Under normoxia, survival remained high (>80%) across a broad thermal range (~20-35 °C),  
578 declining toward the warmest temperatures (Fig. S8). At lower temperatures, larvae  
579 successfully completed endogenous feeding, resulting in high survival-to-first-feeding across  
580 all oxygen levels. In contrast, elevated temperatures caused substantial mortality that  
581 increased progressively with hypoxia severity (all  $p < 0.001$ ; Table S11). Survival declined  
582 below 50% above 34 °C under 50% air saturation, above 32 °C under 25%, and above 27 °C  
583 under 12.5%. Notably, extreme heat (~35°C) combined with hyperoxia also markedly  
584 reduced survival ( $p < 0.001$ ), whereas under normoxia survival closely matched hatching  
585 success. The slight valley at intermediate-high temperatures and hyperoxia appears to be an  
586 artifact of combining experiments rather than a biologically meaningful pattern, as survival  
587 remained relatively high across that range.



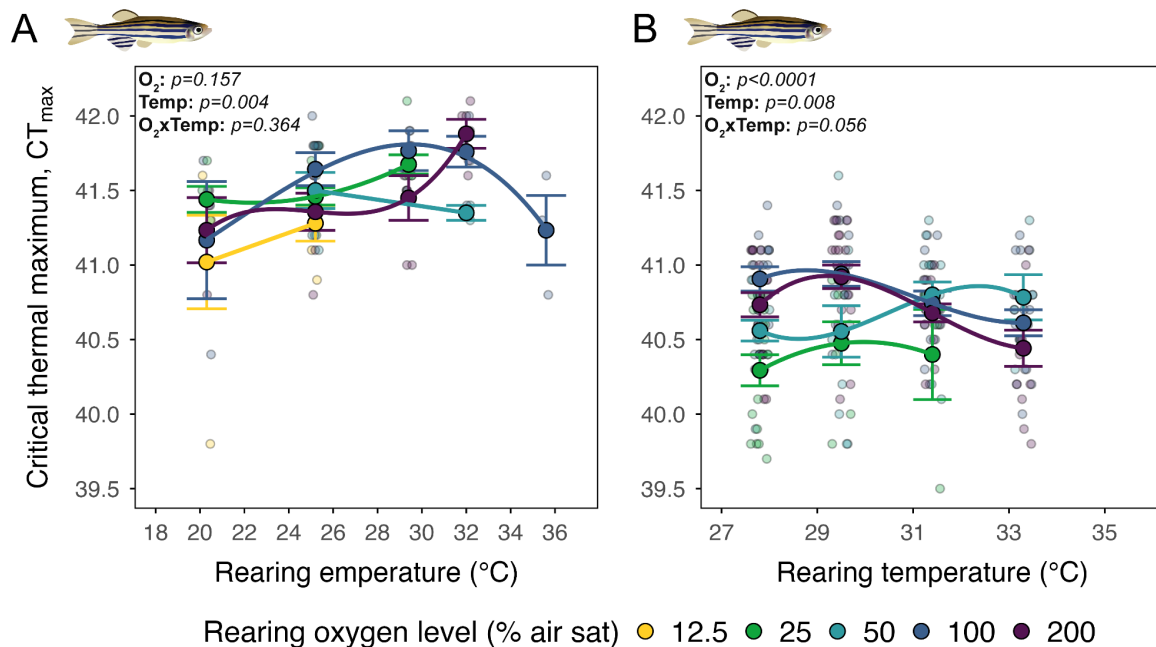
588 **Fig. 6: Three-dimensional surface plot of larval survival across temperature and oxygen**  
 589 **treatments.** 3D surface shows the proportion of fertilized embryos surviving to first feeding  
 590 across temperatures (15.7–39.3 °C) and oxygen levels, combining *Experiments 1* and 2.  
 591 Survival ratios > 0.6 were smoothed using kernel-based normalization (*aRange*,  $\theta = 0.9$ ).  
 592 P-values from binomial GLM-Tmb (Table S11). An interactive version is available at:  
 593 [https://loresilvag.github.io/Interactive-3Dplot/3D\\_SurvivalToFirstFeeding\\_Plot.html](https://loresilvag.github.io/Interactive-3Dplot/3D_SurvivalToFirstFeeding_Plot.html)  
 594  
 595  
 596

### 597 *Fulton's Condition Factor and $CT_{max}$*

598 In *Experiment 1*, larvae from five temperatures and oxygen levels were re-acclimated to  
 599 control conditions before  $CT_{max}$  testing (Table S12). Larvae hatched at 12.5% air saturation  
 600 in the warmer treatments died before transfer, and post-transfer mortality regardless of the  
 601 rearing oxygen level was high at the hottest temperatures, preventing full factorial testing  
 602 (Fig. S13A). Fulton's condition factor of juvenile fish did not differ across rearing  
 603 temperatures or oxygen levels ( $p = 0.076$  and  $p = 0.150$ , respectively; Table S15, Fig. S14A).  
 604  $CT_{max}$  varied significantly with rearing temperature (Anova type III:  $p < 0.001$ ), but not with  
 605 oxygen or the oxygen-temperature interaction (Fig. 7A; Table S13). Post hoc comparisons  
 606 centered on normoxia and 20.3 °C showed that early exposure to severe hypoxia (12.5%)  
 607 reduced  $CT_{max}$  ( $\beta = -0.304 \pm 0.138$ ,  $p = 0.031$ ), while 25%, 50%, and 200% air saturation did  
 608 not differ from normoxia.  $CT_{max}$  was also lower in fish reared at 20.3 °C ( $\beta = -0.324 \pm 0.122$ ,

609  $p = 0.010$ ), unchanged at 25.2 and 32 °C, and marginally reduced at 35.6 °C ( $\beta = -0.436 \pm$   
610  $0.222, p = 0.053$ ).

611 In *Experiment 2*, early mortality under severe hypoxia and warm temperatures similarly  
612 limited the number of treatment combinations available for testing. (Fig. S13B). Fulton's  
613 condition factor again showed no effect of temperature or oxygen ( $p = 0.387$  and  $p = 0.426$ ,  
614 respectively; Table S15, Fig. S14B).  $CT_{max}$  varied with both oxygen level and rearing  
615 temperature (Anova type II: both  $p < 0.001$ ), with a border-line interaction ( $p = 0.056$ ; Fig.  
616 7B, Table S14). Developmental hypoxia (25% air saturation) reduced  $CT_{max}$  ( $\beta = -0.483 \pm$   
617  $0.09, p < 0.001$ ), same in the 50% air saturation fish ( $\beta = -0.158 \pm 0.073, p = 0.032$ ), while  
618 hyperoxia (200%) did not differ from normoxia. Relative to 27.8 °C,  $CT_{max}$  was lower in fish  
619 reared at 33.3 °C ( $\beta = -0.164 \pm 0.082, p = 0.04$ ), while intermediate temperatures produced no  
620 difference. Although overall interactions were weak, moderate hypoxia at higher  
621 temperatures produced small but detectable reductions in  $CT_{max}$  (e.g., at 31.4 °C and 33.3  
622 °C).



623 **Fig. 7: Critical thermal maximum ( $CT_{max}$ ) of juvenile zebrafish following early-life**  
624 **exposure to temperature and oxygen treatment. (A)**  $CT_{max}$  of juveniles in *Experiment 1*.  
625 **(B)** Equivalent data for *Experiment 2*. Points represent individual fish (jittered); circles show  
626 means  $\pm$  s.e., and lines depict polynomial fits. P-values from type III Anova (Table S13-S14).  
627  
628

629  
630

## 631 Discussion

632  
633  
634  
635

*Negligible effects of water oxygen availability on embryo development and hatching*

636 By leveraging the many treatment combinations of the thermal gradient table, we examined  
637 how the thermal-oxygen landscape influences zebrafish early development. Because embryos  
638 and early larvae rely on passive diffusion of oxygen across the chorion and perivitelline fluid,

639 hyperoxia was hypothesized to buffer against oxygen limitation during thermal stress. We  
640 therefore predicted that oxygen availability would play a dominant role in shaping thermal  
641 performance, especially at supraoptimal temperatures. Contrary to these predictions, the role  
642 of oxygen on developmental performance was relatively minor. Increasing oxygen  
643 availability through hyperoxic water did not alleviate key symptoms of thermal stress. Even  
644 at the highest temperatures, hyperoxic water did not improve yolk consumption, hatching, or  
645 larval growth and survival. This lack of benefit from hyperoxia is consistent with  
646 observations in rainbow trout (*Oncorhynchus mykiss*) embryos, where growth was similar  
647 under hyperoxia and normoxia rearing (Ciuhandu et al., 2005), and in Atlantic salmon (*Salmo*  
648 *salar*) where hyperoxic rearing (150% air saturation) through embryonic and alevin  
649 development did not enhance growth or aerobic metabolism (Wood et al., 2019). Together,  
650 these findings indicate that developmental constraints under warming are not readily  
651 explained by OCLTT predictions (Dahlke et al., 2020).

652 Hyperoxia delayed hatching in zebrafish (by 26-50 h), but only at the highest temperatures.  
653 Similar delays were reported in rainbow trout (*Oncorhynchus mykiss*) and Atlantic killifish  
654 (*Fundulus heteroclitus*, Dimichele and Taylor, 1980; Latham and Just, 1989). As hatching  
655 has been hypothesized to be triggered by hypoxia in the embryo (Czerkies et al., 2001;  
656 Teletchea and Pauly 2024), hyperoxic water that reduces diffusive constraints across the  
657 chorion and perivitelline fluid would accordingly delay hatching, although empirical support  
658 for this mechanism remains limited. We found delayed hatching from hyperoxia only at the  
659 highest temperatures, meaning it does not appear to delay hatching in general. The hypothesis  
660 is also not supported by our moderate hypoxia groups, where earlier hatching would have  
661 been predicted. As this was not found, and because hyperoxia did not delay hatching at most  
662 temperatures, we don't see evidence for embryonic oxygen limitation as a universal trigger  
663 for hatching.

664 Similar to the relatively minor effects of hyperoxia, mild hypoxia (50% air saturation) did not  
665 dramatically exacerbate the thermal performance of embryos and larvae in most of our  
666 measurements. There appeared to be a slight slowing of yolk consumption at higher  
667 temperatures, but heart rate, hatching success, and larvae length were mostly unaffected until  
668 the very highest temperatures. Taken together, the limited effects of hyperoxia and mild  
669 hypoxia suggest that tissue oxygen availability is not a major physiological mechanism  
670 restricting development in zebrafish.

671

672 *Severe hypoxia allows early development but imposes physiological costs*

673

674 Remarkably, embryos reared under severe hypoxia (12.5 and 25% air saturation) showed  
675 high hatching success (60-100%) across a broad thermal range (~20-33 °C), indicating  
676 substantial tolerance to low oxygen levels. Yet, severe hypoxia produced clear signs of  
677 developmental disturbance, including reduced heart rate, slowed yolk consumption, reduced  
678 body length, and delayed and underdeveloped hatching, particularly near thermal limits.  
679 These patterns are consistent with hypoxia-induced metabolic depression, a response  
680 observed in many teleosts embryos (Shumway et al., 1964; Hassell et al., 2008; Mueller et  
681 al., 2011; Marks et al., 2012). Edema and diminished skin pigmentation were also observed  
682 in the severe hypoxia-exposed embryos but were not quantified. Notably, embryos exposed to  
683 severe hypoxia exhibited lower heart rates than those reared at higher oxygen levels from the

684 onset of cardiac activity (~24 hpf). Although they eventually reached peak heart rates  
685 comparable to those observed in normoxic embryos, this occurred several days later under  
686 severe hypoxia. Because this pattern is consistent with observed trajectories of cardiac  
687 development in zebrafish (Gierten et al., 2020), it likely reflects delayed cardiac development  
688 rather than persistent bradycardia. While heart rate itself is unlikely to directly limit oxygen  
689 uptake at this stage, delayed cardiac and organ development can nonetheless impair overall  
690 performance. Hatching under severe hypoxia is a common and well-documented response in  
691 fish embryos exposed to suboptimal environmental conditions, including hypoxia and  
692 elevated temperatures (Czerkies et al., 2001; Cowan et al., 2024). Mechanistically, sustained  
693 hypoxia during late embryogenesis can trigger the release of chorionase from hatching gland  
694 cells, softening the chorion and facilitating earlier escape (Czerkies et al., 2001, 2002).  
695 However, if embryos are weakened or hatching glands remain immature, hatching may fail  
696 (Czerkies et al., 2001; Mueller et al., 2011). Thus, while stress-induced hatching may enable  
697 embryos to exit unfavorable environments, it can occur before completion of key  
698 developmental milestones required for post-hatching function.

699 Despite the developmental stress observed before hatching, survival to the first feeding stage  
700 remained high under severe hypoxia at cooler temperatures (18-27 °C), but declined sharply  
701 when hypoxia was combined with supraoptimal temperatures. As in embryos, early larval  
702 oxygen uptake relies primarily on cutaneous diffusion because gills are not yet functional (De  
703 Silva, 1974; Wells and Pinder, 1996). In zebrafish, neuroepithelial cells that facilitate gill-  
704 based oxygen uptake begin developing in the gill filaments at ~5 days post-fertilization at 28  
705 °C (Jonz and Nurse, 2005), coinciding with rising metabolic demands that may render  
706 cutaneous respiration insufficient. This likely explains the time-limited survival and elevated  
707 mortality observed in larvae exposed to severe hypoxia and warming, particularly after  
708 transfer to normoxia for CT<sub>max</sub> testing (Fig. S13). In contrast, larvae reared under severe  
709 hypoxia at cooler temperatures showed high survival after transfer and attained body sizes  
710 comparable to normoxia-reared larvae. Together, these results identify the early post-hatching  
711 transition as a critical window in which rising metabolic demands can outpace diffusive  
712 oxygen uptake under combined hypoxia and warming.

713 Temperature is a key regulator of fish embryonic development (Kamler, 1994; Kamiński et  
714 al., 2006), and in our study, warming predictably accelerated yolk consumption, development  
715 and hatching. Furthermore, severe hypoxia had a temperature-dependent and non-linear effect  
716 on hatching time. When compared to normoxia, the hatching under severe hypoxia occurred  
717 sooner under cooler temperatures (20-50 hours earlier) and was delayed under warming (30-  
718 50 hours later; Fig. 4, Fig. S9). This suggests that at warm temperatures and hypoxia, oxygen  
719 can become limiting to metabolic processes, leading to slowed development and delayed  
720 hatching. At low temperatures, however, where metabolic demands are reduced, the low  
721 oxygen saturation in hypoxia may be sufficient to sustain development, but can still induce  
722 premature hatching. Together, these results demonstrate a complex interaction between  
723 temperature and oxygen availability, whereby severe hypoxia accelerates hatching under  
724 cooler temperatures but delays hatching under warming.

725

726 *Thermal performance curves reveal a broad thermal window for embryonic development*

727

728 The thermal window for successful zebrafish embryonic development and hatching (>80%  
729 success) ranged from 20 to 36 °C under normoxia. This is a broader thermal window than  
730 what has previously been reported for zebrafish (~22-34 °C) (Schirone and Gross, 1968;  
731 Schnurr et al., 2014; Urushibata et al., 2021). A possible explanation for this discrepancy is  
732 that the current experiment used the JU strain of wild-caught zebrafish that have previously  
733 been found to be more plastic than the domesticated AB strain (Morgan et al., 2022; Sundin  
734 et al., 2019). The thermal range is also narrower, especially on the cold side, than the  
735 established thermal window found for juveniles and adults under chronic conditions (Åsheim  
736 et al., 2020; Morgan et al., 2019, 2022). A sharp decline in hatching success and complete  
737 failure below 18 °C and above 36 °C under all water oxygen levels marks clear thermal limits  
738 for the zebrafish embryogenesis. Thermal performance curves further revealed that  
739 intermediate temperatures (25-34 °C) maximized yolk sac consumption and larval size,  
740 suggesting that this range may support the most efficient energy allocation to growth. Taken  
741 together, the embryonic development of zebrafish has a broad thermal window and is  
742 surprisingly robust to thermal challenges.

743

744 *Developmental heat and severe hypoxia marginally shape juvenile thermal limits*

745

746

747 Developmental plasticity, whereby early life conditions confer lasting effects across  
748 subsequent life stages, has been suggested to be an important mechanism shaping ectotherm  
749 thermal tolerance (Scott and Johnston, 2012; Noble et al., 2018). Acute thermal tolerance  
750 tests of juveniles showed that early-life exposure to severe hypoxia and non-optimal  
751 temperatures can have lasting, albeit modest, effects. Fish reared under severe hypoxia  
752 exhibited slightly lower  $CT_{max}$  than those reared under normoxia (0.3-0.4 °C average  
753 difference; Fig. 7). Similarly, fish reared at colder or warmer temperature extremes showed  
754 reduced thermal tolerance relative to those reared near the thermal optimum (0.3 and 0.4 °C  
755 average difference, respectively). These effects should be interpreted cautiously, as severe  
756 hypoxia and warming caused substantial mortality during early development, such that  $CT_{max}$   
757 estimates reflect only individuals that survived to the juvenile stage and do not capture  
758 responses across the full range of developmental conditions. Notably, higher developmental  
759 temperatures did not enhance juvenile heat tolerance, indicating limited capacity for  
760 beneficial developmental plasticity under warming. Overall, the effect sizes associated with  
761 developmental plasticity were small, consistent with meta-analyses showing that ectotherm  
762 thermal tolerance is only weakly influenced by developmental temperature (Pottier et al.,  
763 2022). Together, these results suggest that while early-life oxygen and thermal stress can  
764 influence later thermal limits, their effects are modest and do not confer increased tolerance  
765 to acute warming.

766

767

768

## 769 **Conclusion**

770

771 Early life stages have been viewed as a thermal bottleneck in the fish life cycle, with  
772 warming expected to constrain performance through oxygen limitation. Our results challenge  
773 the view that oxygen limitation sets the upper thermal boundary for early fish development.  
774 Hyperoxia failed to improve early-life performance and even reduced hatching success at the  
775 upper thermal extremes, suggesting potential physiological costs of elevated oxygen under

776 heat stress (e.g. ROS production or oxygen toxicity; Birnie-Gauvin et al., 2016; Tunç et al.,  
777 2025), although these were not directly assessed. Overall, responses to hyperoxia appear  
778 species- and context-dependent.

779

780 In contrast, zebrafish embryos tolerated moderate hypoxia remarkably well, and only severe  
781 hypoxia combined with warming impaired development and reduced larval survival. While  
782 signs of oxygen limitation emerged under these extreme conditions, developmental failure at  
783 high temperatures was not alleviated by additional oxygen. This indicates that mechanisms  
784 other than oxygen supply, likely involving cellular and molecular limits, constrain the upper  
785 thermal tolerance in early life. The broad temperature range supporting successful hatching  
786 further highlights the plasticity of embryonic development in zebrafish. Our study also  
787 indicates only limited carry over effects of early developmental conditions on later thermal  
788 tolerance. Together, these findings underscore the need to understand how multiple  
789 interacting stressors affect early developmental stages to more accurately predict species  
790 resilience and vulnerability in a warming world.

791

792

793

#### 794 **Acknowledgements**

795

796 We thank Eline Østduun for their help with fish husbandry and Claudia Hernández Camacho  
797 for her assistance during the data collection for the first experiment. Thanks to Nicole Aberle-  
798 Malzahn for designing and the NTNU workshop with Øystein Gjervan Hagemo and Robert  
799 Karlsen for constructing the thermal gradient table.

800

801

#### 802 **CRedit authorship contribution statement**

803

804 **Lorena Silva-Garay:** Conceptualization, Methodology, Investigation, Data collection,  
805 Writing – original draft, Data curation, Visualization, Formal analysis, Project administration.

806 **Moa Metz:** Conceptualization, Methodology, Data collection, Review & Editing. **Henning**

807 **H. Kristiansen:** Methodology, Data collection, Data curation, Visualization, Software,

808 Review & Editing. **Leon Pfeufer:** Methodology, Data collection, Review & Editing. **Emily**

809 **R. Lechner:** Methodology, Data collection, Review & Editing. **Rasmus Ern:**

810 Conceptualization, Methodology, Review & Editing. **Anna H. Andreassen:**

811 Conceptualization, Methodology, Review & Editing. **Fredrik Jutfelt:** Conceptualization,

812 Methodology, Investigation, Writing – Review & Editing, Validation, Supervision,

813 Resources, Funding acquisition.

814

815

#### 816 **Conflict of interest declaration**

817

818 We declare we have no competing interests.

819

820

#### 821 **Data availability statement**

822

823 The data supporting the findings of this study is deposited in Zenodo and will be made

824 publicly available upon acceptance of the manuscript. Data are available to editors and

825 reviewers upon request during peer review. [10.5281/zenodo.18500503]

826 **Code availability statement**

827

828 Custom code used to process the data, perform statistical analyses, and generate figures is  
829 deposited in Zenodo and will be made publicly available upon acceptance of the manuscript.

830 Code will be provided to editors and reviewers upon request during peer review.

831

832

833 **References**

834

835

836 Abràmoff, M. D., Magalhães, P. J., & Ram, S. J. (2004). Image processing with ImageJ.  
837 *Biophotonics international*, 11(7), 36-42.

838 Alderdice, D. F., Wickett, W. P., & Brett, J. R. (1958). Some effects of temporary exposure  
839 to low dissolved oxygen levels on pacific salmon eggs. *Journal of the Fisheries*  
840 *Research Board of Canada*, 15(2), 229-250. <https://doi.org/10.1139/f58-013>

841 Andreassen, A. H., Hall, P., Khatibzadeh, P., Jutfelt, F., & Kermen, F. (2022). Brain  
842 dysfunction during warming is linked to oxygen limitation in larval zebrafish.  
843 *Proceedings of the National Academy of Sciences*, 119(39), e2207052119.  
844 <https://doi.org/doi:10.1073/pnas.2207052119>

845 Åsheim, E. R., Andreassen, A. H., Morgan, R., & Jutfelt, F. (2020). Rapid-warming tolerance  
846 correlates with tolerance to slow warming but not growth at non-optimal temperatures  
847 in zebrafish. *Journal of Experimental Biology*, 223(23).  
848 <https://doi.org/10.1242/jeb.229195>

849 Barrionuevo, W. R., & Burggren, W. W. (1999). O<sub>2</sub> consumption and heart rate in developing  
850 zebrafish (*Danio rerio*): influence of temperature and ambient O<sub>2</sub>. *American Journal*  
851 *of Physiology-Regulatory, Integrative and Comparative Physiology*, 276(2), R505-  
852 R513. <https://doi.org/10.1152/ajpregu.1999.276.2.R505>

853 Birnie-Gauvin, K., Costantini, D., Cooke, S. J., & Willmore, W. G. (2017). A comparative  
854 and evolutionary approach to oxidative stress in fish: A review. *Fish and Fisheries*,  
855 18(5), 928-942. <https://doi.org/https://doi.org/10.1111/faf.12215>

856 Burnham, K. P., & Anderson, D. R. (2004). Multimodel inference: understanding AIC and  
857 BIC in model selection. *Sociological Methods & Research*, 33(2), 261-304.  
858 <https://doi.org/10.1177/0049124104268644>

859 Burt, P., & Adelson, E. (1983). The Laplacian Pyramid as a compact image code. *IEEE*  
860 *Transactions on Communications*, 31(4), 532-540.  
861 <https://doi.org/10.1109/TCOM.1983.1095851>

862 Ciuhandu, C. S., Stevens, E. D., & Wright, P. A. (2005). The effect of oxygen on the growth  
863 of *Oncorhynchus mykiss* embryos with and without a chorion. *Journal of Fish*  
864 *Biology*, 67(6), 1544-1551. [https://doi.org/https://doi.org/10.1111/j.1095-](https://doi.org/https://doi.org/10.1111/j.1095-8649.2005.00856.x)  
865 [8649.2005.00856.x](https://doi.org/https://doi.org/10.1111/j.1095-8649.2005.00856.x)

866 Comte, L., & Olden, J. D. (2017). Climatic vulnerability of the world's freshwater and  
867 marine fishes. *Nature Climate Change*, 7(10), 718-722.  
868 <https://doi.org/10.1038/nclimate3382>

869 Cowan, Z.-L., Andreassen, A. H., De Bonville, J., Green, L., Binning, S. A., Silva-Garay, L.,  
870 Jutfelt, F., & Sundin, J. (2023). A novel method for measuring acute thermal tolerance  
871 in fish embryos. *Conservation Physiology*, 11(1).  
872 <https://doi.org/10.1093/conphys/coad061>

873 Cowan, Z.-L., Green, L., Clark, T. D., Blewett, T. A., De Bonville, J., Gagnon, T., Hoots, E.,  
874 Kuchenmüller, L., Leeuwis, R. H. J., Navajas Acedo, J., Rowsey, L. E., Scheuffele,  
875 H., Skeeles, M. R., Silva-Garay, L., Jutfelt, F., & Binning, S. A. (2024). Global

876 change and premature hatching of aquatic embryos. *Global Change Biology*, 30(9),  
877 e17488. <https://doi.org/https://doi.org/10.1111/gcb.17488>

878 Czerkies, P., Brzuzan, P., Kordalski, K., & Luczynski, M. (2001). Critical partial pressures of  
879 oxygen causing precocious hatching in *Coregonus lavaretus* and *C. albula* embryos.  
880 *Aquaculture*, 196(1), 151-158. [https://doi.org/https://doi.org/10.1016/S0044-  
881 8486\(00\)00545-7](https://doi.org/https://doi.org/10.1016/S0044-8486(00)00545-7)

882 Czerkies, P., Kordalski, K., Golas, T., Krysinski, D., & Luczynski, M. (2002). Oxygen  
883 requirements of whitefish and vendace (Coregoninae) embryos at final stages of their  
884 development. *Aquaculture*, 211(1), 375-385.  
885 [https://doi.org/https://doi.org/10.1016/S0044-8486\(02\)00049-2](https://doi.org/https://doi.org/10.1016/S0044-8486(02)00049-2)

886 Dahlke, F. T., Wohrab, S., Butzin, M., & Pörtner, H.-O. (2020). Thermal bottlenecks in the  
887 life cycle define climate vulnerability of fish. *Science*, 369(6499), 65-70.  
888 <https://doi.org/doi:10.1126/science.aaz3658>

889 De Silva, C. (1974). Development of the respiratory system in herring and plaice larvae. In J.  
890 H. S. Blaxter, *The Early Life History of Fish* Berlin, Heidelberg.

891 Dimichele, L., & Taylor, M. H. (1980). The environmental control of hatching in *Fundulus*  
892 *heteroclitus*. *Journal of Experimental Zoology*, 214(2), 181-187.  
893 <https://doi.org/https://doi.org/10.1002/jez.1402140209>

894 Du, W.-G., & Shine, R. (2022). The behavioural and physiological ecology of embryos:  
895 responding to the challenges of life inside an egg. *Biological Reviews*, 97(4), 1272-  
896 1286. <https://doi.org/https://doi.org/10.1111/brv.12841>

897 Ern, R., Johansen, J. L., Rummer, J. L., & Esbaugh, A. J. (2017). Effects of hypoxia and  
898 ocean acidification on the upper thermal niche boundaries of coral reef fishes. *Biology*  
899 *Letters*, 13(7), 20170135. <https://doi.org/doi:10.1098/rsbl.2017.0135>

900 Ern, R., Norin, T., Gamperl, A. K., & Esbaugh, A. J. (2016). Oxygen dependence of upper  
901 thermal limits in fishes. *Journal of Experimental Biology*, 219(21), 3376-3383.  
902 <https://doi.org/10.1242/jeb.143495>

903 Fry, F. E. J., & Hart, J. S. (1948). The relation of temperature to oxygen consumption in the  
904 goldfish. *The Biological Bulletin*, 94(1), 66-77. <https://doi.org/10.2307/1538211>

905 Garside, E. T. (1966). Effects of oxygen in relation to temperature on the development of  
906 embryos of Brook trout and Rainbow trout. *Journal of the Fisheries Research Board*  
907 *of Canada*, 23(8), 1121-1134. <https://doi.org/10.1139/f66-105>

908 Gierten, J., Pylatiuk, C., Hammouda, O. T., Schock, C., Stegmaier, J., Wittbrodt, J., Gehrig,  
909 J., & Loosli, F. (2020). Automated high-throughput heartbeat quantification in  
910 medaka and zebrafish embryos under physiological conditions. *Scientific Reports*,  
911 10(1), 2046. <https://doi.org/10.1038/s41598-020-58563-w>

912 Hassell, K. L., Coutin, P. C., & Nugegoda, D. (2008). Hypoxia impairs embryo development  
913 and survival in black bream (*Acanthopagrus butcheri*). *Marine Pollution Bulletin*,  
914 57(6), 302-306. <https://doi.org/https://doi.org/10.1016/j.marpolbul.2008.02.045>

915 Haugen, L. A. S. (2022). *Feeding ecology and behavior of nudibranchs from the sublittoral*  
916 *zones of Trondheimsfjorden and interactions with fouling communities* [Master's  
917 thesis Norwegian University of Science and Technology].

918 Hayes, F. R., Wilmot, I. B., & Livingstone, D. A. (1951). The oxygen consumption of the  
919 salmon egg in relation to development and activity. *Journal of Experimental Zoology*,  
920 116(3), 377-395. <https://doi.org/https://doi.org/10.1002/jez.1401160302>

921 Jonz, M. G., & Nurse, C. A. (2005). Development of oxygen sensing in the gills of zebrafish.  
922 *Journal of Experimental Biology*, 208(8), 1537-1549.  
923 <https://doi.org/10.1242/jeb.01564>

924 Kamiński, R., Kamler, E., Korwin-Kossakowski, M., Myszkowski, L., & Wolnicki, J. (2006).  
925 Effects of different incubation temperatures on the yolk-feeding stage of *Eupallasella*

926 *percunurus* (Pallas). *Journal of Fish Biology*, 68(4), 1077-1090.  
927 <https://doi.org/https://doi.org/10.1111/j.0022-1112.2006.01008.x>

928 Kamler, E., Szlamińska, M., Kuczyński, M., Hamáčková, J., Kouřil, J., & Dabrowski, R.  
929 (1994). Temperature-induced changes of early development and yolk utilization in the  
930 African catfish *Clarias gariepinus*. *Journal of Fish Biology*, 44(2), 311-326.  
931 <https://doi.org/https://doi.org/10.1111/j.1095-8649.1994.tb01208.x>

932 Keckeis, H., Bauer-Nemeschkal, E., & Kamler, E. (1996). Effects of reduced oxygen level on  
933 the mortality and hatching rate of *Chondrostoma nasus* embryos. *Journal of Fish*  
934 *Biology*, 49(3), 430-440. [https://doi.org/https://doi.org/10.1111/j.1095-](https://doi.org/https://doi.org/10.1111/j.1095-8649.1996.tb00039.x)  
935 [8649.1996.tb00039.x](https://doi.org/https://doi.org/10.1111/j.1095-8649.1996.tb00039.x)

936 Kimmel, C. B., Ballard, W. W., Kimmel, S. R., Ullmann, B., & Schilling, T. F. (1995).  
937 Stages of embryonic development of the zebrafish. *Developmental Dynamics*, 203(3),  
938 253-310. <https://doi.org/https://doi.org/10.1002/aja.1002030302>

939 Latham, K. E., & Just, J. J. (1989). Oxygen availability provides a signal for hatching in the  
940 rainbow trout (*Salmo gairdneri*) embryo. *Canadian Journal of Fisheries and Aquatic*  
941 *Sciences*, 46(1), 55-58. <https://doi.org/10.1139/f89-008>

942 Lauridsen, H., Gonzales, S., Hedwig, D., Perrin, K. L., Williams, C. J. A., Wrege, P. H.,  
943 Bertelsen, M. F., Pedersen, M., & Butcher, J. T. (2019). Extracting physiological  
944 information in experimental biology via Eulerian video magnification. *BMC Biology*,  
945 17(1), 103. <https://doi.org/10.1186/s12915-019-0716-7>

946 Marks, C., Kaut, K. P., Moore, F. B.-G., & Bagatto, B. (2012). Ontogenetic oxygen changes  
947 alter zebra fish size, behavior, and blood glucose. *Physiological and Biochemical*  
948 *Zoology*, 85(6), 635-644. <https://doi.org/10.1086/666508>

949 McArley, T. J., Morgenroth, D., Zena, L. A., Ekström, A. T., & Sandblom, E. (2022).  
950 Prevalence and mechanisms of environmental hyperoxia-induced thermal tolerance in  
951 fishes. *Proceedings of the Royal Society B: Biological Sciences*, 289(1981),  
952 20220840. <https://doi.org/doi:10.1098/rspb.2022.0840>

953 Miller, S. C., Reeb, S. E., Wright, P. A., & Gillis, T. E. (2008). Oxygen concentration in the  
954 water boundary layer next to rainbow trout (*Oncorhynchus mykiss*) embryos is  
955 influenced by hypoxia exposure time, metabolic rate, and water flow. *Canadian*  
956 *Journal of Fisheries and Aquatic Sciences*, 65(10), 2170-2177.  
957 <https://doi.org/10.1139/f08-123>

958 Morgan, R., Andreassen, A. H., Åsheim, E. R., Finnøen, M. H., Dresler, G., Brembu, T., Loh,  
959 A., Miest, J. J., & Jutfelt, F. (2022). Reduced physiological plasticity in a fish adapted  
960 to stable temperatures. *Proceedings of the National Academy of Sciences*, 119(22),  
961 e2201919119. <https://doi.org/doi:10.1073/pnas.2201919119>

962 Morgan, R., Sundin, J., Finnøen, M. H., Dresler, G., Vendrell, M. M., Dey, A., Sarkar, K., &  
963 Jutfelt, F. (2019). Are model organisms representative for climate change research?  
964 Testing thermal tolerance in wild and laboratory zebrafish populations. *Conservation*  
965 *Physiology*, 7(1). <https://doi.org/10.1093/conphys/coz036>

966 Mueller, C. A., Joss, J. M. P., & Seymour, R. S. (2011). Effects of environmental oxygen on  
967 development and respiration of Australian lungfish (*Neoceratodus forsteri*) embryos.  
968 *Journal of Comparative Physiology B*, 181(7), 941-952.  
969 <https://doi.org/10.1007/s00360-011-0573-3>

970 Myrvold, S. L. (2020). *Effect of temperature on the settling rate, survival, ingestion rate and*  
971 *biochemical composition of the polyp stages of A. aurita* [Master's thesis, Norwegian  
972 University of Science and Technology].

973 Negrete, B., Jr, Ackerly, K. L., & Esbaugh, A. J. (2024). Implications of chronic hypoxia  
974 during development in red drum. *Journal of Experimental Biology*, 227(16).  
975 <https://doi.org/10.1242/jeb.247618>

- 976 Noble, D. W. A., Stenhouse, V., & Schwanz, L. E. (2018). Developmental temperatures and  
977 phenotypic plasticity in reptiles: a systematic review and meta-analysis. *Biological*  
978 *Reviews*, 93(1), 72-97. <https://doi.org/https://doi.org/10.1111/brv.12333>
- 979 Pörtner, H.-O. (2010). Oxygen- and capacity-limitation of thermal tolerance: a matrix for  
980 integrating climate-related stressor effects in marine ecosystems. *Journal of*  
981 *Experimental Biology*, 213(6), 881-893. <https://doi.org/10.1242/jeb.037523>
- 982 Pörtner, H.-O., Bock, C., & Mark, F. C. (2017). Oxygen- and capacity-limited thermal  
983 tolerance: bridging ecology and physiology. *Journal of Experimental Biology*,  
984 220(15), 2685-2696. <https://doi.org/10.1242/jeb.134585>
- 985 Pottier, P., Burke, S., Drobniak, S. M., & Nakagawa, S. (2022). Methodological  
986 inconsistencies define thermal bottlenecks in fish life cycle: a comment on Dahlke et  
987 al. 2020. *Evolutionary Ecology*, 36(2), 287-292. <https://doi.org/10.1007/s10682-022-10157-w>
- 989 Raby, G. D., De Bonville, J., Reynolds, L., Storm, Z., Cowan, Z.-L., Metz, M., Andreassen,  
990 A. H., Pfeufer, L., Lechner, E. R., Stewart, E. M. C., Leeuwis, R. H. J., Ern, R., Silva-  
991 Garay, L., Skeeles, M. R., Roche, D. G., Morgan, R., Green, L., Speers-Roesch, B.,  
992 Mills, S. C., . . . Jutfelt, F. (2025). Oxygen supersaturation has negligible effects on  
993 warming tolerance across diverse aquatic ectotherms. *PLOS Biology*, 23(11),  
994 e3003413. <https://doi.org/10.1371/journal.pbio.3003413>
- 995 Rombough, P. J. (1989). Oxygen conductance values and structural characteristics of the egg  
996 capsules of pacific salmonids. *Comparative Biochemistry and Physiology Part A:*  
997 *Physiology*, 92(3), 279-283. [https://doi.org/https://doi.org/10.1016/0300-9629\(89\)90564-1](https://doi.org/https://doi.org/10.1016/0300-9629(89)90564-1)
- 999 Rombough, P. J. (1999). The gill of fish larvae. Is it primarily a respiratory or an  
1000 ionoregulatory structure? *Journal of Fish Biology*, 55(sA), 186-204.  
1001 <https://doi.org/https://doi.org/10.1111/j.1095-8649.1999.tb01055.x>
- 1002 Schirone, R. C., & Gross, L. (1968). Effect of temperature on early embryological  
1003 development of the zebra fish, *Brachydanio rerio*. *Journal of Experimental Zoology*,  
1004 169(1), 43-52. <https://doi.org/https://doi.org/10.1002/jez.1401690106>
- 1005 Schnurr, M. E., Yin, Y., & Scott, G. R. (2014). Temperature during embryonic development  
1006 has persistent effects on metabolic enzymes in the muscle of zebrafish. *Journal of*  
1007 *Experimental Biology*, 217(8), 1370-1380. <https://doi.org/10.1242/jeb.094037>
- 1008 Scott, G. R., & Johnston, I. A. (2012). Temperature during embryonic development has  
1009 persistent effects on thermal acclimation capacity in zebrafish. *Proceedings of the*  
1010 *National Academy of Sciences*, 109(35), 14247-14252.  
1011 <https://doi.org/10.1073/pnas.1205012109>
- 1012 Shumway, D. L., Warren, C. E., & Doudoroff, P. (1964). Influence of oxygen concentration  
1013 and water movement on the growth of steelhead trout and coho salmon embryos.  
1014 *Transactions of the American Fisheries Society*, 93(4), 342-356.  
1015 [https://doi.org/10.1577/1548-8659\(1964\)93\[342:Ioocaw\]2.0.Co;2](https://doi.org/10.1577/1548-8659(1964)93[342:Ioocaw]2.0.Co;2)
- 1016 Silva-Garay, L., Ern, R., Andreassen, A. H., Reiersen, M., & Jutfelt, F. (2025). No oxygen  
1017 limitation of upper thermal tolerance in zebrafish regardless of acclimation  
1018 temperature. *Journal of Thermal Biology*, 131, 104157.  
1019 <https://doi.org/https://doi.org/10.1016/j.jtherbio.2025.104157>
- 1020 Skeeles, M. R., Scheuffele, H., & Clark, T. D. (2022). Chronic experimental hyperoxia  
1021 elevates aerobic scope: a valid method to test for physiological oxygen limitations in  
1022 fish. *Journal of Fish Biology*, 101(6), 1595-1600.  
1023 <https://doi.org/https://doi.org/10.1111/jfb.15213>

1024 Sunday, J. M., Bates, A. E., & Dulvy, N. K. (2012). Thermal tolerance and the global  
1025 redistribution of animals. *Nature Climate Change*, 2(9), 686-690.  
1026 <https://doi.org/10.1038/nclimate1539>

1027 Teletchea, F., & Pauly, D. (2024). Why do fish larvae hatch when they do? *Environmental*  
1028 *Biology of Fishes*, 107(5), 583-591. <https://doi.org/10.1007/s10641-024-01553-y>

1029 Thomas, W. H., Scotten, H. L., & Bradshaw, J. S. (1963). Thermal gradient incubators for  
1030 small aquatic organisms *Limnology and Oceanography*, 8(3), 357-360.  
1031 <https://doi.org/https://doi.org/10.4319/lo.1963.8.3.0357>

1032 Tunç, A., Erdoğan, O., Vural, O., & Aksakal, E. (2025). Impact of acute and long-term  
1033 hypoxia and hyperoxia on antioxidant metabolism and gene expression in juvenile  
1034 rainbow trout (*Oncorhynchus mykiss*). *Aquaculture Research*, 2025(1), 6628284.  
1035 <https://doi.org/https://doi.org/10.1155/are/6628284>

1036 Urushibata, H., Sasaki, K., Takahashi, E., Hanada, T., Fujimoto, T., Arai, K., & Yamaha, E.  
1037 (2021). Control of developmental speed in zebrafish embryos using different  
1038 incubation temperatures. *Zebrafish*, 18(5), 316-325.  
1039 <https://doi.org/10.1089/zeb.2021.0022>

1040 Warkentin, K. M. (2007). Oxygen, gills, and embryo behavior: mechanisms of adaptive  
1041 plasticity in hatching. *Comparative Biochemistry and Physiology Part A: Molecular*  
1042 *& Integrative Physiology*, 148(4), 720-731.  
1043 <https://doi.org/https://doi.org/10.1016/j.cbpa.2007.02.009>

1044 Warkentin, K. M. (2011). Environmentally cued hatching across taxa: embryos respond to  
1045 risk and opportunity. *Integrative and Comparative Biology*, 51(1), 14-25.  
1046 <https://doi.org/10.1093/icb/icr017>

1047 Wells, P. R., & Pinder, A. W. (1996). The respiratory development of atlantic salmon: I.  
1048 morphometry of gills, yolk sac and body surface. *Journal of Experimental Biology*,  
1049 199(12), 2725-2736. <https://doi.org/10.1242/jeb.199.12.2725>

1050 Wood, A. T., Clark, T. D., Elliott, N. G., Frappell, P. B., & Andrewartha, S. J. (2019).  
1051 Physiological effects of dissolved oxygen are stage-specific in incubating Atlantic  
1052 salmon (*Salmo salar*). *Journal of Comparative Physiology B*, 189(1), 109-120.  
1053 <https://doi.org/10.1007/s00360-018-1199-5>

1054  
1055  
1056  
1057  
1058  
1059  
1060  
1061  
1062  
1063  
1064  
1065  
1066  
1067  
1068  
1069  
1070  
1071  
1072  
1073

1074 **Supporting Information for**

1075

1076

1077 Oxygen limitation is not a major physiological mechanism restricting early life development  
1078 in zebrafish

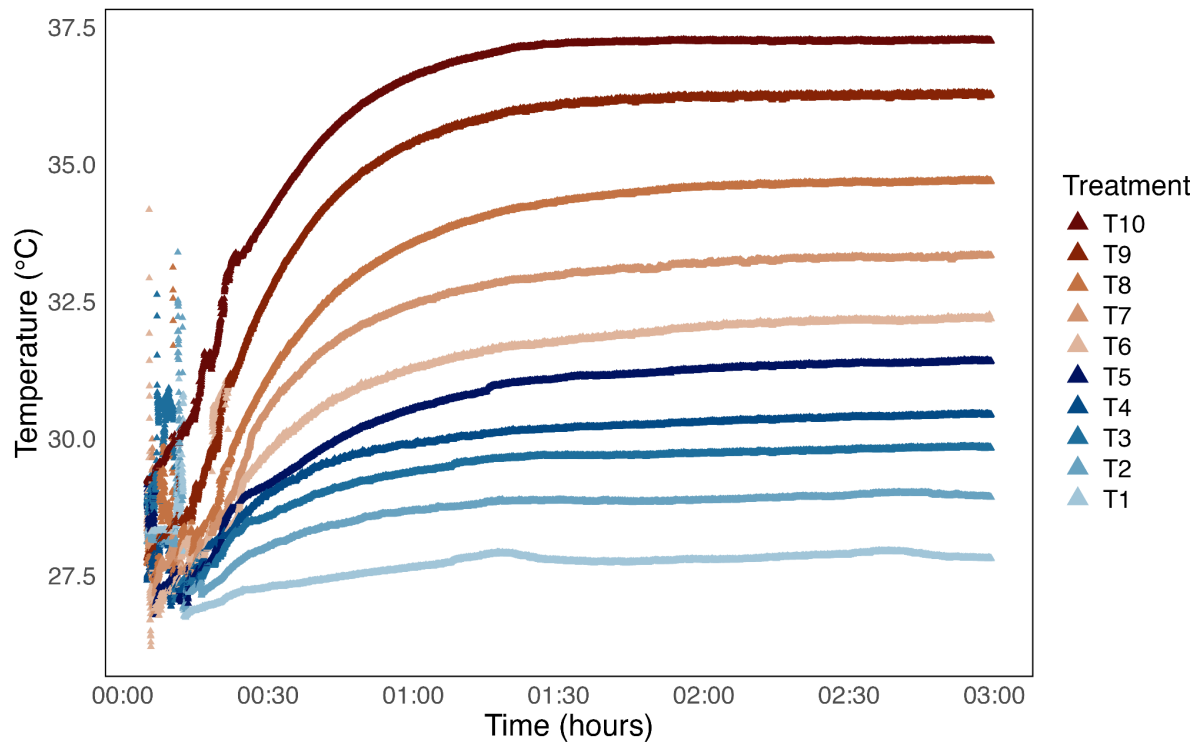
1079

1080

1081

1082

1083



1084

1085 **Fig. S1: Heating rate across treatments in the thermal gradient table.**

1086 Heating rate ( $^{\circ}\text{C h}^{-1}$ ) over time in beakers used in *Experiment 2*. Treatments differ by color  
1087 and correspond to distinct temperature change profiles established in the thermal gradient  
1088 table.

1089

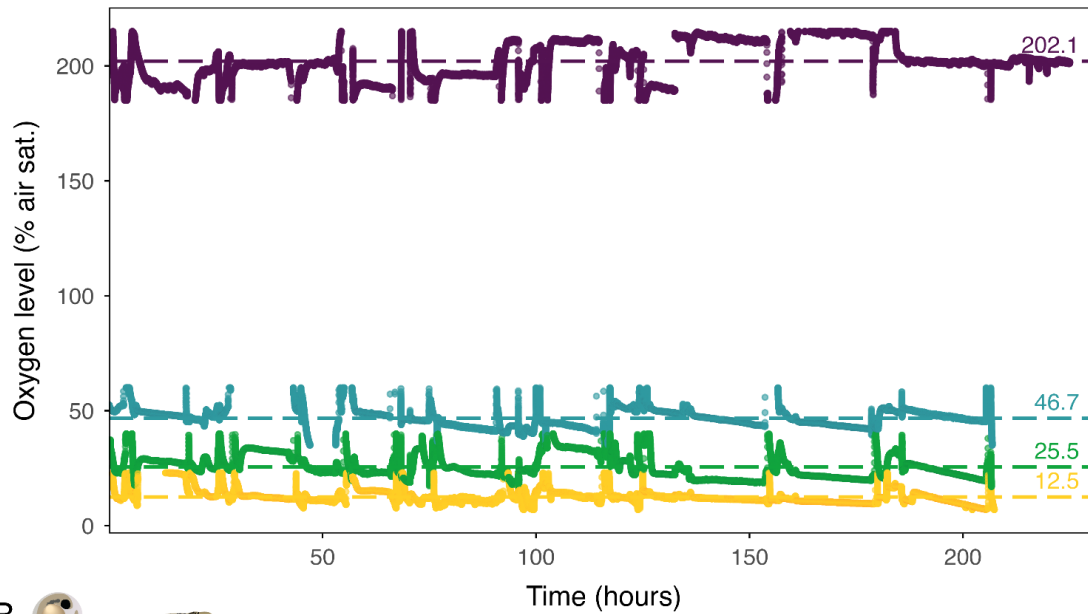
1090

1091



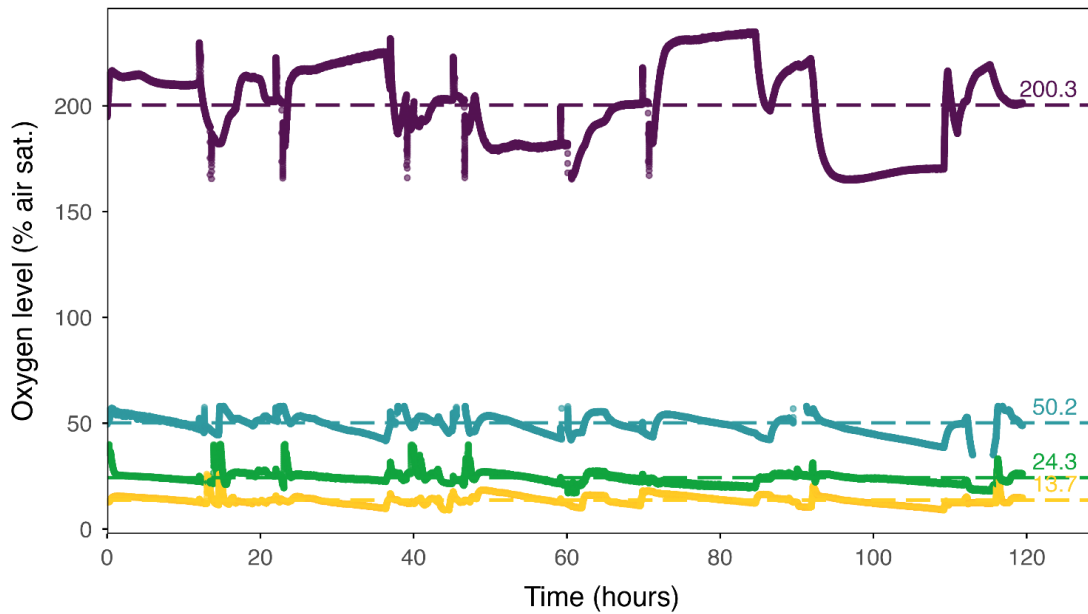
A

Experiment 1: Recording Of Oxygen Level Over Time



B

Experiment 2: Recording Of Oxygen Level Over Time



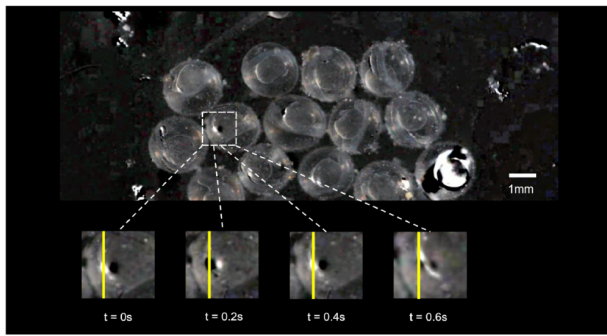
Oxygen level (% air sat.) — 12.5 — 25 — 50 — 200

1092  
1093  
1094  
1095

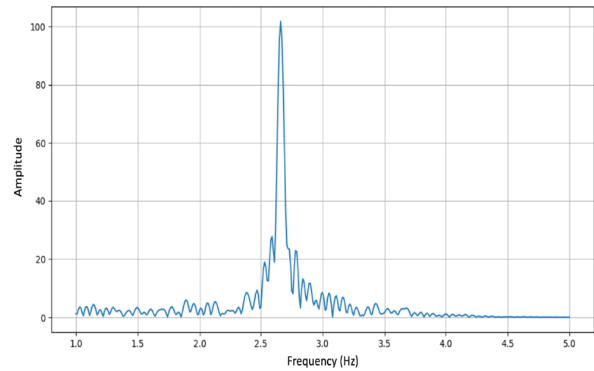
**Fig. S2: Oxygen records over the total experimental time (in hours) of *Experiment 1* and *Experiment 2*.** Raw data and means of the target oxygen treatments during experiments are depicted in colors. *Experiment 1* lasted ~ 10 days and *Experiment 2* lasted ~ 6 days.

**A**

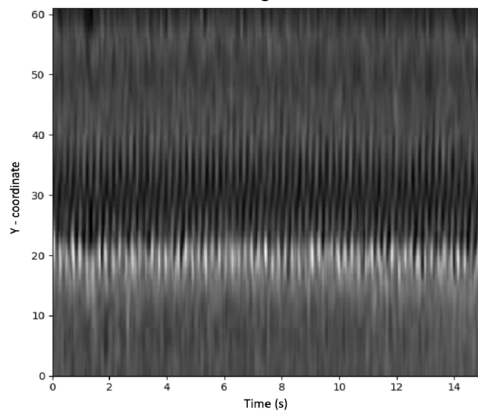
Selected region of interest - vertical scan line of embryo heartbeat

**C**

Frequency spectrum using Fast Fourier Transform

**B**

Vertical scan line of magnified video over time



1096

1097

1098

1099

1100

1101

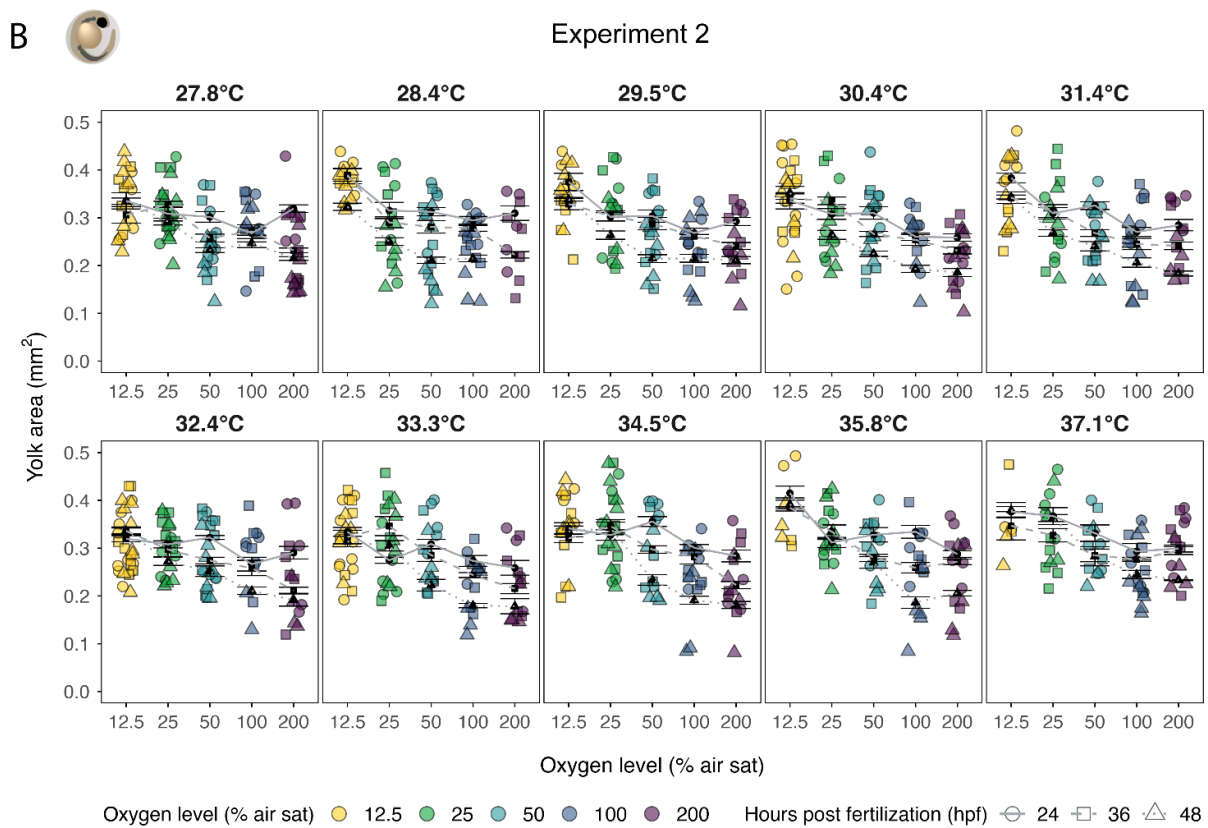
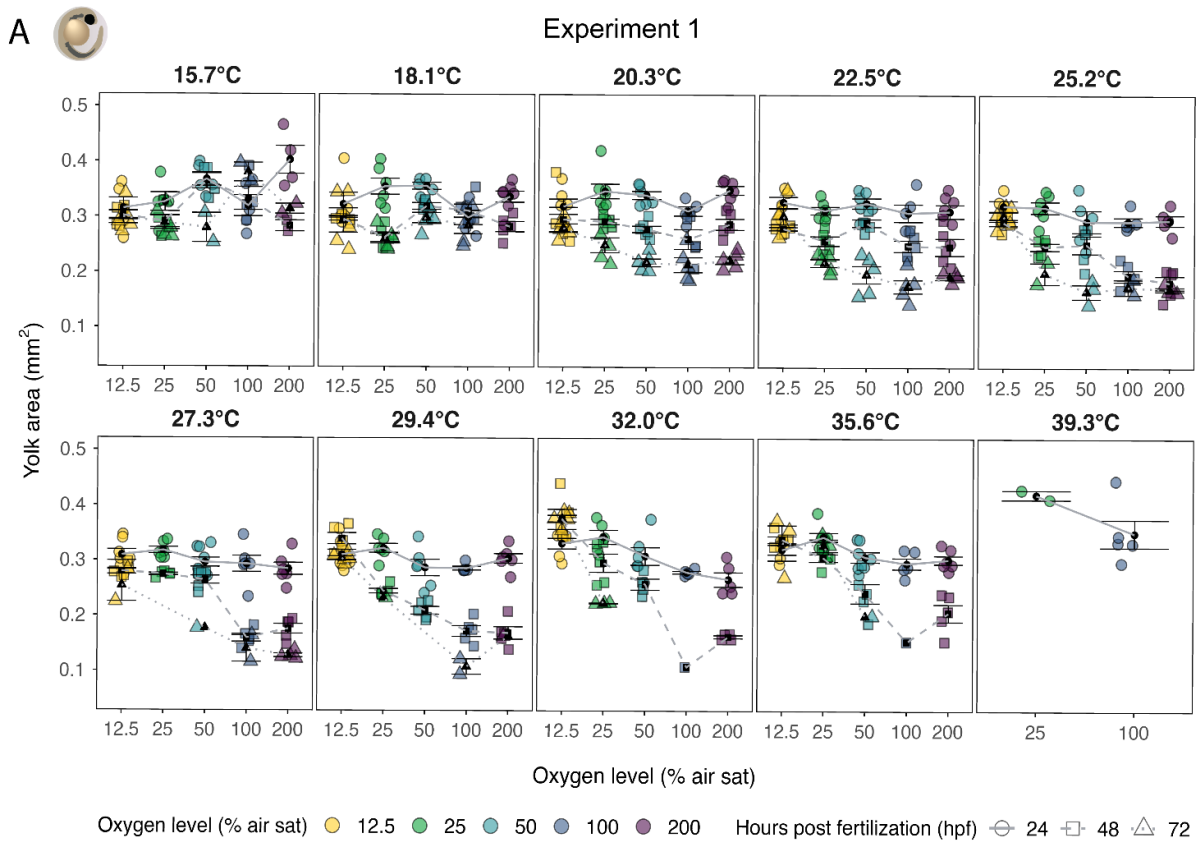
1102

1103

1104

**Fig. S3: Measurement of heart rate in zebrafish embryos using Eulerian video**

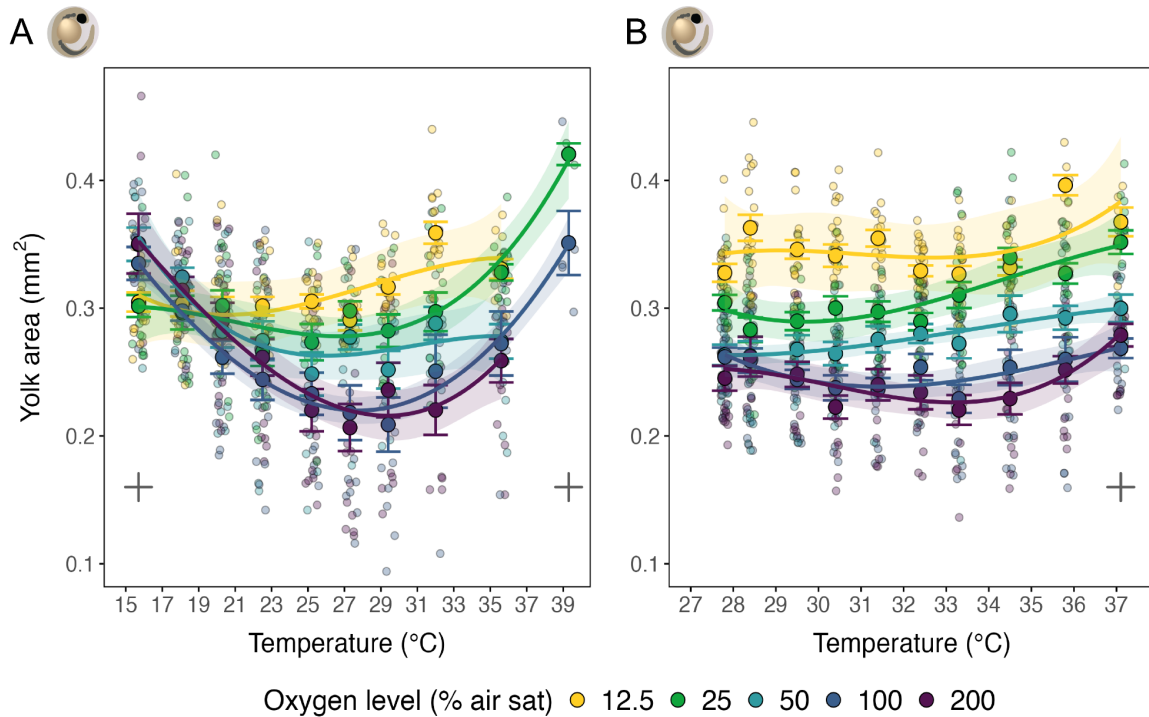
**magnification. (A)** Cropped video frame showing the embryonic heart of *Danio rerio*. The yellow vertical line marks the region where the heartbeat is most visible across the recording, with periodic pixel contrast shifts (white to black) reflecting heartbeat frequency. **(B)** Time-series plot of pixel contrast variation along the yellow line over a 15 s recording, capturing rhythmic heartbeat oscillations. **(C)** Frequency spectrum derived from the same region using a Fast Fourier Transform, showing the dominant heartbeat frequency (Hz). A sharp amplitude peak indicates a strong signal with low noise and a stable heart rate.



1105  
1106  
1107  
1108  
1109

**Fig. S4: Yolk sac area of zebrafish embryos across temperature, oxygen, and developmental time.** Yolk sac area ( $\text{mm}^2$ ) of *Danio rerio* embryos across oxygen levels (colors) and temperatures (vertical panels) over time post-fertilization. Measurements were

1110 taken at 24, 48, and 72 hpf in *Experiment 1*, and at 24, 36, and 48 hpf in *Experiment 2*. Data  
 1111 points represent individual embryos; black triangles indicate group means  $\pm$  s.e., and grey  
 1112 dashed lines connect mean values across sampling times.  
 1113



1114  
 1115 **Fig. S5: Yolk sac area (mm<sup>2</sup>) of zebrafish embryos across temperatures (x-axis) and**  
 1116 **oxygen levels (colors) in *Experiment 1* (A; n = 2–9) and *Experiment 2* (B; n = 2–11).** Points  
 1117 show individual embryos; colored circles indicate means  $\pm$  s.e., and colored lines indicating  
 1118 second-degree polynomial fits.  
 1119

1120  
 1121 **Table S1: Yolk sac consumption (%) of zebrafish embryos across temperature, oxygen,**  
 1122 **and developmental time in *Experiment 1*.** Anova (type III) and linear model (LM) includes  
 1123 oxygen level, temperature centered to 15.7 °C (Temp<sub>1</sub>), and its quadratic term (Temp<sub>2</sub>), their  
 1124 interaction, and developmental time (hpf): Yolk consumption  $\sim$  O<sub>2</sub> + Temp<sub>1</sub> + Temp<sub>2</sub> +  
 1125 O<sub>2</sub>×Temp<sub>1</sub> + O<sub>2</sub>×Temp<sub>2</sub> + hpf. Significance was assessed relative to 15.7 °C and 100% air  
 1126 saturation. Estimates ( $\beta$ ), standard errors (SE), t-values, and p-values are shown for each  
 1127 predictor.  
 1128

<i>Parameters (Anova, type III)</i>	<i>Sum Squares</i>	<i>Df</i>	<i>F-value</i>	<i>P-value</i>
(Intercept)	581	1	6.4054	0.0116*
O <sub>2</sub>	1688	4	4.6523	0.0011**
Temp <sub>1</sub>	11172	1	123.1568	< 0.0001 ***
Temp <sub>2</sub>	8455	1	93.2098	< 0.0001 ***
O <sub>2</sub> :Temp <sub>1</sub>	5232	4	14.4203	< 0.0001 ***
O <sub>2</sub> :Temp <sub>2</sub>	2006	4	5.5294	0.0002***

hpf	37213	1	410.2245	< 0.0001 ***
Residuals	53975	595		
<i>Parameters (LM)</i>	<i>Estimate (B)</i>	<i>Std. Error</i>	<i>t-value</i>	<i>P-value</i>
(Intercept)	-5.860	2.315	-2.531	0.012 *
O <sub>2</sub> (12.5%)	7.661	2.879	2.661	0.008 **
O <sub>2</sub> (25%)	6.136	2.853	2.151	0.032 *
O <sub>2</sub> (50%)	-2.182	3.021	-0.722	0.470
O <sub>2</sub> (200%)	-1.163	3.292	-0.353	0.724
Temp <sub>1</sub>	5.014	0.452	11.098	< 0.0001 ***
Temp <sub>2</sub>	-0.195	0.020	-9.655	< 0.0001 ***
hpf	0.429	0.021	20.254	< 0.0001 ***
O <sub>2</sub> (12.5%):Temp <sub>1</sub>	-4.391	0.648	-6.779	< 0.0001 ***
O <sub>2</sub> (25%):Temp <sub>1</sub>	-2.675	0.635	-4.215	< 0.0001 ***
O <sub>2</sub> (50%):Temp <sub>1</sub>	-1.341	0.678	-1.978	0.048 *
O <sub>2</sub> (200%):Temp <sub>1</sub>	-0.410	0.720	-0.568	0.570
O <sub>2</sub> (12.5%):Temp <sub>2</sub>	0.140	0.031	4.571	< 0.0001 ***
O <sub>2</sub> (25%):Temp <sub>2</sub>	0.073	0.029	2.502	0.013 *
O <sub>2</sub> (50%):Temp <sub>2</sub>	0.064	0.032	2.011	0.045 *
O <sub>2</sub> (200%):Temp <sub>2</sub>	0.035	0.033	1.051	0.294
Residual standard error:		9.524 on 595 degrees of freedom		
Multiple R-squared:		0.6189		
F-statistic:		64.41 on 15 and 595 DF, p-value: < 0.001 ***		

1129  
1130  
1131  
1132  
1133  
1134  
1135  
1136  
1137

**Table S2: Yolk sac consumption (%) of zebrafish embryos across temperature, oxygen, and developmental time in *Experiment 2*.** Anova (type III) and linear model (LM) includes oxygen level, temperature centered to 27.8 °C (Temp<sub>1</sub>), and its quadratic term (Temp<sub>2</sub>), their interaction, and developmental time (hpf): Yolk consumption ~ O<sub>2</sub> + Temp<sub>1</sub> + Temp<sub>2</sub> + O<sub>2</sub>×Temp<sub>1</sub> + O<sub>2</sub>×Temp<sub>2</sub> + hpf. Significance was assessed relative to 27.8 °C and 100% air saturation. Estimates (β), standard errors (SE), t-values, and p-values are shown for each predictor.

<i>Parameters (Anova, type III)</i>	<i>Sum Squares</i>	<i>Df</i>	<i>F-value</i>	<i>P-value</i>
(Intercept)	7128	1	118.067	< 0.0001 ***

O <sub>2</sub>	13295	4	55.053	< 0.0001 ***
Temp <sub>1</sub>	828	1	13.718	0.0002***
Temp <sub>2</sub>	1046	1	17.325	0.00003***
O <sub>2</sub> :Temp <sub>1</sub>	1288	4	5.334	0.0003***
O <sub>2</sub> :Temp <sub>2</sub>	811	4	3.359	0.0097**
hpf	21395	1	354.368	< 0.0001 ***
Residuals	48482	803		

<i>Parameters (LM)</i>	<i>Estimate (B)</i>	<i>Std. Error</i>	<i>t value</i>	<i>P-value</i>
(Intercept)	18.766	1.727	10.866	< 0.0001 ***
O <sub>2</sub> (12.5%)	-21.622	1.907	-11.336	< 0.0001 ***
O <sub>2</sub> (25%)	-8.598	1.910	-4.503	< 0.0001 ***
O <sub>2</sub> (50%)	0.032	1.918	0.016	0.987
O <sub>2</sub> (200%)	1.702	1.955	0.871	0.384
Temp <sub>1</sub>	2.745	0.741	3.704	0.0002 ***
Temp <sub>2</sub>	-0.325	0.078	-4.162	< 0.0001 ***
hpf	0.520	0.028	18.825	< 0.0001 ***
O <sub>2</sub> (12.5%):Temp <sub>1</sub>	-0.245	1.031	-0.238	0.812
O <sub>2</sub> (25%):Temp <sub>1</sub>	-1.975	1.012	-1.952	0.051
O <sub>2</sub> (50%):Temp <sub>1</sub>	-3.399	1.024	-3.320	0.001 **
O <sub>2</sub> (200%):Temp <sub>1</sub>	0.625	1.042	0.600	0.549
O <sub>2</sub> (12.5%):Temp <sub>2</sub>	0.008	0.116	0.073	0.942
O <sub>2</sub> (25%):Temp <sub>2</sub>	0.087	0.109	0.798	0.425
O <sub>2</sub> (50%):Temp <sub>2</sub>	0.296	0.110	2.687	0.007 **
O <sub>2</sub> (200%):Temp <sub>2</sub>	-0.079	0.111	-0.716	0.474

Residual standard error: 7.77 on 803 degrees of freedom

Multiple R-squared: 0.659

F-statistic: 103.2 on 15 and 803 DF, p-value: < 0.001 \*\*\*

Adjusted R-squared: 0.652

1140 **Table S3: Heart rate of zebrafish embryos across temperature, oxygen, and**  
 1141 **developmental time in *Experiment 2*.** Anova (type III) and linear model (LM) includes  
 1142 oxygen level, temperature centered to 27.8 °C (Temp<sub>1</sub>), and its quadratic term (Temp<sub>2</sub>), their  
 1143 interaction, and developmental time (hpf): Heart rate ~ O<sub>2</sub> + Temp<sub>1</sub> + Temp<sub>2</sub> + O<sub>2</sub>×Temp<sub>1</sub> +  
 1144 O<sub>2</sub>×Temp<sub>2</sub> + hpf. Significance was assessed relative to 27.8 °C and 100% air saturation.  
 1145 Estimates (β), standard errors (SE), t-values, and p-values are shown for each predictor.  
 1146

<i>Parameters (Anova, type III)</i>	<i>Sum Squares</i>	<i>Df</i>	<i>F-value</i>	<i>p-value</i>
(Intercept)	379095	1	219.751	< 0.0001 ***
O <sub>2</sub>	338503	4	49.055	< 0.0001 ***
Temp <sub>1</sub>	47756	1	27.683	< 0.0001 ***
Temp <sub>2</sub>	48746	1	28.256	< 0.0001 ***
O <sub>2</sub> :Temp <sub>1</sub>	13286	4	1.925	0.1042
O <sub>2</sub> :Temp <sub>2</sub>	11686	4	1.693	0.1494
hpf	748588	1	433.935	< 0.0001 ***
Residuals	1511201	876		

<i>Parameters (LM)</i>	<i>Estimate (B)</i>	<i>Std. Error</i>	<i>t-value</i>	<i>p-value</i>
(Intercept)	109.803	7.407	14.824	< 0.0001 ***
O <sub>2</sub> (12.5%)	-96.197	8.723	-11.028	< 0.0001 ***
O <sub>2</sub> (25%)	-19.152	8.914	-2.149	0.0319*
O <sub>2</sub> (50%)	2.098	9.916	0.212	0.8325
O <sub>2</sub> (200%)	11.082	9.209	1.203	0.2291
Temp <sub>1</sub>	19.596	3.724	5.261	< 0.0001 ***
Temp <sub>2</sub>	-2.193	0.413	-5.316	< 0.0001 ***
hpf	1.628	0.078	20.831	< 0.0001 ***
O <sub>2</sub> (12.5%):Temp <sub>1</sub>	2.775	5.770	0.481	0.6307
O <sub>2</sub> (25%):Temp <sub>1</sub>	-5.969	5.448	-1.096	0.2736
O <sub>2</sub> (50%):Temp <sub>1</sub>	-12.959	5.837	-2.220	0.0267*
O <sub>2</sub> (200%):Temp <sub>1</sub>	-4.209	5.202	-0.809	0.4187
O <sub>2</sub> (12.5%):Temp <sub>2</sub>	-0.301	0.842	-0.357	0.7208
O <sub>2</sub> (25%):Temp <sub>2</sub>	-0.211	0.658	-0.321	0.7481
O <sub>2</sub> (50%):Temp <sub>2</sub>	1.435	0.669	2.144	0.0323*
O <sub>2</sub> (200%):Temp <sub>2</sub>	0.182	0.573	0.318	0.7504

---

Residual standard error: 41.53 on 876 degrees of freedom

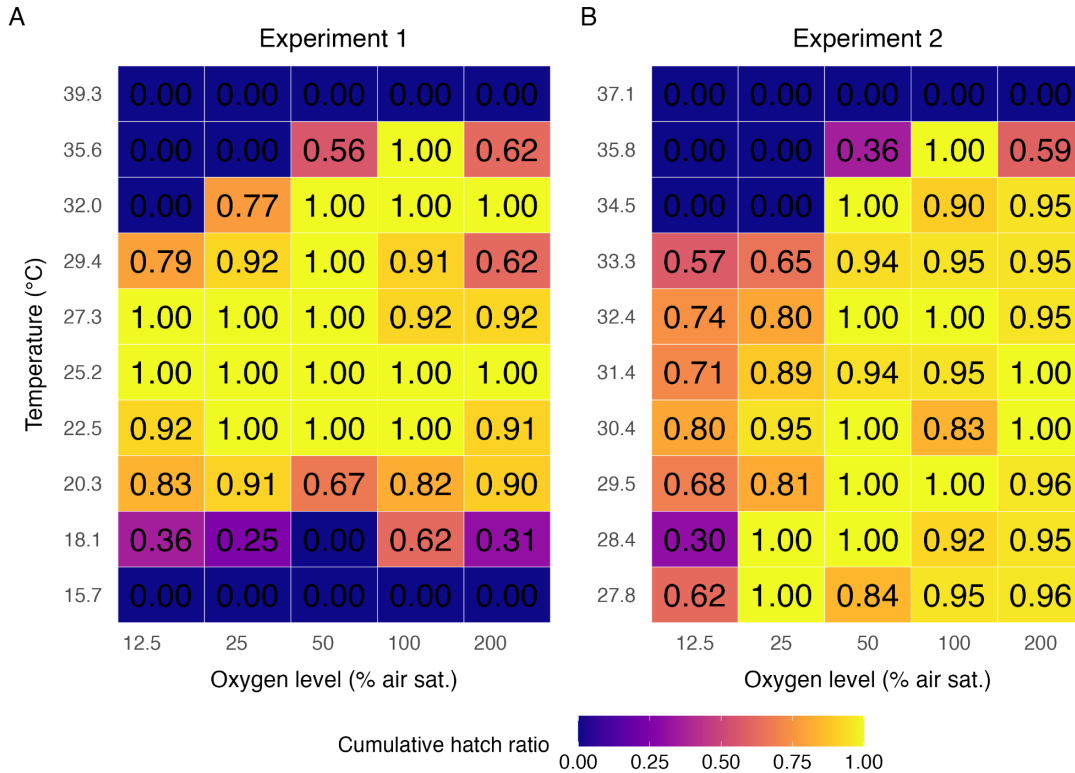
Multiple R-squared: 0.4287

F-statistic: 43.82 on 15 and 876 DF, p-value: < 0.0001 \*\*\*

Adjusted R-squared: 0.587

---

1147



1148

1149

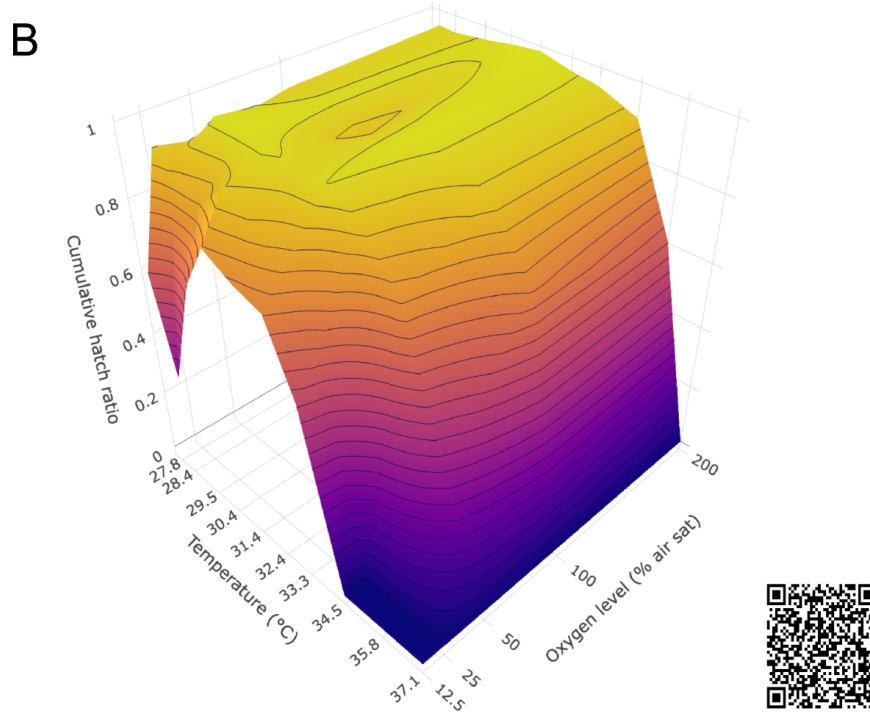
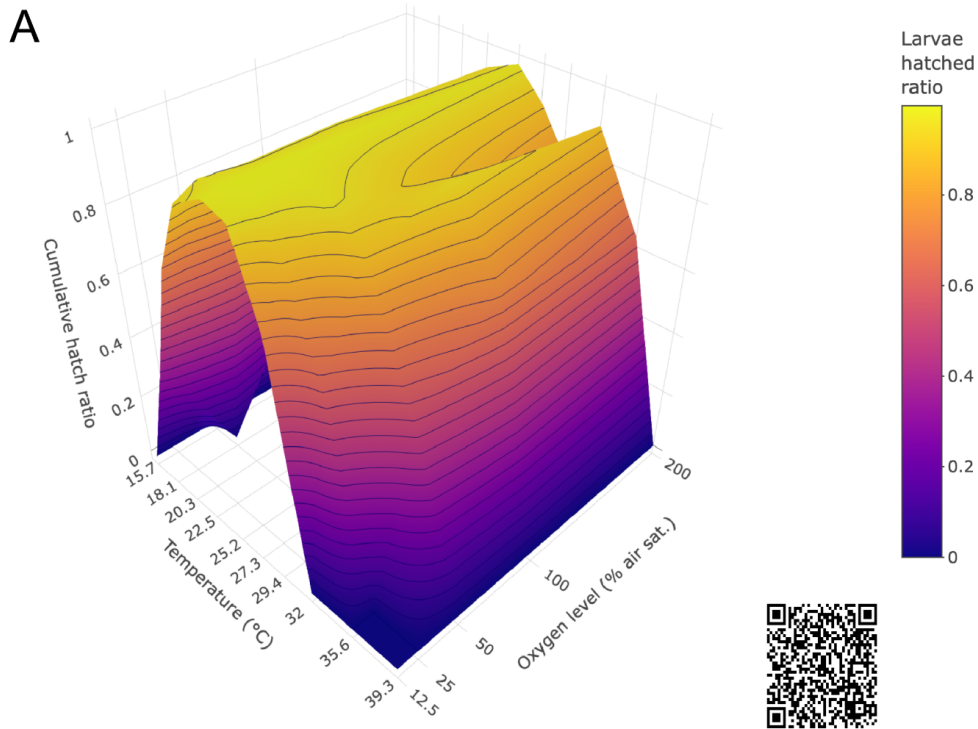
1150

1151

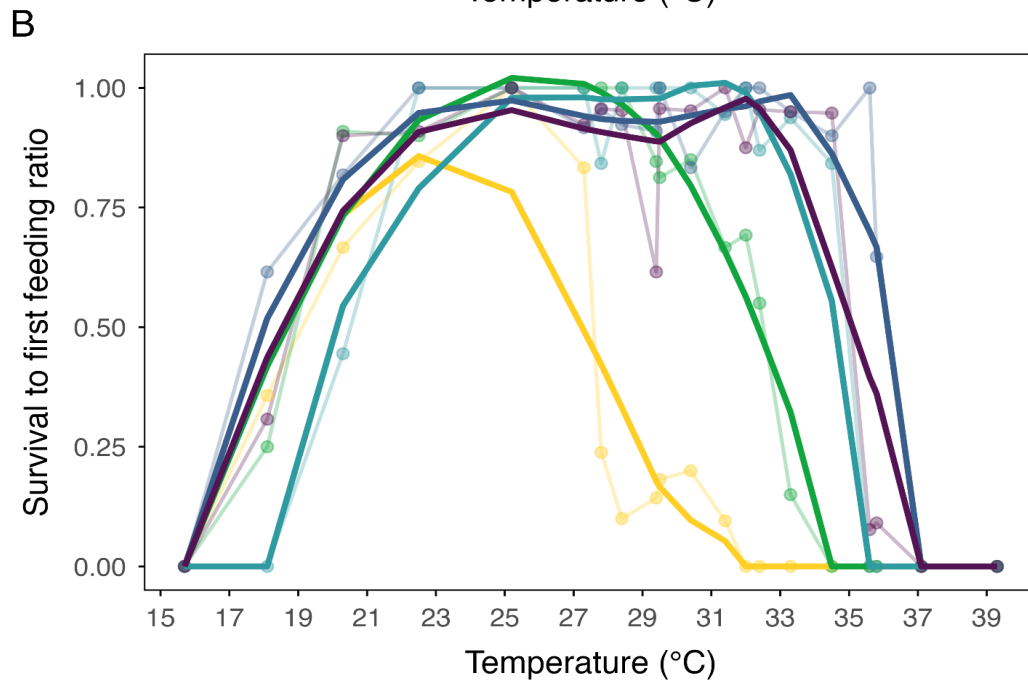
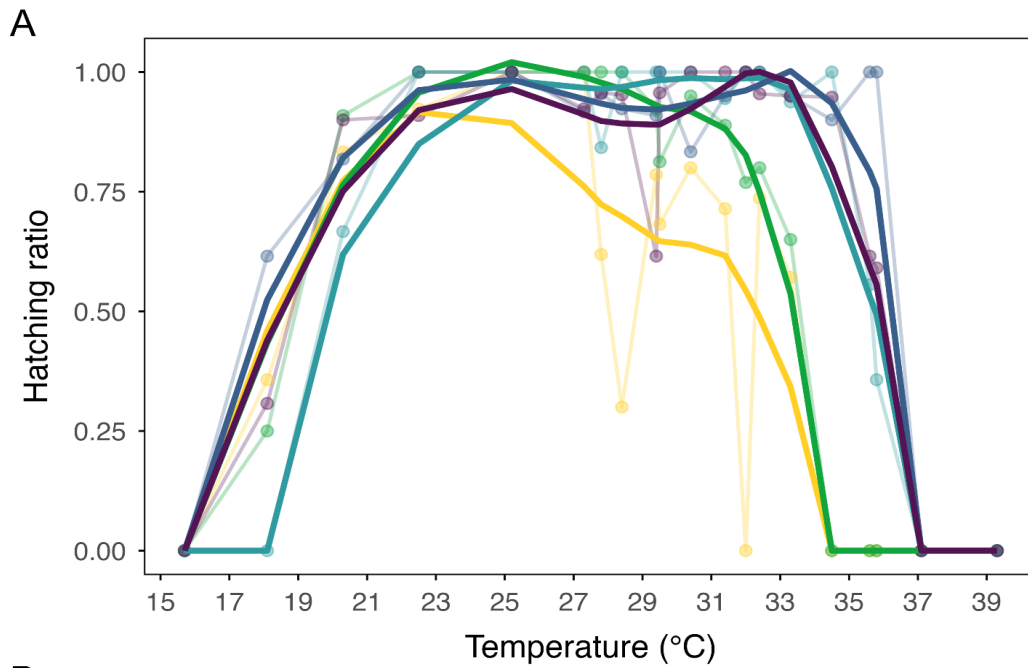
1152

1153

**Fig. S6: Heat map of maximum hatching number across temperature and oxygen treatments.** Heat map showing the accumulated maximum number of hatched *Danio rerio* embryos per temperature and oxygen treatment in (A) *Experiment 1* and (B) *Experiment 2*. Lighter colors (yellow) indicate higher hatching rates.



1154  
 1155 **Fig. S7: Three-dimensional surface plot of cumulative hatching across temperature and**  
 1156 **oxygen treatments.** 3D surface plots showing cumulative hatching of *Danio rerio* larvae  
 1157 across temperature and oxygen levels in (A) *Experiment 1* and (B) *Experiment 2*. Cumulative  
 1158 hatching values are based on observed data. Survival ratios above 0.6 were smoothed using a  
 1159 kernel-based normalization. (function `image.smoother`, `aRange = 0.75`, `theta = 0.75`, `fields`  
 1160 `package`, R), preventing overfitting when hatching nears zero at the extreme temperatures.  
 1161  
 1162



Oxygen level (% air saturation) — 12.5 — 25 — 50 — 100 — 200

1163  
1164  
1165  
1166  
1167  
1168  
1169

**Fig. S8: Thermal performance curve (TPC) of hatching success (A) and survival to first feeding (B) across temperature and oxygen levels.** Points depict maximum hatching ratio per temperature, and TPC lines were fitted using a smoothed maxima *LOESS* function (span = 0.6).

1170  
1171  
1172  
1173  
1174

**Table S4: Effect of oxygen, temperature, and developmental time on hatching success in *Experiment 1*.** GLM includes oxygen level, temperature centered to 18.1 °C (Temp<sub>1</sub>, lowest temperature at which hatching occurred), and its quadratic term (Temp<sub>2</sub>), their interaction, and log-transformed developmental time (hpf): Hatching success ~ O<sub>2</sub> + Temp<sub>1</sub> + Temp<sub>2</sub> + O<sub>2</sub>×Temp<sub>1</sub> + O<sub>2</sub>×Temp<sub>2</sub> + log(hpf) + (1 | Experiment). Significance is shown first with

1175 oxygen as numeric relative to 18.1 °C and subsequently relative to 100% air saturation.  
 1176 Estimates ( $\beta$ ), standard errors (SE), z-values, and p-values are shown for each predictor.  
 1177

<i>Parameters (GLM)</i>	<i>Estimate (B)</i>	<i>Std. Error</i>	<i>z-value</i>	<i>p-value</i>
(Intercept)	-24.4100	0.6950	-35.128	< 0.0001 ***
O <sub>2</sub>	-0.0004	0.0015	-0.288	0.773
Temp <sub>1</sub>	1.3150	0.0484	27.195	< 0.0001 ***
Temp <sub>2</sub>	-0.0665	0.0027	-24.564	< 0.0001 ***
O <sub>2</sub> :Temp <sub>1</sub>	-0.0017	0.0004	-4.380	0.00001
O <sub>2</sub> :Temp <sub>2</sub>	0.0002	0.0000	7.263	< 0.0001 ***
log(hpf)	4.3400	0.1289	33.654	< 0.0001 ***
Null deviance:		6068.2 on 563 degrees of freedom		
Residual deviance:		1498.8 on 557 degrees of freedom		
AIC:		1959		
Num.Fisher Scoring iterations:		3		
<i>Parameters (GLM)</i>	<i>Estimate (B)</i>	<i>Std. Error</i>	<i>z-value</i>	<i>p-value</i>
(Intercept)	-30.6686	0.9320	-32.905	< 0.0001 ***
O <sub>2</sub> (12.5%)	-1.1127	0.3523	-3.159	0.0016 **
O <sub>2</sub> (25%)	-1.0823	0.3568	-3.033	0.0024 **
O <sub>2</sub> (50%)	-3.1413	0.4516	-6.956	< 0.0001 ***
O <sub>2</sub> (200%)	-0.6648	0.3208	-2.072	0.0382 *
Temp <sub>1</sub>	1.0536	0.0597	17.661	< 0.0001 ***
Temp <sub>2</sub>	-0.0306	0.0030	-10.160	< 0.0001 ***
O <sub>2</sub> (12.5%):Temp <sub>1</sub>	1.0454	0.1155	9.048	< 0.0001 ***
O <sub>2</sub> (25%):Temp <sub>1</sub>	0.9531	0.1106	8.615	< 0.0001 ***
O <sub>2</sub> (50%):Temp <sub>1</sub>	0.9264	0.1129	8.206	< 0.0001 ***
O <sub>2</sub> (200%):Temp <sub>1</sub>	0.1588	0.0833	1.907	0.0565 ·
O <sub>2</sub> (12.5%):Temp <sub>2</sub>	-0.1072	0.0081	-13.310	< 0.0001 ***
O <sub>2</sub> (25%):Temp <sub>2</sub>	-0.0774	0.0069	-11.194	< 0.0001 ***
O <sub>2</sub> (50%):Temp <sub>2</sub>	-0.0527	0.0059	-9.004	< 0.0001 ***
O <sub>2</sub> (200%):Temp <sub>2</sub>	-0.0187	0.0045	-4.159	0.00003 ***
log(hpf)	5.6246	0.1727	32.560	< 0.0001 ***

Null deviance: 6102.34 on 563 degrees of freedom  
Residual deviance: 734.34 on 548 degrees of freedom  
AIC: 1212.6  
Num.Fisher Scoring iterations: 4

1178  
1179  
1180  
1181  
1182  
1183  
1184  
1185  
1186

**Table S5: Effect of oxygen, temperature, and developmental time on hatching success in *Experiment 1*.** Effect of oxygen level, temperature, and time post-fertilization (hpf) on hatching success of *Danio rerio* embryos, derived from GLM: Hatching success  $\sim O_2 \times Temp + \log(hpf)$ . Post hoc comparisons were conducted relative to the control treatment (27.3 °C, normoxia). This model was used to predict time to 50% hatching (ET<sub>50</sub>). Coefficients, standard errors; and p-values are shown for each predictor.

<i>Parameters (GLM)</i>	<i>Coefficients</i>	<i>Std. Error</i>	<i>z-value</i>	<i>p-value</i>
(Intercept)	-25.7312	0.8701	-29.5740	< 0.0001 ***
O <sub>2</sub> (12.5%)	1.8225	0.4239	4.2990	0.00002 ***
O <sub>2</sub> (25%)	2.3436	0.4959	4.7260	< 0.0001 ***
O <sub>2</sub> (50%)	1.8628	0.4155	4.4840	0.00001 ***
O <sub>2</sub> (200%)	-0.1948	0.3792	-0.5140	0.60748
Temp(15.7°C)	-10.1363	1.4748	-6.8730	< 0.0001 ***
Temp(18.1°C)	-6.3693	0.4250	-14.9880	< 0.0001 ***
Temp(20.3°C)	-4.6328	0.4008	-11.5590	< 0.0001 ***
Temp(22.5°C)	-1.9670	0.3799	-5.1780	< 0.0001 ***
Temp(25.2°C)	0.5331	0.4179	1.2760	0.20201
Temp(29.4°C)	0.8488	0.4150	2.0450	0.04083 *
Temp(32°C)	3.6409	0.5222	6.9720	< 0.0001 ***
Temp(35.6°C)	3.5634	0.4647	7.6690	< 0.0001 ***
Temp(39.3°C)	0.2245	1.5849	0.1420	0.88736
O <sub>2</sub> (12.5%):Temp(15.7°C)	-2.5674	2.0789	-1.2350	0.21685
O <sub>2</sub> (25%):Temp(15.7°C)	-2.8680	2.0989	-1.3660	0.17181
O <sub>2</sub> (50%):Temp(15.7°C)	-2.3014	2.0830	-1.1050	0.26922
O <sub>2</sub> (200%):Temp(15.7°C)	0.0693	2.0836	0.0330	0.97346
O <sub>2</sub> (12.5%):Temp(18.1°C)	-2.9697	0.6200	-4.7900	< 0.0001 ***
O <sub>2</sub> (25%):Temp(18.1°C)	-3.5675	0.6918	-5.1570	< 0.0001 ***

O <sub>2</sub> (50%):Temp(18.1°C)	-6.1542	1.5286	-4.0260	0.00006 ***
O <sub>2</sub> (200%):Temp(18.1°C)	-1.6456	0.6608	-2.4900	0.01276 *
O <sub>2</sub> (12.5%):Temp(20.3°C)	-0.1308	0.5530	-0.2360	0.81305
O <sub>2</sub> (25%):Temp(20.3°C)	-1.3390	0.6145	-2.1790	0.02933 *
O <sub>2</sub> (50%):Temp(20.3°C)	-2.9215	0.5863	-4.9830	< 0.0001 ***
O <sub>2</sub> (200%):Temp(20.3°C)	0.9848	0.5353	1.8400	0.06582
O <sub>2</sub> (12.5%):Temp(22.5°C)	-1.9238	0.5487	-3.5060	0.00045 ***
O <sub>2</sub> (25%):Temp(22.5°C)	-1.0966	0.6247	-1.7550	0.07917 *
O <sub>2</sub> (50%):Temp(22.5°C)	-1.7295	0.5650	-3.0610	0.0022 **
O <sub>2</sub> (200%):Temp(22.5°C)	-0.5116	0.5226	-0.9790	0.32755
O <sub>2</sub> (12.5%):Temp(25.2°C)	-2.2347	0.6123	-3.6500	0.00026 ***
O <sub>2</sub> (25%):Temp(25.2°C)	-1.2161	0.6700	-1.8150	0.0695
O <sub>2</sub> (50%):Temp(25.2°C)	-2.7798	0.6009	-4.6260	< 0.0001 ***
O <sub>2</sub> (200%):Temp(25.2°C)	-1.1439	0.5702	-2.0060	0.04485 *
O <sub>2</sub> (12.5%):Temp(29.4°C)	-3.8866	0.5854	-6.6400	< 0.0001 ***
O <sub>2</sub> (25%):Temp(29.4°C)	-2.0495	0.6520	-3.1430	0.00167 **
O <sub>2</sub> (50%):Temp(29.4°C)	-0.5201	0.6403	-0.8120	0.41659
O <sub>2</sub> (200%):Temp(29.4°C)	-1.1690	0.5560	-2.1030	0.03549 *
O <sub>2</sub> (12.5%):Temp(32°C)	-13.1201	1.5821	-8.2930	< 0.0001 ***
O <sub>2</sub> (25%):Temp(32°C)	-6.0797	0.7280	-8.3510	< 0.0001 ***
O <sub>2</sub> (50%):Temp(32°C)	-2.4667	0.7134	-3.4580	0.00055 ***
O <sub>2</sub> (200%):Temp(32°C)	-0.6064	0.7152	-0.8480	0.39656
O <sub>2</sub> (12.5%):Temp(35.6°C)	-11.1369	1.5641	-7.1200	< 0.0001 ***
O <sub>2</sub> (25%):Temp(35.6°C)	-11.7437	1.5839	-7.4140	< 0.0001 ***
O <sub>2</sub> (50%):Temp(35.6°C)	-5.9753	0.6571	-9.0940	< 0.0001 ***
O <sub>2</sub> (200%):Temp(35.6°C)	-4.4209	0.5949	-7.4310	< 0.0001 ***
O <sub>2</sub> (12.5%):Temp(39.3°C)	0.4634	2.2625	0.2050	0.83770
O <sub>2</sub> (25%):Temp(39.3°C)	-0.8111	2.2380	-0.3620	0.71705
O <sub>2</sub> (50%):Temp(39.3°C)	-0.2005	2.2286	-0.0900	0.92833
O <sub>2</sub> (200%):Temp(39.3°C)	2.0225	2.2341	0.9050	0.36531
log(hpf)	5.9284	0.1870	31.7010	< 0.0001 ***

---

Null deviance: 6068.18 on 563 degrees of freedom

Residual deviance: 530.22 on 513 degrees of freedom

AIC: 1078.4

Number of Fisher Scoring iterations: 10

1187  
1188  
1189  
1190  
1191  
1192  
1193  
1194  
1195  
1196

**Table S6: Effect of oxygen, temperature, and developmental time on hatching success in Experiment 2.** GLM includes oxygen level, temperature centered to 27.8 °C (Temp<sub>1</sub>, lowest temperature at which hatching occurred), and its quadratic term (Temp<sub>2</sub>), their interaction, and log-transformed developmental time (hpf): Hatching success ~ O<sub>2</sub> + Temp<sub>1</sub> + Temp<sub>2</sub> + O<sub>2</sub>×Temp<sub>1</sub> + O<sub>2</sub>×Temp<sub>2</sub> + log(hpf) + (1 | Experiment). Significance is shown first with oxygen as numeric relative to 27.8 °C and subsequently relative to 100% air saturation. Estimates (β), standard errors, z-values, and p-values are shown for each predictor.

<i>Parameters (GLM)</i>	<i>Estimate (B)</i>	<i>Std. Error</i>	<i>z-value</i>	<i>p-value</i>
(Intercept)	-20.6800	0.4985	-41.4870	< 0.0001 ***
O <sub>2</sub>	0.0062	0.0010	6.1460	< 0.0001 ***
Temp <sub>1</sub>	0.6726	0.0675	9.9660	< 0.0001 ***
Temp <sub>2</sub>	-0.1184	0.0088	-13.4460	< 0.0001 ***
O <sub>2</sub> :Temp <sub>1</sub>	0.0024	0.0006	4.0030	0.0001 ***
O <sub>2</sub> :Temp <sub>2</sub>	-0.0002	0.0001	-3.1210	0.0018 **
log(hpf)	4.7390	0.1118	42.3990	< 0.0001 ***

Null deviance: 7709.4 on 399 degrees of freedom

Residual deviance: 2362.9 on 393 degrees of freedom

AIC: 2885.1

Num.Fisher Scoring iterations: 3

<i>Parameters (GLM)</i>	<i>Estimate (B)</i>	<i>Std. Error</i>	<i>z-value</i>	<i>p-value</i>
(Intercept)	-24.5700	0.6418	-38.278	< 0.0001 ***
O <sub>2</sub> (12.5%)	-3.5550	0.2641	-13.462	< 0.0001 ***
O <sub>2</sub> (25%)	0.4599	0.2571	1.789	0.0737 ·
O <sub>2</sub> (50%)	0.3232	0.2562	1.262	0.2071
O <sub>2</sub> (200%)	-0.0464	0.2430	-0.191	0.8486
Temp <sub>1</sub>	1.2810	0.1000	12.819	< 0.0001 ***
Temp <sub>2</sub>	-0.1703	0.0110	-15.494	< 0.0001 ***

O <sub>2</sub> (12.5%):Temp <sub>1</sub>	0.1941	0.1728	1.123	0.2615
O <sub>2</sub> (25%):Temp <sub>1</sub>	-0.5149	0.1744	-2.953	0.0032 **
O <sub>2</sub> (50%):Temp <sub>1</sub>	-0.1122	0.1434	-0.783	0.4338
O <sub>2</sub> (200%):Temp <sub>1</sub>	-0.1242	0.1340	-0.927	0.3541
O <sub>2</sub> (12.5%):Temp <sub>2</sub>	-0.0623	0.0247	-2.517	0.0118 *
O <sub>2</sub> (25%):Temp <sub>2</sub>	-0.0389	0.0251	-1.552	0.1208
O <sub>2</sub> (50%):Temp <sub>2</sub>	0.0016	0.0163	0.100	0.9201
O <sub>2</sub> (200%):Temp <sub>2</sub>	0.0003	0.0148	0.021	0.9836
log(hpf)	5.8840	0.1459	40.318	< 0.0001 ***
Null deviance:		7709.4 on 399 degrees of freedom		
Residual deviance:		1179.7 on 384 degrees of freedom		
AIC:		1720		
Num.Fisher Scoring iterations:		3		

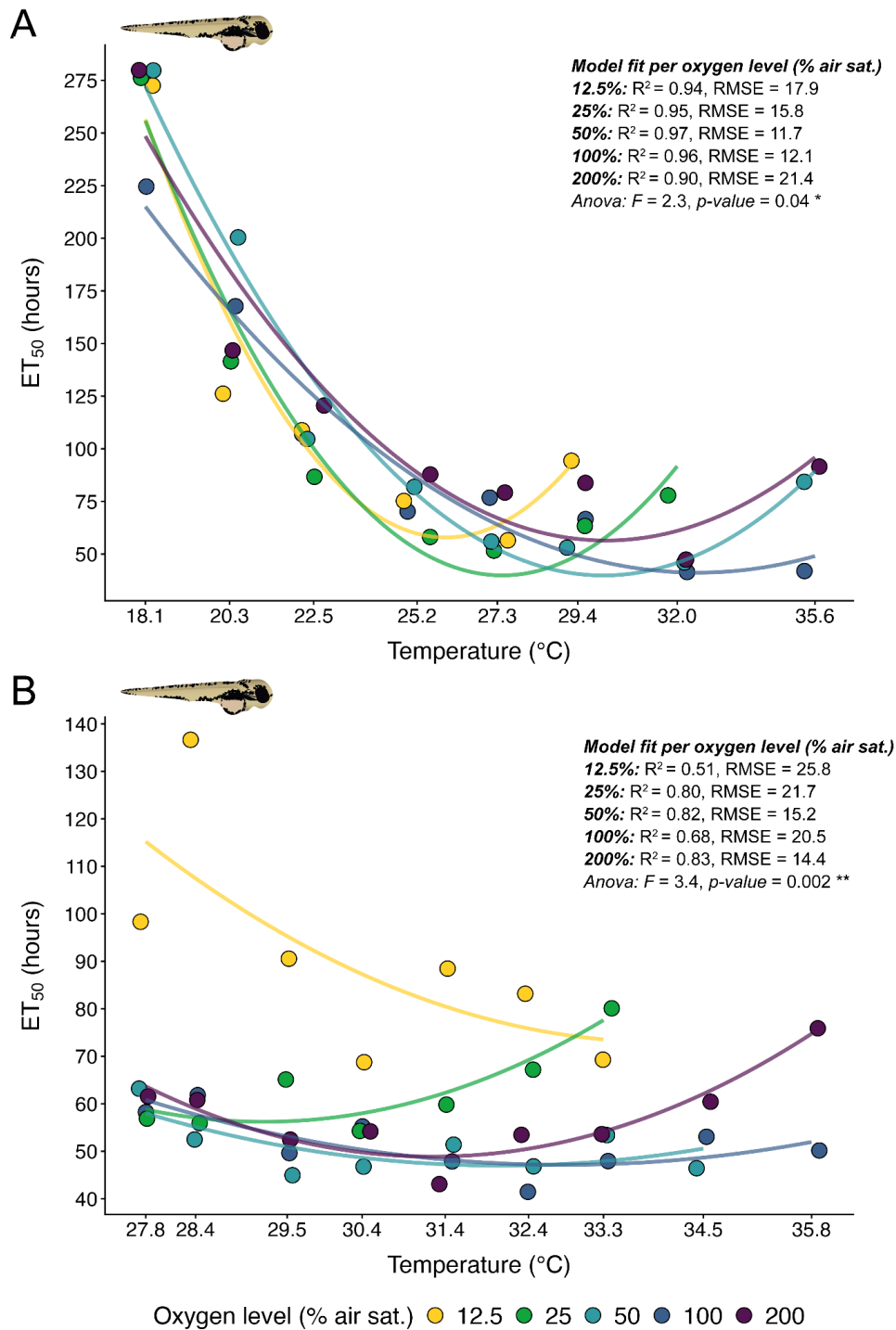
1197  
1198  
1199  
1200  
1201  
1202  
1203  
1204  
1205  
1206

**Table S7: Effect of oxygen, temperature, and developmental time on hatching success in Experiment 2.** Effect of oxygen level, temperature, and time post-fertilization (hpf) on hatching success of *Danio rerio* embryos, derived from a GLM: Hatching success  $\sim$  O<sub>2</sub>  $\times$  Temp + log(hpf). Post hoc comparisons were conducted relative to the control treatment (27.8 °C, normoxia). This model was used to predict time to 50% hatching (ET<sub>50</sub>). Coefficients, standard errors; and p-values are shown for each predictor.

<i>Parameters (GLM)</i>	<i>Coefficients</i>	<i>Std. Error</i>	<i>z-value</i>	<i>p-value</i>
(Intercept)	-25.4008	0.6992	-36.3270	< 0.0001 ***
O <sub>2</sub> (12.5%)	-3.2721	0.3293	-9.9370	< 0.0001 ***
O <sub>2</sub> (25%)	0.1484	0.3442	0.4310	0.66629
O <sub>2</sub> (50%)	-0.5093	0.3468	-1.4680	0.14201
O <sub>2</sub> (200%)	-0.3443	0.3308	-1.0410	0.29791
Temp(28.4°C)	-0.3710	0.3862	-0.9610	0.33670
Temp(29.5°C)	1.0031	0.3624	2.7680	0.00564 **
Temp(30.4°C)	0.3344	0.3626	0.9220	0.35641
Temp(31.4°C)	1.2272	0.3662	3.3510	0.00081 ***
Temp(32.4°C)	2.1239	0.3832	5.5420	< 0.0001 ***

Temp(33.3°C)	1.2181	0.3671	3.3180	0.00091
Temp(34.5°C)	0.5842	0.3549	1.6460	0.09977
Temp(35.8°C)	0.9323	0.3830	2.4340	0.01493 *
Temp(37.1°C)	-7.9833	1.4600	-5.4680	< 0.0001 ***
O <sub>2</sub> (12.5%):Temp(28.4°C)	-1.6848	0.5401	-3.1190	0.00181 **
O <sub>2</sub> (25%):Temp(28.4°C)	0.4760	0.5169	0.9210	0.35713
O <sub>2</sub> (50%):Temp(28.4°C)	1.5334	0.5315	2.8850	0.00392 **
O <sub>2</sub> (200%):Temp(28.4°C)	0.4480	0.5090	0.8800	0.37872
O <sub>2</sub> (12.5%):Temp(29.5°C)	-0.4888	0.4711	-1.0380	0.29939
O <sub>2</sub> (25%):Temp(29.5°C)	-1.8470	0.5152	-3.5850	0.00034 ***
O <sub>2</sub> (50%):Temp(29.5°C)	1.1248	0.5244	2.1450	0.03197 *
O <sub>2</sub> (200%):Temp(29.5°C)	-0.0036	0.4935	-0.0070	0.99413
O <sub>2</sub> (12.5%):Temp(30.4°C)	1.9022	0.5050	3.7670	0.00017 ***
O <sub>2</sub> (25%):Temp(30.4°C)	-0.0434	0.5102	-0.0850	0.93224
O <sub>2</sub> (50%):Temp(30.4°C)	1.5466	0.5309	2.9130	0.00358 **
O <sub>2</sub> (200%):Temp(30.4°C)	0.4625	0.4982	0.9280	0.35330
O <sub>2</sub> (12.5%):Temp(31.4°C)	-0.5664	0.4818	-1.1760	0.23969
O <sub>2</sub> (25%):Temp(31.4°C)	-1.5425	0.5149	-2.9960	0.00274 **
O <sub>2</sub> (50%):Temp(31.4°C)	0.0625	0.5257	0.1190	0.90530
O <sub>2</sub> (200%):Temp(31.4°C)	1.0027	0.5157	1.9440	0.05188 ·
O <sub>2</sub> (12.5%):Temp(32.4°C)	-1.0782	0.5292	-2.0370	0.04161 *
O <sub>2</sub> (25%):Temp(32.4°C)	-3.1643	0.5166	-6.1250	< 0.0001 ***
O <sub>2</sub> (50%):Temp(32.4°C)	-0.2523	0.5239	-0.4820	0.63008
O <sub>2</sub> (200%):Temp(32.4°C)	-1.2446	0.5091	-2.4450	0.01449 *
O <sub>2</sub> (12.5%):Temp(33.3°C)	0.9698	0.5179	1.8730	0.0611 ·
O <sub>2</sub> (25%):Temp(33.3°C)	-3.3581	0.5010	-6.7030	< 0.0001 ***
O <sub>2</sub> (50%):Temp(33.3°C)	-0.1684	0.5317	-0.3170	0.75145
O <sub>2</sub> (200%):Temp(33.3°C)	-0.3551	0.5038	-0.7050	0.48083
O <sub>2</sub> (12.5%):Temp(34.5°C)	-5.4563	1.4939	-3.6520	0.00026 ***
O <sub>2</sub> (25%):Temp(34.5°C)	-8.2046	1.4996	-5.4710	< 0.0001 ***
O <sub>2</sub> (50%):Temp(34.5°C)	1.3427	0.5216	2.5740	0.01005 *

O <sub>2</sub> (200%):Temp(34.5°C)	-0.4701	0.4916	-0.9560	0.33898
O <sub>2</sub> (12.5%):Temp(35.8°C)	-3.9199	1.5096	-2.5970	0.00941 **
O <sub>2</sub> (25%):Temp(35.8°C)	-8.5087	1.5078	-5.6430	< 0.0001 ***
O <sub>2</sub> (50%):Temp(35.8°C)	-2.1024	0.6062	-3.4680	0.00052 ***
O <sub>2</sub> (200%):Temp(35.8°C)	-2.2404	0.5046	-4.4400	< 0.0001 ***
O <sub>2</sub> (12.5%):Temp(37.1°C)	5.3383	2.0750	2.5730	0.01009 *
O <sub>2</sub> (25%):Temp(37.1°C)	1.5752	2.0675	0.7620	0.44611
O <sub>2</sub> (50%):Temp(37.1°C)	1.8417	2.0785	0.8860	0.37559
O <sub>2</sub> (200%):Temp(37.1°C)	0.0890	2.0571	0.0430	0.96548
log(hpf)	6.2491	0.1590	39.3090	< 0.0001 ***
Null deviance:		7620.39 on 399 degrees of freedom		
Residual deviance:		711.17 on 349 degrees of freedom		
AIC:		1321.4		
Num.Fisher Scoring iterations:		5		



1208  
 1209  
 1210  
 1211  
 1212  
 1213  
 1214  
 1215  
 1216  
 1217  
 1218

**Fig. S9: Model-predicted time to 50% hatching ( $ET_{50}$ ) in zebrafish (*Danio rerio*).**

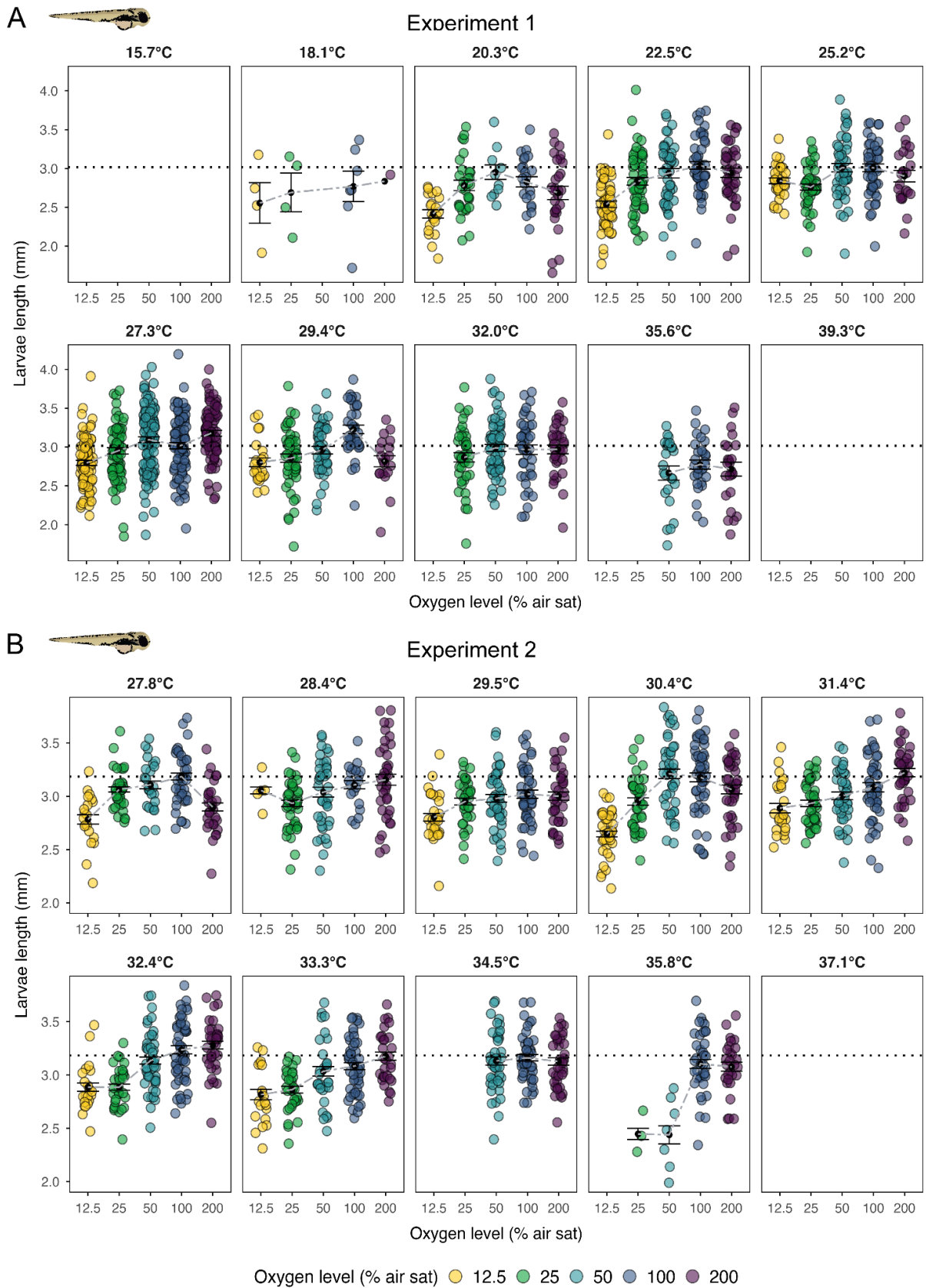
Predicted  $ET_{50}$  (hours) for (A) *Experiment 1* and (B) *Experiment 2* based on GLM: Hatching success  $\sim$  Oxygen  $\times$  Temperature + log(hpf) (Table S5-S7). Oxygen and temperature were included as factors, and hours post-fertilization (hpf) were log-transformed. The models achieved best-fit AIC values. Colored lines represent predicted 50% hatching times for each oxygen level fitted with a second-order polynomial regression (Predicted  $ET_{50} \sim$  poly(Temperature, 2)). Coefficients of determination ( $R^2$ ) and root-mean-square deviation (RMSE) indicate regression fit quality per oxygen level. P-values denote significant effects of oxygen treatment on the temperature–hatching time relationship.

1219 **Table S8: Predicted time to 50% hatching (ET<sub>50</sub> ; hours) for each combination of**  
 1220 **oxygen level and temperature treatment in *Danio rerio* from Experiments 1 and 2.**  
 1221 Predictions were derived from a GLM: Hatching success ~ Oxygen × Temperature + log(hpf)  
 1222 (Table S5-S7), used to generate Fig. S8.  
 1223

Experiment 1			Experiment 2		
Temperature (°C)	Oxygen (% air sat)	Predicted ET <sub>50</sub>	Temperature (°C)	Oxygen (% air sat)	Predicted ET <sub>50</sub>
15.7	12.5	–	27.8	12.5	98.33
18.1	12.5	272.66	28.4	12.5	136.65
20.3	12.5	126.03	29.5	12.5	90.54
22.5	12.5	108.76	30.4	12.5	68.75
25.2	12.5	75.18	31.4	12.5	88.47
27.3	12.5	56.43	32.4	12.5	83.17
29.4	12.5	94.18	33.3	12.5	69.27
32.0	12.5	–	34.5	12.5	–
35.6	12.5	–	35.8	12.5	–
39.3	12.5	–	37.1	12.5	–
<hr/>					
15.7	25	–	27.8	25	56.88
18.1	25	276.24	28.4	25	55.93
20.3	25	141.51	29.5	25	65.10
22.5	25	86.63	30.4	25	54.29
25.2	25	57.99	31.4	25	59.82
27.3	25	51.67	32.4	25	67.18
29.4	25	63.28	33.3	25	80.11
32.0	25	77.97	34.5	25	–
35.6	25	–	35.8	25	–
39.3	25	–	37.1	25	–
<hr/>					
15.7	50	–	27.8	50	63.19
18.1	50	279.83	28.4	50	52.48
20.3	50	200.39	29.5	50	44.95
22.5	50	104.56	30.4	50	46.76
25.2	50	81.87	31.4	50	51.40

27.3	50	56.04	32.4	50	46.83
29.4	50	53.02	33.3	50	53.41
32.0	50	45.98	34.5	50	46.43
35.6	50	84.18	35.8	50	–
39.3	50	–	37.1	50	–
<hr/>					
15.7	100	–	27.8	100	58.26
18.1	100	224.71	28.4	100	61.82
20.3	100	167.61	29.5	100	49.61
22.5	100	106.94	30.4	100	55.21
25.2	100	70.12	31.4	100	47.86
27.3	100	76.72	32.4	100	41.46
29.4	100	66.49	33.3	100	47.93
32.0	100	41.52	34.5	100	53.05
35.6	100	42.07	35.8	100	50.17
39.3	100	–	37.1	100	–
<hr/>					
15.7	200	–	27.8	200	61.55
18.1	200	279.83	28.4	200	60.80
20.3	200	146.73	29.5	200	52.45
22.5	200	120.45	30.4	200	54.19
25.2	200	87.88	31.4	200	43.08
27.3	200	79.30	32.4	200	53.46
29.4	200	83.68	33.3	200	53.61
32.0	200	47.52	34.5	200	60.43
35.6	200	91.64	35.8	200	75.88
39.3	200	–	37.1	200	–

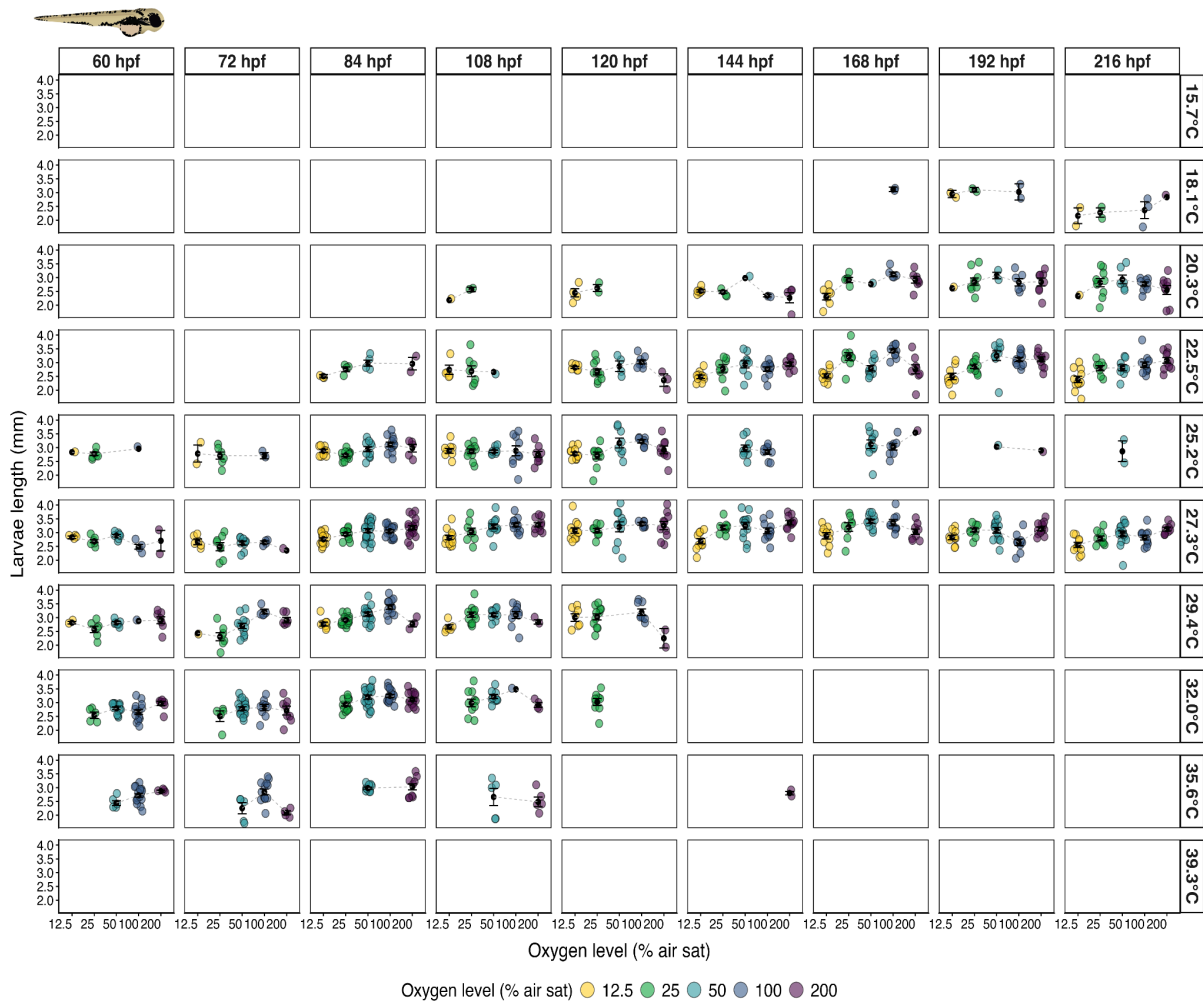
1224  
1225



1226  
1227  
1228  
1229

**Fig. S10: Larval length (mm) of zebrafish (*Danio rerio*) across oxygen levels (colors) and temperatures (panel columns) in *Experiment 1* ( $n = 2-15$ ; A) and *Experiment 2* ( $n = 2-24$ ; B). Points show individual larvae (jittered); black circles and dashed lines indicate group**

1230 means  $\pm$  S.E. Dotted lines mark control means (*Exp 1*: 27.3 °C, normoxia = 3.0 mm; *Exp 2*:  
 1231 27.8 °C, normoxia = 3.2 mm).  
 1232  
 1233



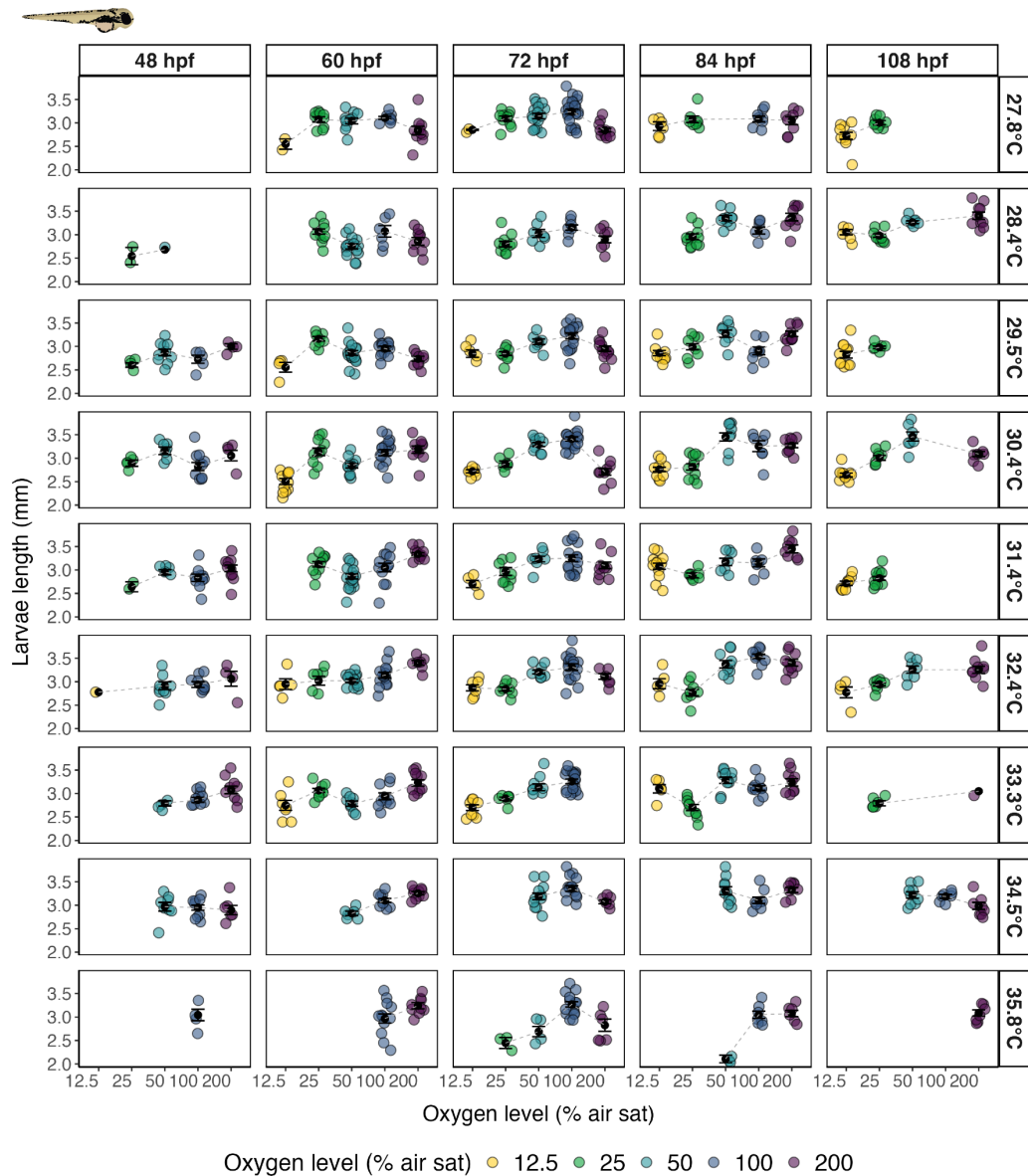
1234  
 1235 **Figure S11 | Larval length of zebrafish across temperature, oxygen, and developmental**  
 1236 **time in *Experiment 1*.** Larval length (mm) of *Danio rerio* across oxygen levels (colors) and  
 1237 temperatures (vertical panels) over time post-fertilization (60, 72, 84, 120, 144, 168, 192, and  
 1238 216 hpf; horizontal panels). Points represent individual larvae; black circles indicate group  
 1239 means  $\pm$  s.e., and grey dashed lines connect mean values across developmental time.  
 1240

1241 **Table S9: Larval length of zebrafish across temperature, oxygen, and developmental**  
 1242 **time in *Experiment 1*.** Anova (type III) and linear model (LM) includes oxygen level,  
 1243 temperature centered to 15.7 °C (Temp<sub>1</sub>), and its quadratic term (Temp<sub>2</sub>), their interaction,  
 1244 and developmental time (hpf): Length  $\sim$  O<sub>2</sub> + Temp<sub>1</sub> + Temp<sub>2</sub> + O<sub>2</sub> $\times$ Temp<sub>1</sub> + O<sub>2</sub> $\times$ Temp<sub>2</sub> +  
 1245 hpf. Significance was assessed relative to 15.7 °C and 100% air saturation. Estimates ( $\beta$ ),  
 1246 standard errors (SE), t-values, and p-values are shown for each predictor.  
 1247

Parameters (Anova, type III)	Sum Squares	Df	F-value	p-value
(Intercept)	96.714	1	747.933	< 0.0001 ***
O <sub>2</sub>	1.662	4	3.212	0.0123*

Temp <sub>1</sub>	3.114	1	24.081	< 0.0001 ***
Temp <sub>2</sub>	3.004	1	23.232	< 0.0001 ***
O <sub>2</sub> :Temp <sub>1</sub>	1.129	4	2.183	0.0687
O <sub>2</sub> :Temp <sub>2</sub>	1.047	4	2.025	0.0886
hpf	1.888	1	14.601	0.00014***
Residuals	185.041	1431		

<i>Parameters (LM)</i>	<i>Estimate (B)</i>	<i>Std. Error</i>	<i>t-value</i>	<i>p-value</i>
(Intercept)	2.533	0.093	27.348	< 0.0001 ***
O <sub>2</sub> (12.5%)	-0.423	0.139	-3.042	0.0024**
O <sub>2</sub> (25%)	-0.023	0.116	-0.203	0.8394
O <sub>2</sub> (50%)	-0.074	0.135	-0.550	0.5822
O <sub>2</sub> (200%)	-0.250	0.117	-2.140	0.0325*
Temp <sub>1</sub>	0.085	0.017	4.907	< 0.0001 ***
Temp <sub>2</sub>	-0.004	0.001	-4.820	< 0.0001 ***
hpf	0.001	0.000	3.821	0.0001***
O <sub>2</sub> (12.5%):Temp <sub>1</sub>	0.007	0.043	0.161	0.8717
O <sub>2</sub> (25%):Temp <sub>1</sub>	-0.037	0.029	-1.273	0.2032
O <sub>2</sub> (50%):Temp <sub>1</sub>	0.017	0.028	0.605	0.5452
O <sub>2</sub> (200%):Temp <sub>1</sub>	0.052	0.026	1.963	0.0498*
O <sub>2</sub> (12.5%):Temp <sub>2</sub>	0.001	0.003	0.305	0.7603
O <sub>2</sub> (25%):Temp <sub>2</sub>	0.002	0.002	1.273	0.2033
O <sub>2</sub> (50%):Temp <sub>2</sub>	-0.001	0.001	-0.771	0.4406
O <sub>2</sub> (200%):Temp <sub>2</sub>	-0.003	0.001	-1.889	0.0591
Residual standard error: 0.3596 on 1431 degrees of freedom				
Multiple R-squared:		0.154		
F-statistic:		17.37 on 15 and 1431 DF, p-value: < 0.0001 ***		
Adjusted R-squared:		0.1452		



1249  
1250  
1251  
1252  
1253  
1254  
1255  
1256  
1257  
1258  
1259  
1260  
1261  
1262  
1263

**Fig. S12: Larval length of zebrafish across temperature, oxygen, and developmental time in *Experiment 2*.** Larval length (mm) of *Danio rerio* across oxygen levels (colors) and temperatures (vertical panels) over time post-fertilization (48, 60, 72, 84, and 108 hpf; horizontal panels). Points represent individual larvae; black circles indicate group means  $\pm$  s.e., and grey dashed lines connect mean values across developmental time.

**Table S10: Larval length of zebrafish across temperature, oxygen, and developmental time in *Experiment 2*.** Anova (type III) and linear model (LM) includes oxygen level, temperature centered to 27.8 °C (Temp<sub>1</sub>), and its quadratic term (Temp<sub>2</sub>), their interaction, and developmental time (hpf): Length  $\sim$  O<sub>2</sub> + Temp<sub>1</sub> + Temp<sub>2</sub> + O<sub>2</sub> $\times$ Temp<sub>1</sub> + O<sub>2</sub> $\times$ Temp<sub>2</sub> + hpf. Significance was assessed relative to 27.8 °C and 100% air saturation. Estimates ( $\beta$ ), standard errors (SE), t-values, and p-values are shown for each predictor.

Parameters (Anova, type III)	Sum Squares	Df	F-value	p-value
(Intercept)	262.798	1	3991.617	< 0.0001 ***

O <sub>2</sub>	3.127	4	11.874	< 0.0001 ***
Temp <sub>1</sub>	0.039	1	0.597	0.4398
Temp <sub>2</sub>	0.037	1	0.556	0.4560
O <sub>2</sub> :Temp <sub>1</sub>	1.466	4	5.566	0.0002***
O <sub>2</sub> :Temp <sub>2</sub>	1.258	4	4.776	0.0008***
hpf	7.414	1	112.605	< 0.0001 ***
Residuals	92.699	1408		

<i>Parameters (LM)</i>	<i>Estimate (B)</i>	<i>Std. Error</i>	<i>t-value</i>	<i>p-value</i>
(Intercept)	2.809	0.044	63.179	< 0.0001 ***
O <sub>2</sub> (12.5%)	-0.410	0.062	-6.577	< 0.0001 ***
O <sub>2</sub> (25%)	-0.166	0.046	-3.586	0.0003***
O <sub>2</sub> (50%)	-0.112	0.048	-2.332	0.0198*
O <sub>2</sub> (200%)	-0.193	0.047	-4.077	< 0.0001 ***
Temp <sub>1</sub>	0.014	0.019	0.773	0.4398
Temp <sub>2</sub>	-0.002	0.002	-0.746	0.4560
hpf	0.004	0.000	10.612	< 0.0001 ***
O <sub>2</sub> (12.5%):Temp <sub>1</sub>	-0.051	0.044	-1.148	0.2512
O <sub>2</sub> (25%):Temp <sub>1</sub>	-0.013	0.031	-0.429	0.6682
O <sub>2</sub> (50%):Temp <sub>1</sub>	0.056	0.029	1.916	0.0555
O <sub>2</sub> (200%):Temp <sub>1</sub>	0.099	0.028	3.579	0.0004***
O <sub>2</sub> (12.5%):Temp <sub>2</sub>	0.013	0.007	1.835	0.0667
O <sub>2</sub> (25%):Temp <sub>2</sub>	-0.004	0.005	-0.857	0.3917
O <sub>2</sub> (50%):Temp <sub>2</sub>	-0.009	0.004	-2.460	0.0139*
O <sub>2</sub> (200%):Temp <sub>2</sub>	-0.011	0.003	-3.154	0.0016**
Residual standard error:		0.2566 on 1408 degrees of freedom		
Multiple R-squared:		0.2336		
F-statistic:		28.61 on 15 and 1408 DF, p-value: < 0.0001 ***		
Adjusted R-squared:		0.2255		

1264  
1265  
1266  
1267

**Table S11: Survival to first feeding of zebrafish across temperature, oxygen, and developmental time in *Experiment 1 and 2*. GLM-TMB includes oxygen level, temperature**

1268 centered to 18.1 °C (Temp<sub>1</sub>, lowest temperature at which hatching occurred), and its  
 1269 quadratic term (Temp<sub>2</sub>), their interaction, log-transformed developmental time (hpf), and  
 1270 Experiment as random effect: Survival to First Feeding ~ O<sub>2</sub> + Temp<sub>1</sub> + Temp<sub>2</sub> + O<sub>2</sub>×Temp<sub>1</sub>  
 1271 + O<sub>2</sub>×Temp<sub>2</sub> + log(hpf) + (1 | Experiment). Significance is shown first with oxygen as  
 1272 numeric relative to 18.1 °C and subsequently relative to 100% air saturation. Estimates (β),  
 1273 standard errors (SE), z-values, and p-values are shown for each predictor.  
 1274

<i>Parameters (GLM-TMB)</i>	<i>Estimate (B)</i>	<i>Std. Error</i>	<i>z-value</i>	<i>p-value</i>
(Intercept)	-26.1100	0.5732	-45.550	< 0.0001 ***
O <sub>2</sub>	-0.0114	0.0022	-5.180	< 0.0001 ***
Temp <sub>1</sub>	0.9085	0.0391	23.230	< 0.0001 ***
Temp <sub>2</sub>	-0.0433	0.0019	-22.370	< 0.0001 ***
O <sub>2</sub> :Temp <sub>1</sub>	0.0028	0.0004	7.020	< 0.0001 ***
O <sub>2</sub> :Temp <sub>2</sub>	-0.0001	0.0000	-5.500	< 0.0001 ***
log(hpf)	4.6060	0.0990	46.510	< 0.0001 ***

Experiment (Intercept): 0.0598 (Var.) 0.2446 (St. Dev.)

Number of obs: 973 groups: Experiment 1, 2

AIC: 6960.7 logLik: -3472.3

<i>Parameters (GLM-TMB)</i>	<i>Estimate (B)</i>	<i>Std. Error</i>	<i>z-value</i>	<i>p-value</i>
(Intercept)	-38.6488	0.8895	-43.450	< 0.0001 ***
O <sub>2</sub> (12.5%)	-0.1135	0.4524	-0.250	0.8019
O <sub>2</sub> (25%)	-1.8757	0.4954	-3.790	0.0001 ***
O <sub>2</sub> (50%)	-4.9287	0.6807	-7.240	< 0.0001 ***
O <sub>2</sub> (200%)	-2.4898	0.5497	-4.530	< 0.0001 ***
Temp <sub>1</sub>	1.2624	0.0596	21.170	< 0.0001 ***
Temp <sub>2</sub>	-0.0442	0.0026	-17.000	< 0.0001 ***
O <sub>2</sub> (12.5%):Temp <sub>1</sub>	0.1149	0.1301	0.880	0.3775
O <sub>2</sub> (25%):Temp <sub>1</sub>	1.1954	0.1088	10.980	< 0.0001 ***
O <sub>2</sub> (50%):Temp <sub>1</sub>	1.1965	0.1247	9.590	< 0.0001 ***
O <sub>2</sub> (200%):Temp <sub>1</sub>	0.6411	0.0995	6.440	< 0.0001 ***
O <sub>2</sub> (12.5%):Temp <sub>2</sub>	-0.0483	0.0091	-5.290	< 0.0001 ***
O <sub>2</sub> (25%):Temp <sub>2</sub>	-0.0919	0.0058	-15.870	< 0.0001 ***
O <sub>2</sub> (50%):Temp <sub>2</sub>	-0.0608	0.0055	-10.990	< 0.0001 ***

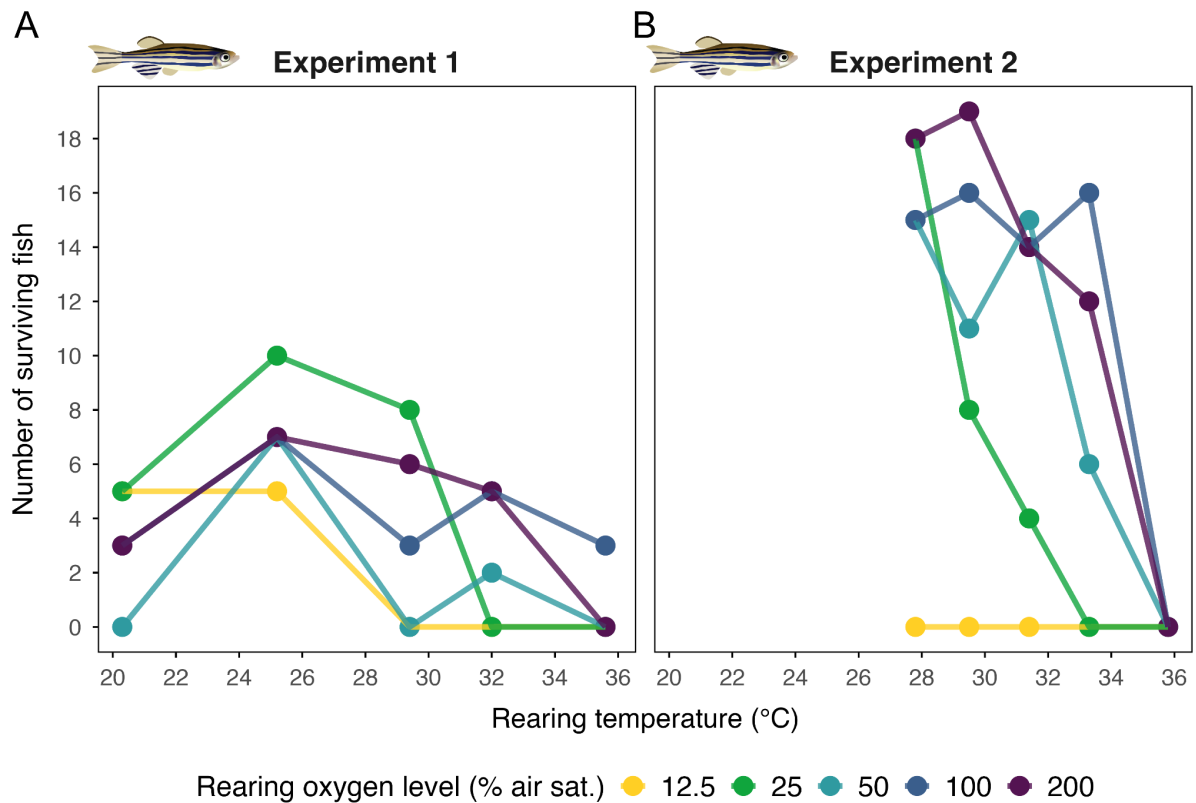
O <sub>2</sub> (200%):Temp <sub>2</sub>	-0.0394	0.0044	-9.000	< 0.0001 ***
log(hpf)	6.8743	0.1509	45.560	< 0.0001 ***
Experiment (Intercept):	0.08689 (Var.)	0.2948 (St. Dev.)		
Number of obs:	973	groups:	Experiment 1, 2	
AIC:	4348.5	logLik:	-2157.2	

1275  
1276  
1277  
1278  
1279  
1280  
1281  
1282

**Table S12: Larval count and survival of zebrafish transferred to control conditions.** Number of larvae transferred to control conditions ( $28.0 \pm 0.5$  °C, normoxia) from *Experiment 1* and ( $27.0 \pm 0.5$  °C, normoxia) from *Experiment 2*. Hatched larvae that died during treatment exposure are indicated by †. Zero values denote treatments in which no hatching occurred.

		Oxygen level (% air sat)					
		Temperature (°C)	12.5	25	50	100	200
<b>Experiment 1</b>	<b>20.3</b>		8	10	4	9	9
	<b>25.2</b>		10	11	10	10	10
	<b>29.4</b>		2	11	9	10	8
	<b>32</b>		0	9	10	9	7
	<b>35.6</b>		0	0	†	13	1
<b>Experiment 2</b>	<b>27.8</b>		†	21	16	21	22
	<b>29.5</b>		†	13	20	20	22
	<b>31.4</b>		†	12	17	19	21
	<b>33.3</b>		†	3	15	19	19
	<b>35.8</b>		0	0	†	11	2

1283  
1284  
1285



1286  
1287  
1288  
1289  
1290  
1291  
1292  
1293  
1294  
1295  
1296  
1297  
1298

**Fig. S13: Survival number of zebrafish reared across temperature and oxygen treatments.** (A) Numbers represent individuals that survived to the juvenile stage after being transferred to control conditions from *Experiment 1* (normoxia; 28 °C) for  $CT_{max}$  testing during the juvenile stage. (B) equivalent data for *Experiment 2* (normoxia; 27 °C).

**Table S13: Critical thermal maximum ( $CT_{max}$ ) of zebrafish across rearing temperature and oxygen treatments in *Experiment 1*.** Anova (type III) and linear model (LM) includes oxygen level ( $O_2$ ), temperature (Temp), and their interaction:  $CT_{max} \sim O_2 \times Temp$ . Significance was assessed relative to 20.3 °C and 100% air saturation. Estimates ( $\beta$ ), standard errors (SE), t-values, and p-values are shown for each predictor.

Parameters (Anova, type III)	Sum Squares	Df	F-value	P-value
$O_2$	0.747	4	1.717	0.1566
Temp	1.863	4	4.283	0.0038**
$O_2:Temp$	0.849	7	1.115	0.3644
Residuals	7.288	67		

Parameters (LM)	Estimate (B)	Std. Error	t value	P-value
(Intercept)	41.669	0.113	370.304	< 0.0001***
$O_2(12.5\%)$	-0.304	0.138	-2.197	0.0311*
$O_2(25\%)$	-0.022	0.109	-0.198	0.8439

O <sub>2</sub> (50%)	-0.165	0.144	-1.147	0.2551
O <sub>2</sub> (200%)	-0.134	0.107	-1.248	0.2160
Temp(20.5°C)	-0.324	0.122	-2.656	0.00967**
Temp(25.5°C)	-0.107	0.103	-1.042	0.3009
Temp(32°C)	0.156	0.133	1.170	0.2457
Temp(36°C)	-0.436	0.222	-1.962	0.05347
<hr/>				
Residual standard error:	0.3316 on 74 degrees of freedom			
Multiple R-squared:	0.2794			
F-statistic:	3.587 on 8 and 74 DF, p-value: 0.00144			
Adjusted R-squared:	0.2015			

1299  
1300  
1301  
1302  
1303  
1304  
1305  
1306

**Table S14: Critical thermal maximum (CT<sub>max</sub>) of zebrafish across rearing temperature and oxygen treatments in *Experiment 2*.** Anova (type III) and linear model (LM) includes oxygen level (O<sub>2</sub>), temperature (Temp), and their interaction: CT<sub>max</sub> ~ O<sub>2</sub>×Temp. Significance was assessed relative to 27.8 °C and 100% air saturation. Estimates (β), standard errors (SE), t-values, and p-values are shown for each predictor.

Parameters (Anova, type III)	Sum Squares	Df	F-value	P-value
O <sub>2</sub>	4.265	3	10.797	< 0.0001***
Temp	1.588	3	4.020	0.0084**
O <sub>2</sub> :Temp	2.049	8	1.945	0.0559
Residuals	24.097	183		
Parameters (LM)	Estimate (B)	Std. Error	t value	P-value
(Intercept)	40.808	0.065	629.348	< 0.0001***
O <sub>2</sub> (25%)	-0.483	0.088	-5.490	< 0.0001***
O <sub>2</sub> (50%)	-0.158	0.073	-2.163	0.0318*
O <sub>2</sub> (200%)	-0.094	0.067	-1.407	0.1611
Temp(29.5°C)	0.115	0.069	1.657	0.0991
Temp(31.4°C)	0.025	0.072	0.340	0.7344
Temp(33.3°C)	-0.164	0.082	-2.014	0.0455*
<hr/>				
Residual standard error:	0.37 on 191 degrees of freedom			
Multiple R-squared:	0.1714			

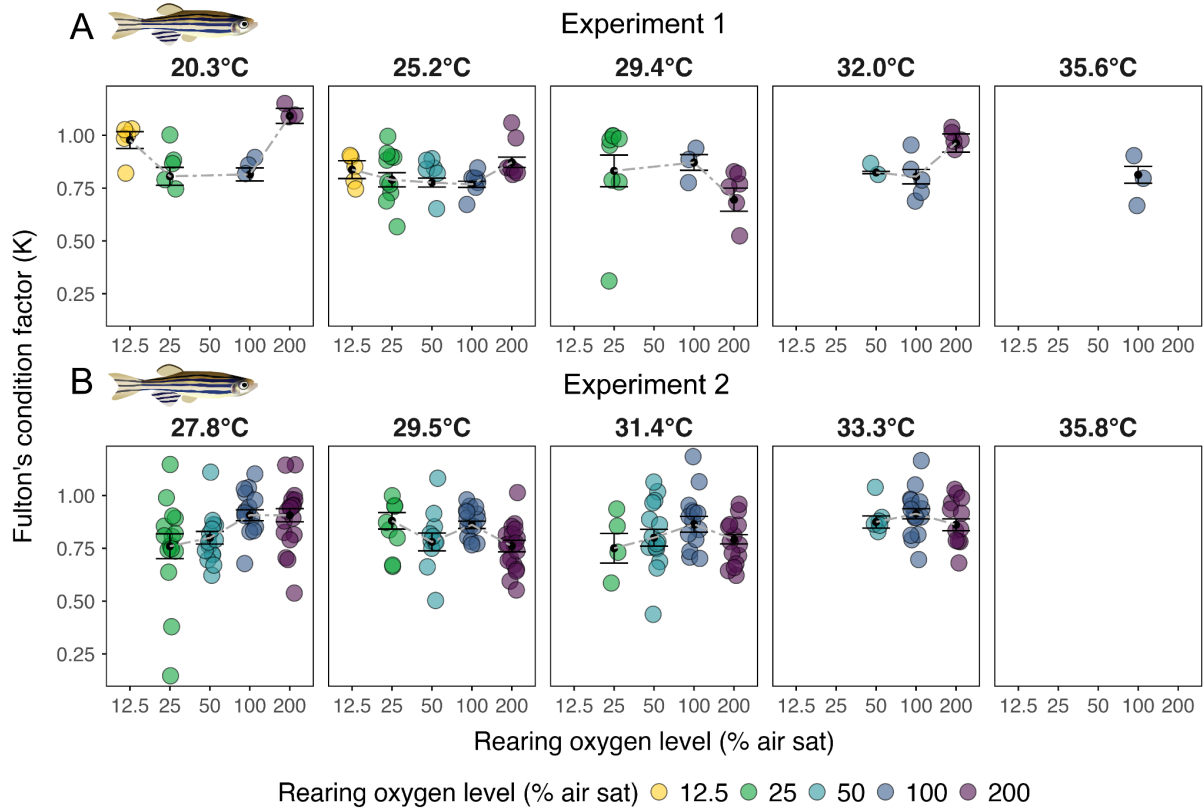
F-statistic:

6.583 on 6 and 191 DF, p-value: < 0.0001\*\*\*

Adjusted R-squared:

0.1453

1307  
1308



1309  
1310  
1311  
1312  
1313  
1314  
1315  
1316

**Fig. S14: Fulton's condition factor (K) of juvenile zebrafish across rearing temperature and oxygen treatments.** Fulton's condition factor (K) of juvenile *Danio rerio* reared during the embryonic stage under five oxygen levels (colors) and temperature treatments (horizontal panels) in (A) *Experiment 1* and (B) *Experiment 2*. Points represent individual fish (jittered), with color indicating oxygen treatment.

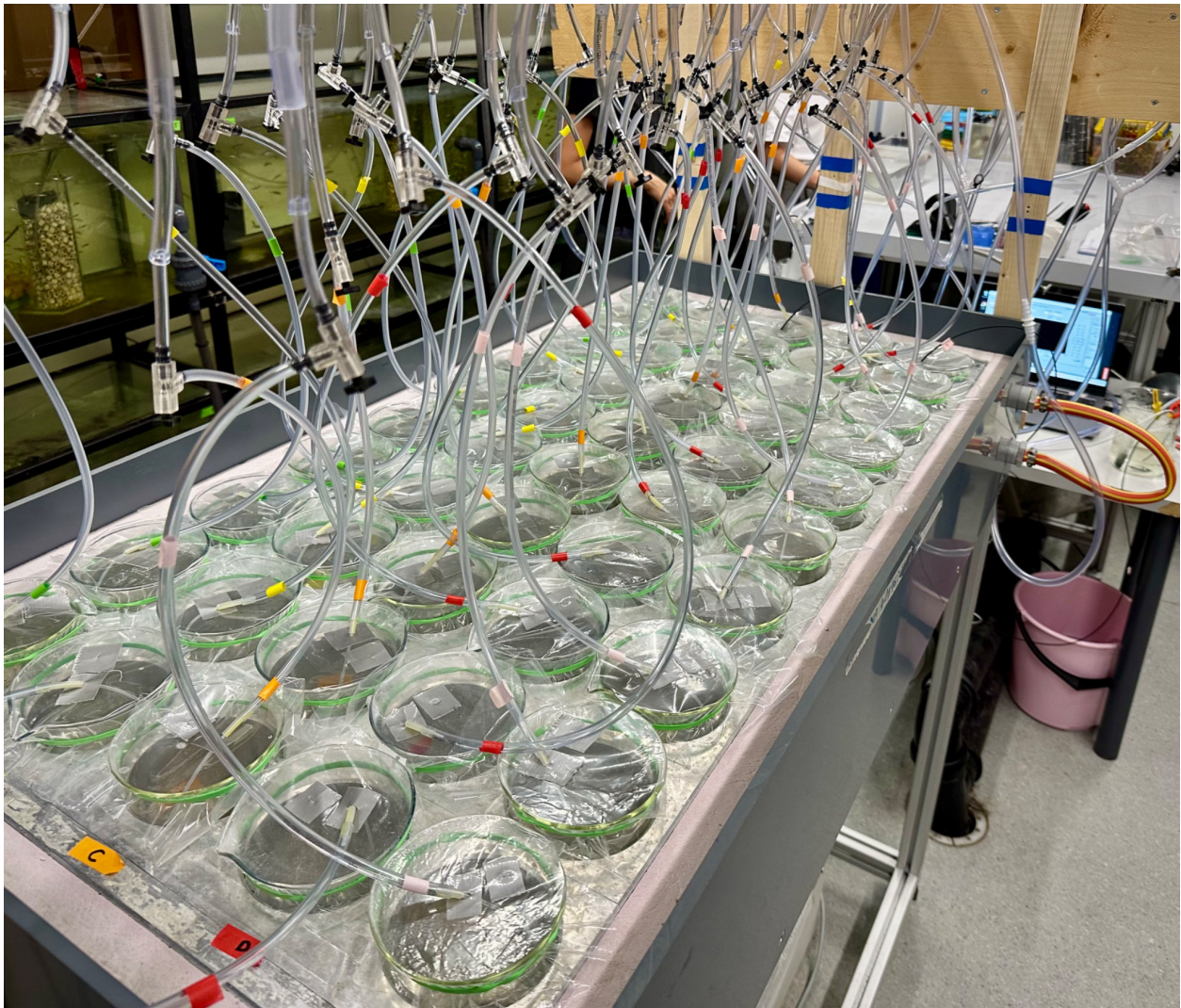
1317  
1318  
1319  
1320

**Table S15: Fulton's condition factor (K) of juvenile zebrafish across rearing temperature and oxygen treatments for *Experiment 1* and *2*.** Anova (type III) includes oxygen level ( $O_2$ ) and temperature (Temp):  $K \sim O_2 + \text{Temp}$ . P-values are shown for each predictor.

Experiment 1				
Parameters (Anova, type III)	Sum Squares	Df	F-value	P-value
(Intercept)	1.818	1	113.872	< 0.0001***
$O_2$	0.034	1	2.111	0.1502
Temp	0.052	1	3.237	0.0758
Residuals	1.277	80		
Experiment 2				

<i>Parameters (Anova, type III)</i>	<i>Sum Squares</i>	<i>Df</i>	<i>F-value</i>	<i>P-value</i>
(Intercept)	0.417	1	22.120	< 0.0001***
O <sub>2</sub>	0.012	1	0.635	0.4264
Temp	0.014	1	0.753	0.3868
Residuals	3.672	195		

1321



1322

1323

1324

1325

1326

1327

1328

1329

1330

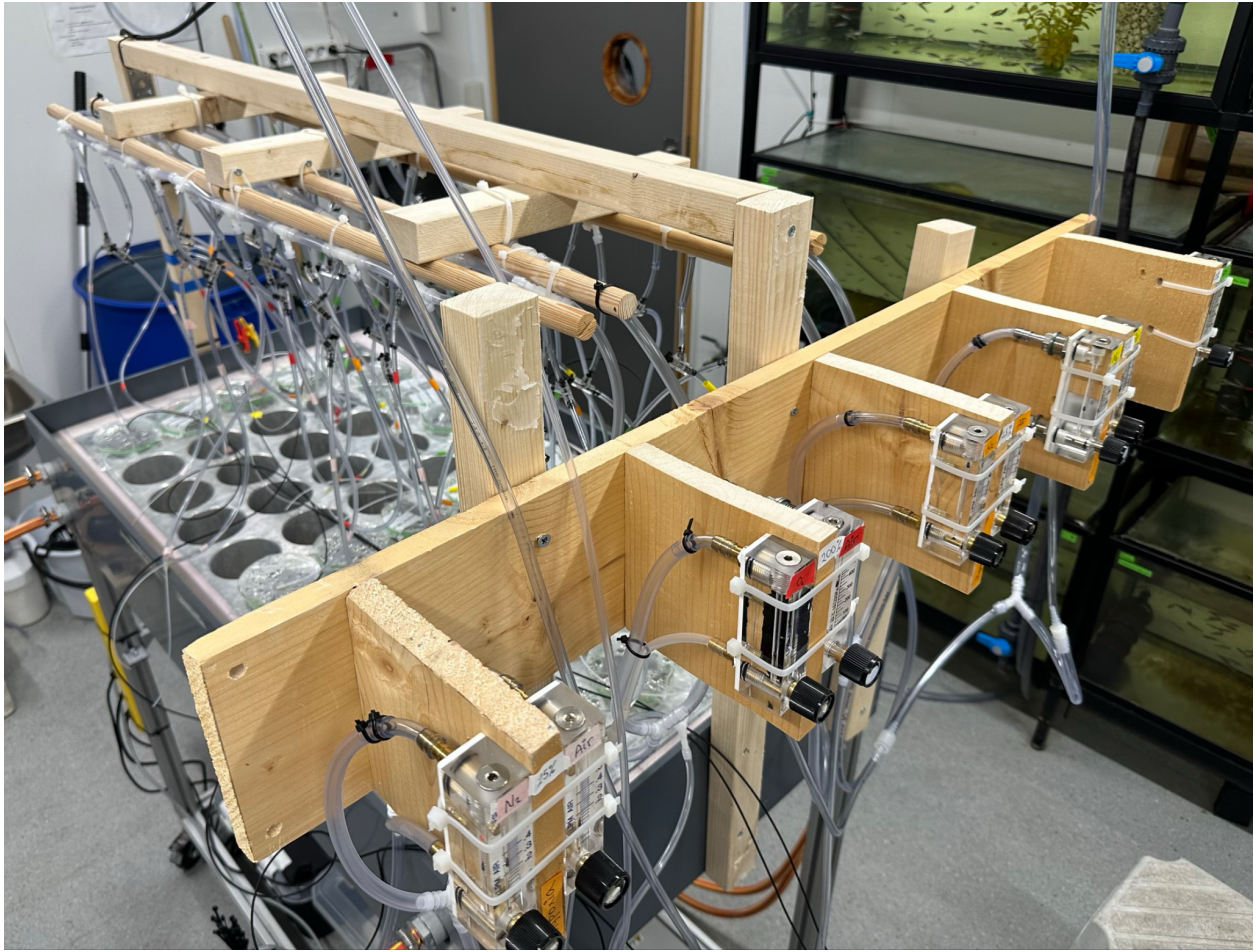
1331

**Fig. S15: Gradient table set up depicting a factorial design of 10 temperatures and 5 oxygen levels yielding 50 unique temperature-oxygen combinations.** Color coded tubes supplied with air to each beaker, where different color lines represent an oxygen level. Beakers were hermetically covered to keep a constant DO<sub>2</sub> concentration per treatment. The mixed gas was delivered to the respective column of 10 beakers via a 10 mm diameter outflow tube. Each beaker was aerated through an individual air tube tightly inserted through the lid and fitted with an air valve, providing gentle bubbling.



1332  
1333  
1334  
1335  
1336

**Fig. S16: Beaker (800 mL) filled with 300 mL treated fresh water held the embryos and early larvae during the rearing period. The aluminium wells holding a beaker had a 17 cm depth.**



1337  
1338  
1339  
1340  
1341  
1342  
1343  
1344  
1345  
1346

**Fig. S17: Set up with five gas mixing stations per oxygen level (12.5, 25, 50, 100, and 200% air saturation).** Oxygen concentrations were regulated using manual gas flow controllers (RS Pro, 500 ml/min) that mixed air with either nitrogen (50 L, 99.6% N<sub>2</sub>) or oxygen (50 L, 99.5% O<sub>2</sub>, Linde Co.) to create hypoxia or hyperoxia, respectively. Normoxia was achieved using ambient air. The two flow controllers supplied with the target oxygen concentration via a 10 mm diameter outflow tube to each column (10 beakers) of the thermal gradient table. Each beaker was aerated through an individual air tube tightly inserted through the lid and fitted with an air valve, providing gentle bubbling.



1347  
1348  
1349  
1350  
1351  
1352  
1353  
1354  
1355  
1356  
1357  
1358

**Fig. S18: Aluminium gradient table connected to a cool and warm temperature water bath at each extreme.** The system consisted of a cooler (Titan 200, Aqua Medic, Germany) and a heater circulator (Grant Instruments, GD100), each with a built-in thermostats that maintain their respective water baths at a set temperature. Water from each bath was pumped to the respective edges of the table using an Eheim Universal 1000 pump (Germany), generating a consistent thermal gradient, from cold to warm, across the aluminium slab of the table.

1359  
1360  
1361  
1362  
1363  
1364  
1365  
1366  
1367  
1368  
1369  
1370  
1371  
1372